Swansea University
Prifysgol Abertawe

An investigation into BMP9-induced postnatal maturation of articular cartilage

Miles Christopher Anderson-Watters

Submitted to Swansea University in fulfilment of the requirements for the Degree of Maters of Science by Research
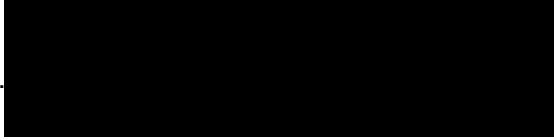
September 2022

Swansea University

Abstract

Postnatal maturation is a process of articular cartilage development in which the tissue acquires biomechanical properties allowing lifelong cyclical loading in adults. During postnatal maturation cartilage undergoes structural and morphological changes, including the reorganisation of the collagen network from isotropic to one that is anisotropic, forming distinct zonal regions of collagen architecture and chondrocyte organisation. However, the mechanisms underlying the process of maturation are poorly understood. Currently there are no *in vitro* biological models of maturation, limiting study of this phenomenon to snapshots of histological, biochemical and biophysical changes. In this study we have shown that *in situ* culture of immature bovine cartilage explants with BMP9 induces changes in collagen structure and chondrocyte organisation recapitulating the zonal features of mature articular cartilage. We found BMP9 stimulates reorganisation of the collagen network causing the reorientation of mid and deep zone fibres perpendicular to the cartilage surface. Inhibition of matrix metalloproteinases (MMPs) via doxycycline prevented the changes observed in collagen alignment. Our results demonstrate that there is increased *MMP3* expression and a reduction in tissue inhibitors of metalloproteinases-1 and -2 resulting in an increase in proteoglycan turnover and uptake of water. Of significant note were observations that show that cellular proliferation is involved in maturation, contrary to findings in mouse cartilage postnatal development, and immunological data showing that remodelling of collagen does not require enzymatic cleavage of pre-existing fibres. Whilst observations of BMP9 induced postnatal maturation in explants were variable, *in vitro* analysis using isolated chondrocytes grown as pellet cultures provided unequivocal evidence of the role of BMP9 in postnatal organisation of collagen fibrils in immature chondrocytes. In addition, pellet cultures show that mature chondrocytes have an intrinsic ability to recapitulate the mature cartilage collagen architecture, but even this is enhanced in the presence of BMP9. Therefore, we have developed useful models of postnatal maturation that have shone light on several important mechanisms that regulate the transition to maturity. We anticipate that our models of BMP9 induced postnatal maturation will provide the basis for further research into understanding the detailed mechanisms involved, guiding the development of more successful tissue engineering strategies.

Declaration

This work has not previously been accepted in substance for any degree and is not being concurrently submitted in candidature for any degree.

Signed ...

Date ....08/09/22.......................................

STATEMENT 1

This thesis is the result of my own investigations, except where otherwise stated. Where correction services have been used, the extent and nature of the correction is clearly marked in a footnote(s).

Other sources are acknowledged by footnotes giving explicit references.   A bibliography is appended.

Signed ....

Date ....08/09/22.......................................

STATEMENT 2

I hereby give consent for my thesis, if accepted, to be available for photocopying and for inter-library loan, and for the title and summary to be made available to outside organisations.

Signed ....

Date   ....16/04/24.....................................

STATEMENT 3

The University's ethical procedures have been followed and, where appropriate, that ethical approval has been granted.

Signed............

Date.................16/04/24...

Contents

Acknowledgements

Firstly, I would like to thank my supervisor, Dr Ilyas Khan for adopting me as a second son and helping me throughout my research project. I will carry the lessons I have learned from this project with me for the rest of my life, trying to be tenacious in whatever I do.

To my parents I cannot explain how grateful I am for everything you have done for me, without your love and support I would not be the person I am today.

Thank you to my close friends, who have been there to provide me with many a distraction whenever I have been overwhelmed by my research.

A special thanks to Mugha, you have been there to keep me calm throughout my project, university would not have been half as enjoyable without you.

Abbreviations

AC	Articular cartilage
ACAN	Aggrecan gene
AFM	Atomic force microscopy
ALK	Activin-like kinases
Amp	Ampicillin
BMP2	Bone morphogenetic protein 2
BMP9	Bone Morphogenetic protein 9
BrdU	Bromodeoxyuridine
cDNA	Complementary DNA
CM	Chloramphenicol
COL2	Type II collagen gene
CON	Control
CS	Chondroitin sulphate
DAPI	(4', 6-diamidino-2-phenylindole) – nuclear stain
DDW	Double distilled water
DM	Dorsomorphin
DMEM	Dulbecco's modified Eagles media
DMEM-HG	Dulbecco's modified Eagles media – High Glucose (4.5g/L)
DMMB	Dimethylmethylene blue assay
DMSO	Dimethyl sulphoxide
DNA	Deoxyribonucleic acid
DNase	Deoxyribonuclease
Dox	Doxycycline
DPX	Distyrene, plasticizer, and xylene synthetic resin mounting media
DTT	Dithiothreitol
ECM	Extracellular matrix
EDTA	Ethylenediaminetetraacetic acid
ENG	Endoglin
FBS	Foetal bovine serum
FCC	Frozen competent cells
FGF2	Fibroblast Growth Factor 2
FT	FGF2 and TGFβ1
GAG	Glycosaminoglycan
Gal	Galactose
GDF	Growth differentiation factor
HA	Hyaluronan
HCL	Hydrochloric acid
HEPES	4-(2-Hydroxyethyl)Piperazine-1-Ethanesulfonic acid
HHT	Hereditary haemorrhagic telangiectasia
Hr	Hour
IM	Immature
ITS	Insulin transferrin selenium
KL	Kellegren Lawrence scale
LB Broth	Lysogeny broth
LOX	Lysyl oxidase
m	Minutes
MA	Mature

MAPK	Mitogen-activated protein kinase
ML	ML347 Inhibitor
MMP	Matrix metalloproteinase
NaOH	Sodium hydroxide
NBFS	Neutral buffered formalin solution
NTC	No template control
OA	Osteoarthritis
PBS	Phosphate buffered saline
PCR	Polymerase chain reaction
PD	PD166793 inhibitor
PG	Proteoglycan
PLA	Poly(lactic acid)
PLM	Polarised light microscopy
PRG4	Proteoglycan 4/lubricin
PSR	Picrosirius red
RM	Reaction mixture
RNA	Ribonucleic acid
RNase	Ribonuclease
RT	Room temperature
RT-qPCR	Reverse transcriptase - quantitative polymerase chain reaction
SMAD	Suppressor of mothers against decapentaplegic
SOB	Super optimal broth
SOC	Super optimal broth with catabolite
TBE	Tris – borate – ethylenediaminetetraacetic acid
TBS	Tris-buffered saline
TBS-T	Tris-buffered saline – with 0.1% v/v tween20
TE	Tris-ethylenediaminetetraacetic acid
TGFβ	Transforming growth factor beta
TGFβ1	Transforming growth factor beta 1
TIMP	Tissue inhibitor of metalloproteinases
Wnt	Wingless-related integration site

Chapter 1: Introduction

1.1 Why study articular cartilage maturation?

Articular cartilage is a highly specialised tissue that lines the bones of synovial joints, responsible for protecting joint surfaces from cyclic mechanical loads. To provide sufficient protection cartilage tissue adopts a highly organised architecture of cells and extracellular matrix (ECM) components in response to mechanical loading. Juvenile articular cartilage is a thick, soft tissue, isotropic in structure. Through the process of postnatal maturation cartilage adopts a zonal anisotropic organisation, containing collagen fibres aligned parallel to the surface in the superficial zones transitioning to perpendicularly aligned fibres within the mid and deep zones (Clark et al., 1997). Distinct zonal changes in chondrocyte morphology can also be observed, increasing in size and circularity with depth. These zonal changes in collagen and chondrocyte organisation are crucial to mature cartilages superior biomechanical properties (Williamson et al., 2003).

Repair of cartilage tissue through tissue engineering strategies under the umbrella of regenerative medicine provides a potential solution for treating OA. Currently stem cells are used as they provide an economically viable option to generate cartilage tissue. However, there is a limited understanding of the mechanisms that lead to the formation and postnatal development of structurally mature cartilage. Any tissue constructs that lack the unique zonal architecture of mature cartilage are destined to fail (Hunziker, 2009). Therefore, it is important to understand the mechanisms modulating joint formation and maturation to engineer successful tissues.

The zonal structure of articular cartilage degenerates when articular cartilage is damaged especially when diseased. Osteoarthritis (OA) is the most prevalent musculoskeletal disease, resulting in pain and loss of joint function. It has been identified as the 11th leading global cause of physical disability (Cross et al., 2014). Knee OA is the most common type of arthritis effecting 3.8% of the population globally. It is the predominant cause of knee replacements, accounting for 97% of prosthetic replacements in the UK (Chen et al., 2012). Interestingly incidence rates are disproportionally higher for females 4.8% than males 2.8%, but both are projected to increase due to demographic trends due to increased longevity (Cross et al., 2014).

Osteoarthritis places a large burden on the health system due its high incidence rates. The Royal British Collage of GPs estimated that in 2006 over 1 million adults had GP appointments for OA related issues (Chen et al., 2012). The UK Arthritis Research Council estimated in 2002 that 4.4 million patients suffered from hand arthritis, 550,000 from knee OA, and 210,000 from hip OA. Financially the costs relating to the treatment of OA are direct through treatment or indirect expenditure on for example community health services and loss of income. In the UK alone direct costs of hip and knee replacements were estimated at £850 million with indirect economic impacts estimated to reach a loss of up to £3.2 billion (Chen et al., 2012). A similar French study conducted in 2002 estimated that the direct costs of OA treatment in Europe exceeded 1.6 billion euros, covering 80,000 hip replacements and 38,000 knee replacements, with over 13 million hospital admissions relating to OA treatments (Le Pen et al., 2005).

The financial burden on the health system is only expected to worsen with increasing obesity and ageing populations having a serious effect on OA incidence in the future. Between 2001 and 2018 OA incidence increased by 2.9% and 3.8% for knee and hip OA per year. In this period there was a total of 3.14 million patients with OA symptoms with a significant rise in

OA of younger adults below the age of 65 (Morgan et al., 2019). In the UK OA incidents are projected to reach 96,000 hip replacements and 119,000 knee replacements by 2035. The increase in treatments is mostly driven by increasing trends in obesity and an ageing population (Culliford et al., 2015).

Therefore, it is critical to develop more effective treatment methods to ease the burden OA poses on the health system. To develop more effective treatment methods the underlying mechanisms of joint formation and homeostasis must be applied. In particular, increasing our understanding of the postnatal transition of immature cartilage to a highly structured, stiff and durable joint surface is critical to developing tissue-engineered implants and drug treatments to repair and regenerate damaged joints.

1.2 Synovial joint physiology

Synovial joints are the most common type of joint in the musculoskeletal system, consisting of a fluid-filled cavity surrounded by articular cartilage and a fibrous capsule lined by the synovium. Joints of the musculoskeletal system are defined by their range of motion; fixed (synarthrosis), partially movable (amphiarthroses), or freely movable (diarthrosis).

The fibrous capsule that surrounds the synovial joint is composed of tendons and ligaments forming two distinct layers, a dense fibrous outer layer and an inner membrane. Each has unique roles; the outer fibrous layer provides the mechanical structure of the synovial capsule, supported by larger external ligaments. The inner synovial membrane is responsible for supplying the synovial fluid with nutrients and key molecules such as hyaluronan and lubricin also known as proteoglycan type 4 (PRG4), essential for normal joint function. Synovial fluids provide the joint surfaces with the lubrication required for almost frictionless articulation.

The key lubricating factors in synovial fluid, lubricin and hyaluronan, are produced by synoviocytes and chondrocytes. Furthermore, synovial fluid is responsible for the transportation of nutrients and waste from the synovial membrane to the tissues of the inner synovium, including the transportation of oxygen and the removal of waste metabolites. It is the primary nutrient supplier of articular cartilage as calcification of deep zone cartilage prevents nutrient flow from below the tissue (Hui et al., 2012). Synovial fluid also contains tissue remodelling enzymes such as matrix metalloproteinases (MMPs) and a family of extracellular proteases with a disintegrin and metalloproteinase with thrombospondin motifs (ADAMTS) secreted by Type-A synoviocytes involved in the processes of tissue remodelling.

The ends of skeletal bones in synovial joints are covered by articular cartilage a type of connective tissue known as hyaline cartilage, responsible for protecting the end plates of bones, allowing frictionless articulation and transmission of forces through the skeleton (Haywood & Walsh, 2001). Hyaline cartilage is an avascular tissue unlike the other tissues lining the synovial cavity with unique biomechanical properties required for it to protect bone from compressive and shear loads. Together the different tissue types of a synovial joint collaborate to function effectively as a singular joint system. The formation of multiple tissue types within a single joint structure requires complex signalling and a highly controlled mechanism.
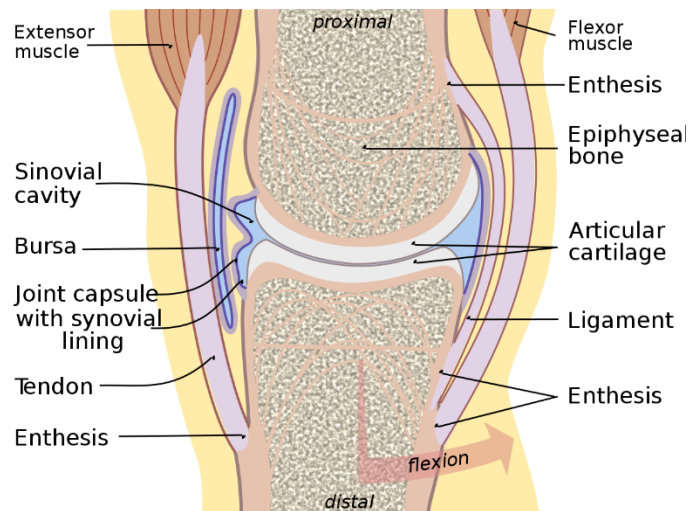
Figure 1. Structural anatomy of a synovial knee joint. Image source: (al Kabbani, 2019)

1.2.1 Synovial joint formation

Joint formation is a multi-step process which requires complex signalling pathways. Initially the bones of a developing limb are formed of continuous uniform mesenchymal condesations. Joint formation begins with the determination of the joint site within the mesenchymal condensations by expression of overlapping genetic factors, followed by the appearance of a denser region of planar mesenchymal cell condensations at the predetermined joint sites. Within these distinct mesenchymal condesations the interzone forms consisting of three regions that will become the joint. After the interzone has been established cavitation of the interzones central region occurs accompanied by the production of synovial fluid. Finally, morphogenesis of the opposing joint surfaces produces complementary structures. Some of the key signalling factors involved in joint formation include growth and differentiation factor 5 (GDF5), *wingless* (wnt), *Indian hedgehog* (IHH), *bone morphogenetic protein* (BMP), *transforming growth factor β* (TGFβ), and *fibroblast growth factor* (FGF). The timing of joint development varies based on location: forelimb preceding hindlimb, and proximal joints before distal. In humans the process of synovial joint formation occurs during embryonic and feotal development between gestational weeks 7-14. Cavitiaiton occurring during weeks 9-11 (Mérida-Velasco *et al.*, 1999; Chijimatsu and Saito, 2019).

1.2.2 Joint site determination

Joint site determination is the first step in joint formation, little is known about which genetic factors pattern the location of joint formation. Several studies have identified potential genes involved in the process. Homeotic genes *Hox a* and *d 9-13* are responsible for patterning during limb formation and have been hypothesised to determine joint locations along the limb where gene expressions overlap, however, this has never been substantiated (Meyerowitz, 1991). *Noggin,* a bone morphogenetic protein (BMP) antagonist, is another potential gene involved in joint site determination. Studies using *Noggin* knock-out mice produce cartilaginous limbs lacking joints, implicating its activity in joint patterning (Brunet et al., 1998).

1.2.3 Interzone formation

Formation of the interzone is the first visible stage in joint formation, chondrocytes of the cartilaginous anlagen are interrupted by condensed flat mesenchymal cells at the presumptive joint site (Decker et al., 2015). Work by Hartmann and Tabin (2001) identified *wnt14* (now known as wnt9) as a factor initiating interzone formation in joints and also ectopic interzone formation in chick limbs. The interzone can easily be distinguished by a central region of dense cells flanked by two lighter, less dense regions which are co-incident with *GDF5* expression. The denser intermediate region of the tissue goes on to form articular chondrocytes and permanent cartilage, whilst the flanking regions are destined to participate in the early phases of endochondral ossification during skeletal development (Hyde et al., 2008). Interzone cells have been shown to form other structures within the joint, specified later in the development process contributing to structures such as the synovial lining, ligaments and other internal tissues.

1.2.4 Cavitation

Cavitation of the interzone is the process that leads to the physical formation of the synovial cavity at the location of the joint. There are multiple different theories for how the process of cavitation occurs. Some of the leading studies suggest that cell death is responsible for the formation of the cavity (Abu-Hijleh et al., 1997; Mitrovic, 1978). Others have suggested that cell death is unimportant, and that collagen fibril reorganisation, accumulation of hyaluronan (HA), and muscle-driven separation of the opposing tissue surfaces form the cavity (Dowthwaite et al., 1998; Ito & Kida, 2000). Pacifici (2005) theorised that it is likely to be a combination of both cell death and ECM accumulation and reorganisation. Initially, cell death occurs within the interzone to a very limited number of cells forming a gap, followed by the reorganisation of the collagen matrix flanking the new joint site. An accumulation of HA and potentially lubricin localised to the cells of the intermediate zone leads to further tissue degradation filling the cavity, lubricating it for further separation. Finally, physical separation of the joint surfaces is achieved mechanically by muscle contraction (Pacifici et al., 2005).

1.2.5 Morphogenesis

Morphogenesis is the final and least understood stage of joint formation. During morphogenesis the two joint surfaces change in shape forming complementary structures. Current explanations suggest that cells of the distal side undergo differentiation and hypertrophy to form a convex shape whilst the proximal joint cells proliferate at the periphery forming a concave surface (Pacifici et al., 2005).

1.2.6 Signalling during joint formation

Although little is known about the cell fates and lineages of the interzone there is abundant data on the signalling mechanisms required. Many members of the TGFβ superfamily participate in interzone and joint formation: BMP2 and -4, GDF5 and -6, *Wnts4/-14/-16, chordin* and *noggin* signalling factors have all been identified in the process of joint formation. Additionally, some members of the FGF signalling family FGF2/-4/-13 modulate early joint formation. GDF5 is one of the key signalling factors in early joint formation, expressed by mesenchymal cells located in the interzone, recruiting cells to the interzone and inducing differentiation of chondrogenic cells. Reduced expression of GDF5 results in

joint defects, and over-expression causes increased cartilage growth and joint fusion (Storm & Kingsley, 1996, 1999). *Wnt14* is another gene expressed in the early stages of interzone formation as an upstream regulator of GDF5 expression, shown to inhibit chondrogenesis (Hartmann & Tabin, 2001). On the otherhand *Noggin*, *chordin*, and BMP2 growth factors define the location and boundaries of the interzone once it has been formed.

Noggin expression localises to the epiphysial chondrocytes of the long bones, preventing early differentiation of mesenchymal cells into chondrocytes. Studies have shown a loss of *Noggin* expression results in a loss of joint formation. Indian hedgehog (*Ihh*) has a similar function to noggin maintaining the mesenchymal cell phenotypes of the interzone, regulating proliferation and differentiation of chondrocytes located in developing joints. Loss of Ihh signalling in double knockout mice produces uniterurupted digits failing to develop joint cavities as prehypertrophic chondrocytes undergo abnormal hypertrophy and differentiation (Bechtold *et al.*, 2019).

1.3 Articular cartilage

1.3.1 Overview of articular cartilage

Articular cartilage (AC) is a highly specialised tissue with the sole purpose of protecting bones from the forces that synovial joints are exposed to. AC is a type of hyaline cartilage characterised by its low cellularity and avascular structure giving it a translucent glassy appearance, hence its description as hyaline (*Gr. Hualos,* glass). AC is composed mostly of water making up 80% of the tissues wet weight, the remaining weight is composed of 10-15% collagen, and 5% proteoglycan (Cohen et al., 1998). Cartilage contains only one cell type called a chondrocyte which is responsible for maintaining the ECM and controlling tissue remodelling. AC is typically segregated into three distinct zones based on cellular morphology, the superficial zone occupying 0-10% of the tissue volume, the mid or transitional zone 10-20%, and the deep or radial zone 80% (Hunziker et al., 2002; Wong et al., 1996). Below the deep zone lies the calcified cartilage and subchondral bone plate, delineated by the tidemark where articular and calcified cartilage interface. The proportion each of the zones forms of the overall tissue varies between animals, in many models the ratios of 0-10%, 10-40% and 40-100% are used for superficial, transitional and deep (radial) zones respectively (Hunziker 1992, Sophia Fox et al., 2009).

1.3.2 Cartilage zones

The superficial zone forms the surface of AC, it contains the highest concentration of water and lowest concentration of proteoglycans of the three zones, making it softer and able to deform under compressive forces to absorb the initial shock during cyclic compression. Chondrocytes within the superficial zone have a flattened discoid morphology and the highest cell density of all the zones, usually found as single cells or doublets (Bush & Hall, 2003; Poole, 1997). However, dependent on the type of joint, planar-oriented chodron clusters have been observed in the superficial zone (Schumacher et al., 2002). Collagen fibres within the superficial zone are relatively thin, 40-60nm in diameter, running parallel to

the surface of the tissue and are aligned in this way to provide mechanical resistance to the shear forces that the cartilage surface is exposed to (Clark et al., 1997).

The mid or transitional zone lies just below the superficial zone, chondrocytes in this zone are not as densely populated and slightly more circular in shape, elongated along their long axis in an oblique orientation to the surface. Collagen fibres of the mid zone are also orientated in an oblique fashion to the surface transient to the parallel superficial fibres above and perpendicular fibres below. Due to the transitional nature of these fibres, they are less organised in structure and are slightly larger in diameter than those of the superficial region (Poole, 1997). Increases in collagen fibril diameter, content, and proteoglycan content are present in the midzone relative to the superficial, however, water content is reduced.

The deep or radial zone accounts for the remaining cartilage tissue up until the tidemark. The deep zone has the highest proteoglycan content and lowest water content of the three layers providing the tissue with increased mechanical stiffness due to reduced osmolarity and increased hydrostatic pressure. Cells within this region are the largest and more circular in morphology, slightly elongated along their long axis perpendicular to the surface. Chondrocytes are arranged into vertical columns in alignment with the collagen fibrils orientated perpendicular to the cartilage surface (Poole, 1997). Collagen fibrils are thickest within this zone and continue to increase in diameter with depth (Clark et al., 1997).

A layer of calcified cartilage and the subchondral bony plate lie below the upper three zones transitioning from cartilage tissue into the underlying trabecular bone. Collagen fibres of the deep zone extend down into the subchondral bone providing an interface between the two main types of skeletal tissue. During endochondral ossification, type X collagen is synthesised by hypertrophic chondrocytes which facilitates calcification and mineralisation; a remnant of this epiphyseal growth remains as the calcified layer.

1.3.3 Extracellular matrix regions

The ECM of articular cartilage is delineated by three regions based on composition and proximity to the chondrocytes. The thinnest of these regions is the pericellular matrix (PCM) which surrounds the chondrocyte cell membrane; together the pericellular matrix and chondrocyte form the chondron (Hughes et al., 2005; Poole, 1997). It is mostly composed of proteoglycans e.g. biglycan and decorin, glycoproteins and type VI collagen. Type VI collagen is only found in the PCM of healthy articular cartilage (Poole et al., 1988). The main function of the pericellular matrix is to transmit signals from the ECM to the chondrocytes in response to mechanical load and changes in ECM composition (Guilak et al., 2006). This is possible through type VI collagen's interaction with aggrecan and type II collagen of the territorial and interterritorial matrices (Wiberg et al., 2003). Secondary to its mechanotransductive capabilities the PCM provides the chondrocyte with a protective layer and a storage site for sequestered growth factors (Macri et al., 2007).

The territorial matrix of articular cartilage surrounds the PCM and is slightly thicker, comprised of proteoglycans (mainly aggrecan) and type II collagen. It provides a protective capsule for the chondron from greater mechanical forces than the PCM is capable of withstanding. Type II collagen fibres of the territorial matrix are relatively thin, and most are aligned parallel to the surface of AC (Poole et al., 1984; Servin-Vences et al., 2016; Sophia Fox et al., 2009).

The interterritorial matrix (IM) forms the third and final region in AC, it is the thickest of the three regions containing large type II collagen fibres and aggregating proteoglycans, contributing to the biomechanical resistance to compression. The concentrations of type II collagen, aggrecan and water of the interterritorial matrix vary depending on the zone. Type II collagen fibres have different orientations, diameters and levels of anisotropy dependent on which zone they are located in, forming arcade-like structures (Benninghoff, 1925).

1.3.4 Postnatal maturation of cartilage

Immature articular cartilage is thicker, more elastic and lacks the complex compositional and structural architecture of adult cartilage. It is only through the process of postnatal maturation that immature articular cartilage adopts the cellular and compositional architecture of adult cartilage.

During cartilage maturation distinct changes in chondrocyte organisation and morphology occur that distinguish the two types of tissue. Immature cartilage has a relatively high cellular density in the superficial region of the tissue compared to mature tissue (Williamson et al., 2003). Within the superficial zones of mature cartilage cells have a planar orientation found within the first 50μm of tissue, in immature tissue the presence of discoid cells is limited to a much shallower depth, marking a thinner superficial layer and an earlier progression into the transient zone (Jadin et al., 2005). The mid and deep zones of immature cartilage retain the same cellular density and organisation, whereas in mature tissue chondrocytes of the deep zone are sparser, forming distinctive cellular columns that are used to differentiate between the mid and deep zones of mature cartilage (Jadin et al., 2005). Chondrocytes of the deeper zones are more spherical in immature cartilage compared to the elongated chondrocytes of mature tissue (Clark et al., 1997)

Throughout postnatal maturation the ECM of cartilage also undergoes compositional and organisational changes. In the early stages of postnatal maturation there is an increase in collagen content, type II collagen fibres increase in diameter and density. However, no significant changes in collagen content occur during the later stages of maturation. (Blaschke et al., 2000; Williamson et al., 2001, 2003). In addition to compositional changes, collagen undergoes structural changes, transitioning from an isotropic organisation in immature cartilage, with most sub-superficial zone fibres orientated parallel to the surface, to an anisotropic structure containing perpendicularly aligned fibres (van Turnhout et al., 2010). The collagen matrix of mature tissue forms leaf-like structures known as "Benninghoff arcades", which transition from parallel fibres at the surface to perpendicularly arranged fibres within the deeper zones (Benninghoff, 1925). This change in collagen organisation is a key hallmark of cartilage maturation (van Turnhout et al., 2010).

Proteoglycans are the second most abundant ECM component within cartilage, responsible for controlling the influx and efflux of water due to its negative charges. During postnatal maturation the concentration of proteoglycans in articular cartilage decrease relative to the tissues wet weight (Williamson et al., 2003). The changes in cartilage composition and organisation during postnatal maturation result in a stiffer tissue capable of withstanding greater mechanical loads.

1.3.5 Biochemical composition of cartilage

1.3.6 Collagen

Collagen is the most abundant protein in articular cartilage accounting for 60% of the total dry weight. Type I, II, III, VI, IX, XI collagen can all be found in articular cartilage. However, type II collagen is the most abundant member comprising 90% of all the collagens located within the tissue. Type II collagen is a triple helical homodimer and heteropolymer containing minor amounts of collagens IX and XI, required for microfibril formation and regulating fibril diameter (Blaschke et al., 2000). Type II collagen forms a staggered polymer crosslinked by lysyl oxidase (LOX) enzymes (Holmes et al., 2001; Wu et al., 1992). The remaining collagens found in cartilage play very minor roles within the tissue. Type III Collagen is capable of crosslinking with type II collagen, type VI collagen is found in the pericellular matrix regulating chondrocyte signal transduction (Young et al., 2000). Whilst type X collagen is only found within the mineralised tissue of the calcified cartilage at the sites of endochondral ossification (Watt et al., 1992).

Collagen is synthesised by the chondrocytes as preprocollagen with propeptide domains at either ends of the peptide chain. The peptides form hydrogen interactions between individual chains producing a triple-helix structure called tropocollagen. It is only after the formation of the triple helixes that the propeptides are removed allowing multiple tropocollagen to interact and self-assemble into microfibril, larger microfibrils are cross-linked intra- and inter-molecularly by LOX enzymes (Rich & Crick, 1955).

Type II collagen fibres in adult cartilage form Benninghoff arcades or leaf-like structures, horizontal in the superficial zone transitioning to become vertical fibres in the deep zones, increasing in diameter with depth (Benninghoff, 1925; Notzli & Clark, 1997). In addition to their primary function to provide the ECM with structural integrity collagen fibres also interact with the proteoglycans of AC, acting as a mesh to lock them into the tissue and resist their swelling potential which provides articular with its hydrostatic biomechanical properties.

1.3.7 Proteoglycans

Proteoglycans make up 10-15% of the wet weight of cartilage, they are formed of a core protein with covalently bound glycosaminoglycans. In cartilage, the proteoglycans aggrecan, lubricin, decorin, and biglycan are required for normal cartilage function. Aggrecan is the largest and most common of the proteoglycans found in cartilage. It is composed of a core protein, a linker region and hundreds of chondroitin sulfate and keratin sulfate side chains. Aggrecan interacts with hyaluronan sugar chains (HA) via link proteins forming large aggregates with negatively charged chondroitin and keratin side chains which form electrostatic interactions with water (Sophia Fox et al., 2009). The interactions between aggrecans side chains and water provide cartilage tissue with its hydrostatic properties enabling it to withstand compressive forces. With increasing depth in cartilage, the concentration of aggrecan increases and so does the negative charge density, reducing the permeability of the tissue making it stiffer (Maroudas, 1968).

Smaller proteoglycans lubricin, decorin and biglycan are required for normal cartilage function. Decorin and biglycan are much smaller than aggrecan, containing dermatan sulfate side chains which participate in collagen fibre formation. Decorin forms interactions with type II collagen whereas biglycan is involved in type VI collagen interactions within the pericellular matrix. Lubricin, also known as superficial zone protein or proteoglycan four (SZP, PRG4) is expressed within the superficial regions of articular cartilage its main function, as its name suggests, is to lubricate the surfaces of the synovial joint to form a low friction bearing surface.

1.3.8 Water

Water accounts for 80% of cartilages wet weight, decreasing in concentration with depth, from 80% within the superficial zone to 65% within the deeper zones. The water content of cartilage is located within three different regions of the tissue. The majority is found in the ECM pores, with lower concentrations found interacting with the collagen intrafibrillar space or contained within chondrocytes. The water in the interfibrillar space interacts with the negative charge densities of the proteoglycans within the tissue, preventing through-flow, giving cartilage a low permeability and high osmotic pressure, allowing it to withstand large compressive forces (Sophia Fox et al., 2009).

1.3.9 Chondrocytes

Chondrocytes are the singular cell type found in cartilage, they are responsible for the development, maintenance, and remodelling of the ECM. In articular cartilage chondrocytes are most abundant in the superficial zone where they have a discoid shape, reducing in number and increasing in size towards the deeper zones (Hunziker et al., 2002). Due to the avascular nature of cartilage chondrocytes are capable of synthesising ECM components within an environment of low oxygen tension and nutrient supply (Stockwell, 1978). Chondrocytes produce a unique pericellular microenvironment formed of a fluid-filled capsule surrounded by dense type VI collagen (Poole et al., 1988). The chondrocyte, pericellular matrix, and fibrillar pericellular capsule delineating the chondron from the surrounding territorial matrix form a singular chondron unit. These chondron units can be found alone or as doublets, triplets, and columns (Poole, Flint and Beaumont, 1984; Poole, Ayad and Schofield, 1988; Chang and Poole, 1996; Poole, 1997). Integrins contained within the chondron mediate signal transduction between chondrocytes and the surrounding ECM, relaying information in response to changes in ECM composition and mechanical forces (Gao et al., 2014)
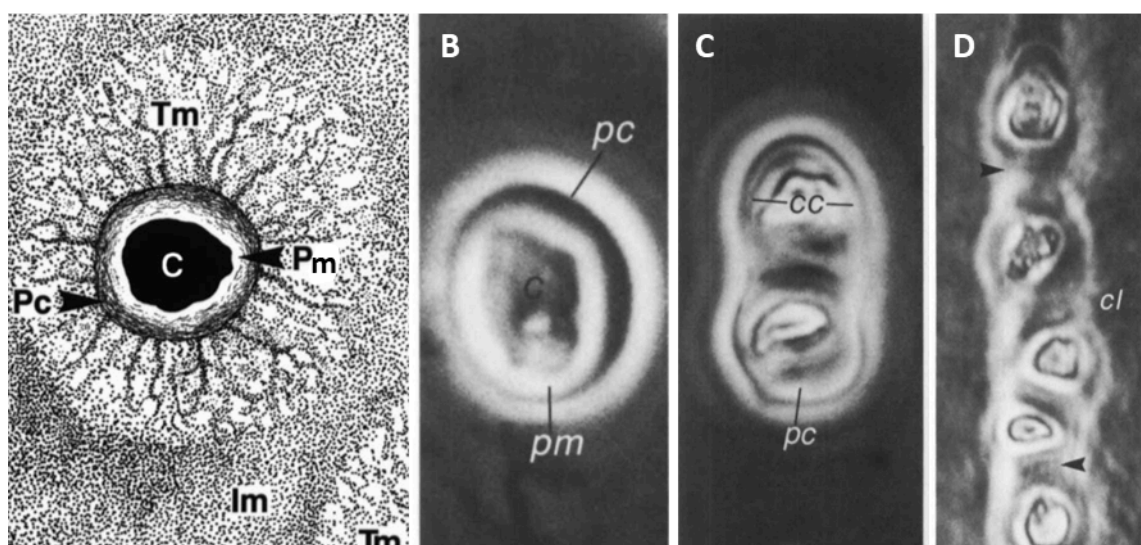
Figure 2. Structure of a chondron, A Diagram of a singular chondron unit consisting of the Chondrocyte (c), Pericellular matrix (Pm), and Pericellular capsule (Pc). Surrounded by but not including the Territorial matrix (Tm) and Interterrritorial matrix (Im). **B** Singular chondron unit, **C** Chondron douplet formed of two chondron units, **D** Chondron column containing 5 individual chondron units. Figure source (Poole, Ayad and Schofield, 1988)

1.4   Osteoarthritis

OA is the most prevalent musculoskeletal disease globally, characterised by degradation and eventual destruction of articular cartilage. OA develops as a byproduct of adverse biomechanical forces applied to a susceptible joint, age being the most significant risk factor for the onset of OA. It is a complex condition that effects the whole joint, resulting in the complete destruction of the cartilage tissue and is generally accompanied by episodic inflammatory flares. Loss of the articular cartilage layer from the joint results in symptomatic tenderness, pain, and a loss of mobility in the effected joint.

1.4.1   Diagnosis

X-ray radiography is the most common clinical practice for diagnosing OA. Initially Kellegren and Lawrence (KL) developed a classification system for grading the severity of OA in effected patients. The KL scale grades OA from 0-4 increasing in number with severity based on the presence of osteophytes, joint space narrowing, and abnormal bone structure observed in radiography images (Kellgren & Lawrence, 1956). However, the KL grading system has limitations, assuming that OA pathology always progresses in the same linear manner. Since the development of KL scale many other grading systems have been developed and hence there is no single universal recognised grading system (Galli et al., 2003; Hefti et al., 1993; Scheller et al., 2001; Yan et al., 2018). MRI imaging is now used alongside X-ray radiography when diagnosing OA as it provides higher resolution images of the joint tissues (including soft tissues that cannot be seen by X-ray) allowing earlier detection and treatment (Stolz et al., 2009). Lab studies have shown that OA can be detected before macroscopic changes in tissue by using nanoprobe atomic force microscopy (AFM), however, it is not possible to perform nano AFM clinically.

1.4.2   Pathogenesis

Early diagnosis of osteoarthritis is hard as the changes that occur during early onset are only detectable on a nano-level. Initially there is a loss of proteoglycan content from the cartilage surface inducing an uptake of water and swelling of the tissue. Eventually, as OA proceeds the collagen matrix is affected, resulting in a decrease in content and loss of structural organisation (fibrillation). The breakdown of cartilage tissue is catalysed by matrix metalloproteinases (MMPs) and ADAMTS4, -5. MMP13 is the predominant enzyme activated in OA expressed by hypertrophic chondrocytes located within cartilage. However, MMP1, which like MMP13 is a collagenase, is also expressed by the cells of the synovium and released into the synovial fluid causing cartilage surface degradation (Mehana et al., 2019). In OA the other joint tissue are also affected, the subchondral bone undergoes features of early developmental changes reminiscent of endochondral ossification, increasing in vascularity and resorbing some of the cartilage layer, raising the tidemark. Also synoviocytes undergo a reduction in the synthesis of lubricin and hyaluronan into the synovial space affecting lubrication and reducing the frictionless movement of the joint.

1.4.3   OA treatment

Treatment methods for OA range from basic lifestyle changes to advanced surgical and regenerative methods, however all treatments to date are limited in their success due to the

degenerative nature of the disease. For minor OA cases weight loss and exercise can reduce symptoms by increasing muscle strength of effected joints and restoring motility, ensuring patients are exercising regularly is becoming increasingly important as obesity rates are increasing (Thomas et al., 2002). With increasing severity and symptoms non-steroidal anti-inflammatory drugs (NSAID) or opioid anti-inflammatory drugs are used to treat the pain associated with OA but don't prevent further degradation of the joint tissue. Alternatively, treatment of OA tissue using matrix metalloproteinase (MMP) inhibitors such as doxycycline are used to reduce further progression of articular cartilage breakdown with moderate success, however they provide little to no improvement in symptoms (Rutjes et al., 2009). Slightly more invasive treatments such as hyaluronic acid injections into the affected joints to increase joint space separation and lubrication can provide longer-term pain relief and limited improvement in joint function (Bellamy et al., 2006). For severe OA cases surgical treatment methods are often required to correct joint alignment and movement, easing stress and reducing the pain associated. In extreme circumstances transplantation of osteochondral plugs from unaffected areas of the joint are implanted into focal areas of cartilage degradation or total joint replacements, arthroplasty, is required (Bedi et al., 2010). All of the traditional treatments covered only provide a temporary solution to the problem with a lifespan of up to 20 years before requiring additional treatment (Tübingen, 2011). They are limited with respect to the fact that they are preventative measures none of which are restorative. Thus, it is important to develop treatments that can restore the architecture of cartilage tissue with the correct mechanical and structural qualities required to recapitulate normal joint function. Regenerative medicine offers a unique opportunity to develop treatment methods able to restore artefacts of normal joint cartilage tissue to improve function and relieve pain. Regenerative methods focus on the use of cell culture, 3D scaffolds, and growth factor stimulation to generate more effective treatments than the traditional methods used.

1.4.4 Regenerative medicine approaches

Early regenerative techniques used microfracture surgery to induce cartilage regeneration of full-thickness defects in the hope of releasing chondroprogenitors from the subchondral bone, which in turn differentiate into chondrocytes and synthesise new tissue. However, micro-fracture techniques produce fibrocartilage, limited by its weaker mechanical properties (Bedi et al., 2010; Franke et al., 2007). Autologous chondrocyte cultures have also been used since the mid 1980s, reimplanting cell masses into focal lesions up to 10cm's in diameter (Brittberg et al., 1994). Early autologous regenerative treatments had little improvement over a 5-year review period compared to standard microfracture methods (Vanlauwe et al., 2011). In recent years the development of scaffolds, matrix-assisted chondrocyte implantation (MACI), have been used in clinical treatments to improve cartilage regeneration. Collagen based scaffolds used in combination with micro-fracture promote cartilage regeneration or are used to secure autologous chondrocytes to focal defects (Crawford et al., 2009; Gille et al., 2013). Alternatively, hydrogel scaffolds developed for direct injection into microfracture sites have shown the potential to promote osteogenesis and chondrogenesis, characterised by type II collagen and proteoglycan synthesis, with the added benefit of being biodegradable (Gomoll, 2012). Chondrocytes cultured *ex vivo* and seeded in hyaluronan-based scaffolds for implantation have also been found to improve type II collagen and proteoglycan synthesis. The scaffolds themselves providing the ideal environment for chondrocyte differentiation (Grigolo et al., 2002). Through further development of scaffolds and regenerative techniques better treatments will be developed.

Rather than using autologous chondrocytes that are limited in number and proliferative capabilities mesenchymal or induced pluripotent stem cell (MSC, IPSC) approaches have also been developed to obtain autologous chondrocytes through directed differentiation cultures. MSCs can be obtained from bone marrow, articular cartilage, synovium, or adipose tissue. MSCs obtained from the synovial lining have been shown to have the best potential for differentiating into chondrocytes compared to alternative sources (Sakaguchi et al., 2005). These MSC based treatments have been shown to match the effectiveness of chondrocyte-based allografts (Mollon et al., 2013). Alternatively Embryonic stem cells (ESCs) can be used. ESCs are pluripotent in their nature, able to differentiate into many cell linages with an unlimited potential to replicate, but they can only be obtained from embryos. Thus, IPSCs are the preferred choice which can be used for similar tissue engineering techniques as MSCs and normal chondrocytes via directed differentiation (Takahashi & Yamanaka, 2006). One example of an MSC based approach used bone marrow MSCs seeded into collagen-based sheets for implantation into chondral defects, however symptom improvements were limited (Fomby et al., 2010).

The application of growth factors to cell cultures or tissue scaffolds have been used to improve the viability of the cell or tissue prior to implantation, improving long-term effectiveness. Growth factors are used when differentiating MSC and IPSCs into chondrocytes for use in regenerative treatments. Using improved differentiation and regenerative methods will provide cell types with a more specific/desired phenotype. This will attribute the cell with certain phenotypic markers qualifying it for enhanced cartilage tissue regeneration. Growth factors are also used when culturing tissue constructs to stimulate cell functions that improve the quality of the tissue. This includes the upregulation of ECM components such as type II collagen or proteoglycans in the case of articular cartilage production. Alternatively, growth factors have been used to help supplement current surgical treatments via direct application to effected joints during micro-fracture or osteochondral transplants. By understanding these growth factors involved in normal cartilage more effective tissue-engineered treatments can be developed.

1.4.5 Disadvantages of tissue-engineered constructs

The current gold standard in cartilage repair is osteochondral transplantation, but this is not a scalable method. Therefore, regenerative medicine offers the ability to use stem cells to generate a transplantable tissue. However, as stated above the production of cartilage is inferior biomechanically and morphologically (Bedi et al., 2010; Franke et al., 2007). Therefore, it is logical that we must understand how the transition from immature to mature cartilage occurs so that we can produce cartilage implants that are able function in a challenging biomechanical environment with cyclic loads of 1MPa as found in adults.

The literature is full of studies that describe the differences between the two postnatal developmental states of articular cartilage however no-one has been able to study the key stimuli and changes that drive postnatal maturation. To date the favoured explanation for the induction of postnatal maturation is that biomechanical cues provide the inducing stimuli, and this has led to the thought that conditioning tissue-engineered cartilage with cyclic loading will generate mature adult articular cartilage (Carter et al., 2004; Houard et al., 2013). Recently, it has become clear that aspects of postnatal maturation can be induced through growth factor stimulation of immature articular cartilage (Khan et al., 2011; Zhang et al., 2017). These studies have shown that the combination of FGF2 and TGF-β1 induce biochemical, morphological, and biomechanical changes consistent with maturation of immature articular cartilage. In the latter study no significant changes in collagen alignment

were noted. However, the same authors discovered that BMP9 (GDF2) also induces key changes associated with postnatal maturation specifically changes in collagen alignment rendering them perpendicular to the surface fibrils (Morgan et al., 2020). Therefore, as BMP9 appears to induce an earlier phase of maturation it provides an ideal model system to study how changes in collagen alignment occur.

1.5   BMP9

Bone morphogenetic protein 9 also known as growth differentiation factor 2 belongs to the TGFβ superfamily along with many other growth factors involved in skeletal development. BMP9 is one of the least studied members of the TGFβ superfamily with known osteogenic and chondrogenic capabilities making it an ideal molecule for further study as a musculoskeletal regeneration therapeutic.

BMPs were first discovered by Dr Marshal Urist in the 1960s and subsequently 22 different BMPs have been identified (Urist & McLean, 1965). However not all BMPs belong to the TGFβ superfamily, BMP1 doesn't fit into this category as it is a MMP and not a growth factor (Kessler et al., 1996). Most BMPs were identified due to their osteogenic or chondrogenic properties during bone formation or related skeletal developmental processes. Out of the BMPs discovered to date BMP2,-4,-6,-7 and -9 have the most osteogenic potential, with BMP9 surpassing the rest. The reason for its elevated osteogenic capacity is not yet fully understood but has been hypothesised to related with its high affinity for activin-like kinase receptor 1 (ALK1) and its immunity to BMP antagonists BMP3 and Noggin (Kang et al., 2004). In addition to its osteogenic and chondrogenic capabilities BMP9 signalling is required through-out the body as an angiogenic factor involved in vascular quiescence and cardiac tissue development (Kang et al., 2004). Loss of BMP9 signalling in humans causes hereditary haemorrhagic telangiectasia (HHT) a genetic disorder in which the blood vessels don't develop properly.

1.5.1 Structure

BMP9 like all other TGFβ superfamily molecules is translated into a protein consisting of three main domains, a signal sequence, propeptide domain, and the active protein. Prior to secretion precursor proteins form homodimers in the cytoplasm linked by 3 disulphide bonds (Carreira et al., 2014). BMP9 and -10 are unique as they are released from the cell with their pro-domain attached which remains tightly bound in circulation. The pro-domains of BMP9 and -10 do not affect the proteins signalling or affinity for receptor binding, eliciting the same responses as unbound formations (Salmon et al., 2020). Both BMP9 and -10 share 16 conserved residues at the centre of their homodimer interfaces. This conserved region is responsible for type 1 and 2 receptor binding. A single residue K368 within this region has been identified as the cause for their high ALK1 binding affinity, due to interactions with a complementary residue in ALK1 (Salmon et al., 2020).

1.5.2 BMP9 receptors

BMP9 signalling is achieved through a hetero-tetrameric complex composed of a combination of type 1 and 2 serine-threonine kinase receptor complexes. BMP9 was

originally thought to signal through type 1 receptors Activin-like kinases (ALK) -1, -2 and -5. However, it has recently been shown that during osteogenesis BMP9 signalling only occurs through ALK1 and 2 receptors. To form the active heterodimer receptor type 2 receptors BMPRII, ACTRII, and ACTRIIB participate in BMP9 osteogenic signalling pathways. Activation of the receptors occurs via the initial binding of a BMP9 dimer to a type 2 receptor, followed by its co-binding to a type 1 receptor which activates SMAD1/5/8 cell signalling pathways.

Endoglin (ENG) and BMP and activin membrane-bound inhibitor (BAMBI) receptors are also capable of binding to BMP9 dimers. Endoglin (ENG, also identified as CD105) is a TGFβ coreceptor with the same binding affinity for BMP9 as ALK1. It assists with BMP9 signalling by capturing it to the cell surface so higher concentrations are available to bind with BMP type 1 and type 2 receptors (Saito et al., 2017). BAMBI is another cellular receptor that binds with BMP9, however, unlike endoglin it has an inhibitory function acting as a pseudo-receptor preventing BMP9 from binding to functional receptors. Together endoglin and BAMBI provide an additional level of extracellular BMP9 regulation. Interestingly BMP9 receptor concentrations have been found to vary significantly depending on cell type and maturity providing contextually specific responses to BMP9 activation.
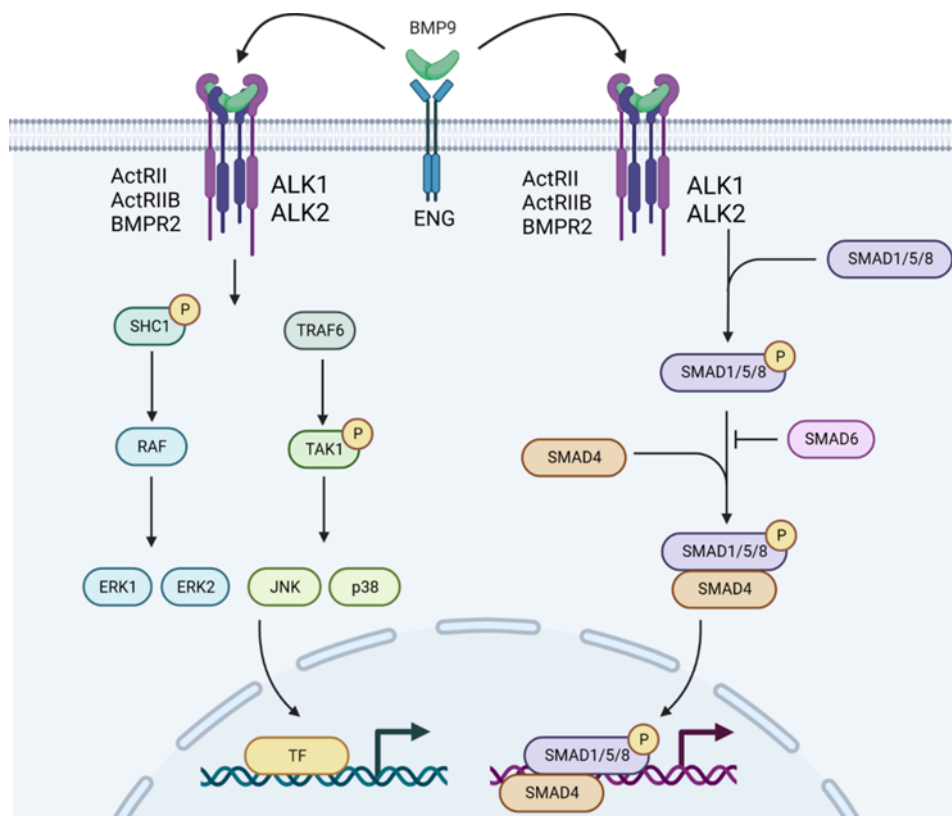
Figure 3 BMP9 SMAD-dependent and non-canonical signalling pathways. BMP9 **SMAD-dependent** signalling initiates when BMP9 binds to a receptor complex formed of type 1 (ALK1 or -2) and type 2 (ActRII, ActRIIB, or BMPR2) receptors. The receptor complex induces phosphorylation of SMADs1/5/8 which translocate to the nucleus with the assistance of SMAD4. Within the nucleus the complex activates transcription of factors such as RUNX2 and SOX9. **Non-canonical** or **SMAD-Independent** signalling is initiated by BMP9 binding to the same receptor complexes, however, the internal regions are different and activate either the ERK signalling cascade via SHC1 or TAK signalling cascade through TRAF6. Both of theses cascades are MAPK signalling pathways resulting in the activation of ERKs, JNK, p38, or other MAPKs. These factors translocate to the nucleus where they form transcription complexes inducing transcription factors

such as c-MYC, c-JUN or NFkB. BMP = Bone morphogeneric protein 9, ALK = Activin-like kinase, ACTRII = Activin type 2 receptor, BMPR2 = Bone morphogenetic type 2 receptor, ENG = Endoglin, SHC1 = SHC-transforming protein 1, TRAF6 = TNF receptor-associated factor 6, TAK1 = TGFβ-activated kinase 1, JNK = c-Jun N-terminal kinase, p38 = p38 MAPK, RAF = RAF serine/threonine-protein kinase, ERK = Mitogen-activated protein kinase 3, c-MYC = MYC proto-oncogene, c-JUN = Jun proto-oncogene.

1.5.3 Signalling mechanisms

BMP9 signalling via ALK1 and -2 receptors activates SMAD signalling pathways. Receptor activation occurs when BMP9 binds to a homodimer receptor bringing the two halves together, facilitating the activation of the type 1 receptor by a constitutively active type 2 receptor. ALK 1, 2, 3 and 6 receptors activate cytoplasmic signalling proteins *small mothers against decapentaplegic* (SMAD) -1, 5 and -8 whilst ALK4, -5 and -7 activate SMAD2, -3 pathways. Both signalling pathways require downstream SMAD4 assisted translocation to the nucleus where the SMAD proteins bind to DNA via the recruitment of transcription factors altering gene transcription. BMPs can activate different ALK receptors which function via similar signalling pathways.

Alternatively, BMP9 can induce non-canonical signalling pathways via mitogen-activated protein kinase (MAPK) signalling. Induction of the MAPK signalling ultimately results in the activation of either extracellular signal-related kinases (ERK) 1/2, Jun amino terminal kinases (JNKs), or p38 MAP kinases. BMP9 activated MAPK signalling regulates the effects of SMAD signalling by regulating phosphorylation. P38 signalling enhances phosphorylation of SMAD signalling induced by BMP9 whilst ERK 1/2 inhibits SMAD signalling phosphorylation. Together the SMAD and MAPK signalling pathways provide additional internal regulation of BMP9 activation (Xu et al., 2012).

1.5.4 Osteogenesis and bone formation

BMP9 has been studied extensively for its potent osteogenic effects using both *in vitro* and *in vivo* methods, in which it has been shown to induce mesenchymal stem cell (MSC) differentiation, bone formation and fracture healing. Using MSC cell lines BMP9 signalling induces osteogenic differentiating potential. C3H10T1/2 mouse cells cultured with BMP9 produce mineralised osteoid nodules (Cheng et al., 2003). Alternatively, C2C12 mouse cell lines stimulated with BMP9 upregulated the expression of osteocalcin, a downstream marker of osteogenesis (Cheng et al., 2003). When injected into the quadriceps of mice C2C12 stimulated cells induced orthotopic bone formation within the muscle tissue. Both features induced by BMP9 are clear markers of osteogenesis (Luther et al., 2011). The osteogenic effects of BMP9s in animal models using adenoviral BMP9 (AdBMP9) demonstrate its osteogenic potential. In animal studies, BMP9 transduced cells or direct injection of adenoviral BMP9 into the quadricep muscles of mice led to mineralization or ectopic bone formation of the muscle tissue. Interestingly MC3T3-E1 cells cultured with BMP9 were not affected by *noggin* a BMP9 antagonist but heterotopic ossification of damaged muscle tissue in mice was inhibited by soluble ALK (Bergeron et al., 2009). This emphasizes the importance of ALK1 receptors for BMP9-induced osteogenesis.

1.5.5 Chondrogenesis

BMP9 signalling in chondrocytes is activated via the same type 1 and 2 receptors as osteogenesis, inducing SMAD and MAPK signal transduction pathways. BMP9 acts as a potent modulator of MSC chondrogenic differentiation, inducing expression of *COL2A1*, *ACA*

and *SOX9* chondrogenic markers (Butler et al., 2007; Majumdar et al., 2001). BMP9-directed chondrogenesis also results in cellular hypertrophy, and in some cases, low levels of *COLX* expression and mineralisation of collagen has been observed in chondrocyte pellet and scaffold-based cultures. These three features are markers of late-stage hypertrophy and terminal differentiation, typically signs of early osteogenesis (Blunk et al., 2003; B. J. Morgan et al., 2020; van Caam et al., 2017). Surprisingly co-culture of TGFβ1 with BMP9 improves chondrogenesis of pellet cultures. Inducing *ACAN* and *COL2A1* expression whilst downregulating *COLX* and *MMP13* expression, markers of late-stage hypertrophy (Quiros et al., 2020). TGFβ1 signals though SMAD2 and -3 signal transduction pathways and so SMAD1/5 and SMAD2/3 signalling pathways have contrasting effects on chondrocyte differentiation. The synergistic effects of TGFβ1 and BMP9 signalling may therefore be responsible for normal cartilage development and homeostasis.

1.5.6 Angiogenesis

BMP9 is a well-documented angiogenic factor circulating in the blood as an active factor responsible for maintaining vascular quiescence, inhibiting endothelial cell migration and growth (David et al., 2008). BMP9 maintains quiescence via ALK1 and ENG endothelial cell signalling. Endoglin and ALK1 receptors are highly expressed on epithelial cells and vital to BMP9 signalling. Endoglin co-receptors are more abundantly expressed on the cell surface than ALK 1 and thus provide a pool of available BMP9 molecules for serine-threonine type 1 and 2 receptor binding (Saito et al., 2017). Genetic mutations to the genes encoding BMP9 and its receptors ALK1 and ENG cause multiple variants of hereditary haemorrhagic Talgeictasia (HHT). HHT is characterised by abnormal formation of arteriovenous microvasculature due to a loss of BMP9 signalling. 85% of HHT cases are caused by mutations to either the *Endoglin* or ALK1 (*ACVRL1*) genes, HHT1 and HHT2 respectively (Tillet & Bailly, 2014). Mutations to SMAD4 and BMP9 proteins also cause variants of HHT however they are not as prevalent. Although BMP9 mutations only account for a small percentage of HHT cases it highlights the necessity of ALK1 and endoglin for BMP9 signalling (Saito et al., 2017).

1.5.7 BMP9 signalling in osteoarthritis

Changes in TGFβ family signalling pathways have been identified in the formation and progression of osteoarthritis. Variations of TGFβ receptor expressions in chondrocytes have been observed in mice, humans, pigs and cows. In bovine tissue a decrease in ALK2, -3, -4, and -5 receptor expression during ageing has been observed, interestingly ALK1 is the only receptor that is not affected by ageing and so the ratio of remaining ALK receptors shifts in favour of ALK1 signalling (Blaney Davidson *et al.*, 2009; van Caam *et al.*, 2016). Thus, BMP9 signalling is not affected with age however other morphogenetic proteins are, increasing BMP9-activated SMAD1/5/8 signalling and reducing the protective TGFβ SMAD2/3 signalling. Increases in SMAD1/5/8 signalling with age are known to lead to an increase MMP13 expression, an enzyme commonly observed in OA cartilage degradation (Blaney Davidson et al., 2009; van der Kraan et al., 2016). Therefore it is plausible that uninhibited BMP9 signaling via the SMAD1/5/8 signalling is responsible for the increase in *MMP13* expression and thus OA onset.

Mechanical loading of cartilage has also been shown to effect OA onset in cartilage tissue, inducing SMAD2/3 signalling via TGFβ expression. Older cartilage is less responsive to mechanical loading and does not induce the same levels of SMAD2/3 signalling as young

cartilage. It has been shown that cartilage not subject to any mechanical loading has radically increased tissue degradation combined with high levels of *COLX* and *MMP13* expression (Madej et al., 2016).

1.5.8   Clinical applications of BMP9

As the previous sections describe BMP9 signalling has potent osteogenic and chondrogenic capabilities. These unique properties of BMP9 could be useful for developing regenerative treatments. With this same goal in mind multiple studies have investigated BMP9's potential clinical applications for the treatment of bone defects and skeletal formation.

One related study with potential clinical applications used adenoviral BMP9 (adBMP9) to repair cranial defects in mice. In which, transduced immortalised murine calvaria progenitor cells were seeded into a thermo-sensitive scaffold. The scaffold was then placed into a cranial defect and after 12 weeks mice with BMP9 transduced cells had significantly more bone regeneration than controls. The bone produced was mature in structure and filled the defects (Dumanian et al., 2017). Another translatable study using scaffold-based approaches to repair critical-size cranial defects in mice observed improved bone repair with BMP9 transduced cell lines. The study compared the effectiveness of recombinant BMP9 and BMP2 treatment of cranial defects, finding that rhBMP9 produced highly mineralised bone that was denser and less fatty than rhBMP2 treatments (Nakamura et al., 2017). A similar *in vitro* study in rabbits compared the effectiveness adBMP2 and adBMP9 induced muscle-derived stem cells for the treatment of large bone defects. They found that after 16 weeks the bones of the BMP9 treated group had reconnected, taking an additional 2 weeks for BMP2 to achieve similar levels of repair (X. Li et al., 2012). Together these studies demonstrate the therapeutic potential for BMP9 in the repair of bone defects.

Most recently an *in vitro* mouse study showed sequential treatment of amputated bone stumps with BMP2 followed by BMP9-induced bone regeneration, including features that resembled an articulating joint. The joint structures generated included the formation of an articular cartilage surface lining the bone inside a synovial cavity. The articular cartilage layer generated resembled histologically normal cartilage. Demonstrating BMP9s therapeutic ability to regenerate tissues of the synovial joint, most importantly generation of histologically normal articular cartilage, for potential future clinical treatments (Yu et al., 2019).

In summary, the previous literature highlights BMP9s potential use for therapeutic treatments by harnessing its osteogenic and chondrogenic capabilities. Most of the current treatments are focused on the repair of bone defects, however, its potential for joint regeneration and articular cartilage formation also presents a promising avenue for further research.

1.6   Summary and hypothesis

Osteoarthritis is the most prevalent musculoskeletal disease in the world characterised by loss of articular cartilage. Treatments to repair damaged cartilage fail to reproduce the complex structure of this tissue, making it an ideal target for regenerative approaches. Tissue engineering provides a possible solution to this clinical problem. Postnatal maturation during puberty is critical for the tissue to develop its resistive biomechanical properties, during maturation reorganisation of the extracellular matrix occurs. Collagen fibrils of the extracellular matrix form arcade-like patterns providing the source of the tissue's structural integrity. There is limited knowledge regarding the processes involved in cartilage

maturation, but recent papers studying BMP9-induced differentiation of chondrocytes show morphological characteristics mimicking those of native mature cartilage including the reorganisation of collagen fibrils. Therefore, this project aimed to determine the major mechanisms involved in BMP9-induced maturation and discover if it is possible to engineer more effective implants using the knowledge gathered.

We hypothesise that BMP9 can induce postnatal maturational changes in immature articular cartilage *in situ*, causing structural and morphological reorganisation of the extracellular matrix that recapitulate features of adult cartilage.

The hypothesis was tested in four ways:

1. Histological, biochemical, and image analysis of BMP9-treated immature bovine cartilage explants was conducted to identify and quantify changes in tissue structure and morphology.
2. RT-qPCR studies were performed to determine which genes are key to BMP9-induced articular cartilage maturation.
3. Inhibitor studies of BMP9-treated explant cartilage cultures were used to identify the roles of participating enzymes and signalling pathways in the maturation process.
4. The effect of BMP9 treatment on engineered cartilage pellet constructs was evaluated biochemically and histologically.

By the end of the project, we hoped to have a much better understanding of BMP9-induced articular cartilage maturation. This understanding will span across histological, biochemical and gene expression analyses providing a comprehensive outlook of the mechanisms that regulate the maturation processes. These insights will help to instruct us on how to engineer tissue constructs resembling mature cartilage extracellular matrices, opening the doors to the production of grafts and further development of chondrocyte scaffold-based tissues for repair, replacement, or regeneration.

Chapter 2: General methods and materials

2.1   Sample collection and processing

2.1.1 Feet collection
This study was approved by the ethical committee at Swansea University, Wales. The requisite regulatory permissions from National Authorities were obtained upon application to The Department for Environment, Food & Rural Affairs (DEFRA) UK. Mature and immature bovine feet were retrieved from local abattoirs; the samples acquired comprised of the lower portion of the leg that would otherwise be disposed of as waste. All animals were killed humanely in accordance with the law. The bovine feet were collected on the day of slaughter from the abattoirs and transported directly back to the laboratory for processing.

2.1.2 Feet sterilisation
Each foot was first washed with detergent and hot water to remove any surface dirt, spraying with virkon and ethanol to sterilise the outer surface. Followed by the removal of the skin from the feet, being careful not to damage the joint. Scoring along the length of the foot using a scalpel with size 23 surgical blades (Swann-Moton, #0123). After all the feet had been processed, they were washed again with detergent, sprayed with ethanol and virkon, and caped at the ends of each leg with surgical gloves. The feet were then placed on a stainless-steel surgical tray for transportation into the tissue culture lab for dissection and sample acquisition.

2.1.3 Explant collection
Legs were resprayed with 70% ethanol before being placed in the tissue culture hoods. Under sterile conditions the feet were dissected at the metacarpophalangeal joint revealing the joint surfaces. Any joints that displayed visible signs of damage or infection on dissection were discarded immediately. 4mm or 6mm biopsies (Kai Medical #BP-40F, #BP-60F) were taken from the inner flanks of the metacarpophalangeal condyle head, explants were collected from one side of the joint and controls from the adjacent position to mitigate differences in tissue composition across the joint affecting results. Biopsies were placed directly into the wells of a 24-well plate containing 1.5mL of DMEM (wash step). After all the biopsies had been collected the DMEM was removed and replaced with culture media, adding fresh ascorbate, growth factors or FBS depending on the culture.

2.1.4 Volumetric measurements of explants
After all the explants had been collected and placed in DMEM in the 24-well plates sterile Bijou tubes were filled with 1mL of DMEM and weighed one at a time. Using sterile autoclaved forceps each explant was placed into a bijou tube containing 1mL of DMEM and reweighed to calculate the wet weight of the explants. Tubes were returned to the culture hood and explants moved to sterile petri dishes where they were measured using a vernier calliper for height, width, and volume. After the explants had been measured the DMEM from the wells was replaced with chondrogenic growth medium. At the end of the culture period the same process was repeated to record the final volumetric values. Samples were then fixed in 10% NBFS, or flash frozen in liquid nitrogen.

2.1.5 Histological processing of explants

Explants were fixed in 10% NBFS at 4°C overnight and loaded into cassettes for embedding. The explants were dehydrated through immersion in a series of graded ethanol baths from 30%-100% to remove the water, cleared using xylene (Sigma, #534056-5L) before infiltration with paraffin wax at 65°C – 70°C and embedding back onto the wax cassettes (Histological fixing was provided by Singleton Hospital Pathology Department)

The explant cassettes were sectioned to a depth of 800μm before the collection of samples. Samples were cut using a microtome at 7μm thicknesses. Wax sections were placed in a 45°C water bath and adhered to positively charged slides. POLYSINE slides (Thermo Scientific #J2800AMNZ) were left on 60°C hot plates for 20 minutes to melt the wax and complete adhesion.

2.1.6 RNA processing of explants

Explants were fed with fresh media 2 hours before removal from culture to ensure any genes induced via growth factors were activated at the time of collection, day 0 explants were processed immediately after collection. A small container was filled with dry ice, placing a small glass beaker containing 20mL of n-hexane into the dry ice. The surrounding container was filled with 100% ethanol until the glass beaker was partially covered. Explants were removed from culture, allowing time for the n-hexane to reduce in temperature. Explants were then frozen in n-hexane one after the other and placed into Eppendorfs on dry ice. Once all explants were frozen, they were transferred for storage at -80°C.

Explants were processed for RNA extraction using a dismembranator. The samples were removed from -80°C storage and kept on dry ice. The holders and ball bearings used for dismembranation were cooled by submerging in liquid nitrogen, retaining liquid nitrogen within the smaller half of the holder. RTL lysis Buffer (QIAGEN #1015762) and a sample were added to the holder containing liquid nitrogen, adding additional liquid nitrogen to the sample holder if required to cool the sample. The dismembranator was shaken for 1-2mins, holders were removed and placed on a heated plate to melt the sample before pipetting into sterile DNase and RNase-free Eppendorfs. RNA was stored at -20°C until use.

2.2 Tissue culture

2.2.1 Culture conditions

All cultures were conducted in humidified incubators at 37°C, with 4% carbon dioxide, sodium hydroxide was diluted into the water tray to prevent bacterial growth within the incubator due to persistent contamination issues. Explants were cultured in 24-well plates and pellets were cultured in 1.5mL Eppendorfs. Medium in explant cultures was changed every third day. Supplemental media components such as ascorbate and growth factors were added freshly during every feed from stock solutions.

2.2.2 Chondrogenic media

For all cultures, unless specified, standard chondrogenic media was used. Chondrogenic medium was prepared by weighing 25mg of L-proline (Sigma #P5607) into a sterile 50mL Falcon tube which was sprayed with 70% ethanol and transferred to a sterile tissue culture hood. 5mL HEPES pH 7.5 (Sigma #H3375), 500μL 2% Gentamicin, and 5mL 100x ITS-insulin transferrin selenium (Gibco #51500-056) was pipetted into the Falcon tube. The tube was topped up to the 50mL mark with DMEM-HG mixing the solutions by hand until all the L-proline had dissolved. The contents of the Falcon tube were transferred into a 500mL vacuum filter top attached to a freshly autoclaved bottle, rinsing the tube with an additional 50mL of DMEM. The filter top was filled up to the 500mL mark with the remaining DMEM-HG and vacuum filtered into the bottle using a pump. Chondrogenic medium was stored in a fridge at -7°C until feeding. 345μm of fresh ascorbate, BMP9 3.7nM (Preprotech), or any other additional inhibitors where specified were added to the culture media just before feeding.

Control Chondrogenic Growth Medium	BMP9
DMEM – HG (high glucose) – (Corning #10-013-CVR) ITS – Insulin transferrin selenium (Gibco #51500-056) 10mM HEPES pH 7.5 (Sigma #H3375) 100μM Gentimicin 345μM Ascorbate (Sigma #A4034) 172μM L-proline (Sigma #P5607)	3.7nM BMP9 (Preprotech #120-01)

2.2.3 Doxycycline inhibitor culture media

To investigate BMP9s mechanism of function doxycycline (dox) was added to control and BMP9 cultured 4mm diameter immature bovine explants. Standard chondrogenic medium was used as the culture media, adding 3.7nM BMP9, 345μm ascorbate, and 100μm dox fresh for each culture feed. Cultures were fed with 1.5mL of media every 3 days collecting 0.5mL of the waste medium for biochemical analysis.

2.2.4 PD166793 inhibitor culture media

To investigate BMP9s mechanism of function PD166793 was added to control and BMP9 cultured 4mm diameter immature bovine explants. Standard chondrogenic medium was used as the culture media, adding 3.7nM BMP9, 345μm ascorbate, and 10μm of PD166793 fresh for each culture feed. Cultures were fed with 1.5mL of media every 3 days collecting 0.5mL of the waste medium for biochemical analysis.

2.3   Histological staining

All stains that were produced in the lab were filtered through paper (Fisherbrand) before use to remove any impurities.

2.3.1   Haematoxylin and eosin

0.25% eosin Y stain was made by diluting 25mL of 5% eosin Y (TCS Biosciences, #HS255-500) in 475mL 80% ethanol and 2.5mL acetic acid glacial (Fischer #A/0400/PB17). Sections were deparaffinised in xylene for 5 minutes followed by 5 minutes in histochoice (Agar Scientific, #HS-202). They were rehydrated in a series of ethanol baths 100%, 100%, 95%, 70% and a final tap water rinse. Sections were stained for 8 minutes in Mayers haematoxylin solution (TCS Biosciences, #HS351) then rinsed again in running water for 10 minutes and dipped into 95% ethanol prior to staining with 0.25% eosin Y solution for 2 minutes. Sections were then dehydrated in 100% ethanol for 4 minutes, histochoice for 5 minutes, and xylene for 5 minutes before mounting with DPX (agar scientific #R1340).

2.3.2   Safranin O

0.1% safranin O was produced by dissolving 0.5g safranin O crystals (Gurr Microscopy materials, #34067) in 500mL of distilled water. Sections were deparaffinised in xylene for 5 minutes followed by 5 minutes in histochoice. Sections were rehydrated in a series of ethanol baths 100%, 100%, 95%, 70% and a final tap water rinse. Stained for 8 minutes in Mayers haematoxylin solution then rinsed again in running water for 10 minutes, dipped in 0.005% Fast green for 5 minutes, dipped into 1% acetic acid for 30 seconds, and stained with 0.1% safranin O for 5 minutes. Sections were then dehydrated in 100% ethanol, histochoice, and xylene before mounting with DPX.

2.3.3   Toluidine blue

1% toluidine blue stain was prepared by dissolving 5g of toluidine blue crystals (Sigma #C.I.52040) in 500mL of distilled water. Sections were deparaffinised in xylene for 5 minutes followed by 5 minutes in histochoice. Sections were rehydrated in a series of ethanol baths 100%, 100%, 95%, 70% and a final tap water rinse, sections were washed for 2 minutes in each grade. Sections were stained for 30 seconds in 1% toluidine blue O (Sigma #C.I.52040) rinsed in running tap water for a further 10 minutes and left to air dry at 37°C until completely dehydrated. Sections were treated for 5 minutes in xylene and mounted with DPX. The ideal length of time for staining with 1% toluidine blue was determined using immature cartilage samples.

2.3.4   Picrosirius red

0.1% picrosirius red was prepared by dissolving 0.2g of sirius red / direct red 80 (Sigma #365548) in 200mL of 1.3% picric acid (Sigma, #p6744-1ga), mixing until all the solids were dissolved. Acidified water was prepared by diluting 5mL of acetic acid (glacial) added in 1L of distilled water. Sections were deparaffinised in xylene for 5 minutes followed by 5 minutes in histochoice. Sections were rehydrated in a series of ethanol baths 100%, 100%, 95%, 70% and a final tap water rinse, 2 minutes in each grade. Sections were stained for 8 minutes in Mayers haematoxylin solution and then rinsed in running water for 10 minutes.

Sections were ringed using an ImmEdge wax pen (Vector Laboratories, #H-4000) prior to picrosirius red staining and left for 2 hours. Sections were then washed twice with acidified water for 5 minutes, dehydrated in 100% ethanol, histochoice, and xylene for 5 minutes each before mounting with DPX.

2.4 Microscopy

Histological sections were imaged using a Lecia light microscope, images were taken at magnifications ranging from 2.5x up to 20x. For picrosirius red-stained sections images were captured using a Leica polarised light microscopy (PLM) to view the birefringence (fluorescence) of the stained collagen fibres. PLM images were captured for image analysis when the birefringence observable provided the best representation for what could be viewed at all planes, both control and BMP9 samples were imaged at the same plane.

2.5 Immunofluorescent staining

2.5.1 BrdU application in culture

Bromodeoxyuridine (BrdU) was added to cultures during the last feed, three days before the end of the culture period to allow for its incorporation into the tissue. BrdU was used at a concentration of $10\mu m$. At the end of the culture period the cells were washed with fresh media for 2 hours to remove any unincorporated BrdU from within the tissues.

2.5.2 Section preparation

Sections were deparaffinised in xylene for 5 minutes followed by 5 minutes in histochoice. Sections were rehydrated in a series of ethanol baths 100%, 100%, 95%, 70% and a final tap water rinse, 2 minutes in each grade. Samples were ringed with a wax pen to reduce the reagents required. 3 x 5 minute wash in TBS-T (Tris buffered saline containing 0.1% Tween 20) (Sigma #P1754-500ML), followed by 0.3% H_2O_2 (Sigma #H1009) for 5 minutes, and another 3 x 5 minute TBS-T wash.

2.5.3 Section hydrolysis

Sections were hydrolysed to denature the DNA and make BrdU available for antibody binding using 2M HCL (Merk #HC6067563) for 30 minutes, 0.1M $NaBO_3$ (sodium borate) v/v in distilled water was used to neutralise the HCL for 20 minutes, followed by 3 x 5 minute TBS-T washes at 4°C to remove any residual solutions.

2.5.4 Antibody binding

First, the sections were blocked with 20% goat serum made up in TBS-T at room temperature for 1 hour, followed by a 3 x 5 minute TBS-T wash. $1\mu gmL^{-1}$ or 1/45 dilution of the primary antibody G3G4 anti-BrdU (DSHB) was prepared in TBS-T and applied to sections overnight at 4°C. Sections were washed 3 x 5 minutes in TBS-T to remove any residual primary antibody before covering the sections with $1\mu gmL^{-1}$ Alexa Fluor 594 goat anti-mouse (Abcam) antibody for 1 hour followed by 3 x 5 minute TBS-T washes. Sections were mounted immediately after the three wash cycles using a DAPI mountant (Vectashield

laboratories #H-1200). Optimial antibody concentrations were determined using a range of dilutions on test samples.

2.6   ImageJ analysis

Histological images were processed using ImageJ software (National Health Institute) for cell and collagen fibril analysis. For both analysis techniques the first 500μm of tissue from the surface was measured using the same 5 zones 100μm in depth, increasing in depth from the tissue surface.

ImageJ particle analysis software was used to analyse cell morphology and density. Toluidine blue stained sections were converted to binary 8bit images, selecting 15 cells randomly spread across each zone. ImageJ particle analysis software was used to analyse area, circularity, and the orientation of the cells long axis relative to the surface. To measure cell density DAPI stained sections were converted to greyscale images and ImageJ particle analyser was used to count the number of labelled nuclei within each zone. These values were used to determine the changes in chondrocyte shape and organisation with depth in cultured cartilage tissue

FibrilJ plugin tool for ImageJ was used to measure the orientation and anisotropy of collagen fibrils in the histological sections. Picrosirius red sections imaged using PLM were converted into 8bit grey-scale images. Sections were measured in 5 zones of 100μm in depth and equal width starting from the surface of the cartilage tissue. Fibre orientations were measured from 0°- 90° relative to the tissue surface. Collagen anisotropy was measured in arbitrary values between 0 and 1, 1 representing anisotropic collagen directionality and 0 representing isotropic directionality. Fibril data was outputted as a mean value for all the fibres within the zone being analysed. These values were used to determine the changes in fibril orientation and anisotropy with increasing depth in cultured cartilage tissue.

2.7   Biochemical techniques

2.7.1 Papain digest of tissue

Papain digest buffer containing 20mM NaAC pH 6.8 (Sigma-Aldrich #W302406-1KG-K), 1mM Ethylenediaminetetraacetic acid (EDTA) (Sigma) was prepared as a large 1L stock and stored at room temperature. Papain crystals (Sigma #P3375-25G) were suspended in double distilled water at a concentration of 25mg mL^{-1}, 60mg of papain was used to prepare 2.4mL of the enzyme in solution. The papain solution was stirred at 60°C to fully dissolve the crystals with periodic vortexing. A 1mL syringe (BD Plastipak sterile #303172) with a 22μm filter tip (MILLIEXGP #SLGP033RS) was used to filter sterilise the papain solution.

1M Dithiothreitol (DTT) stock was prepared from crystals diluted in double distilled water and filter sterilised through a 22μm syringe tip and stored at -20°C. 40mL of the papain digest buffer was pipetted into a 50mL Falcon tube followed by 200μL of 1M DTT and 400μL of 25mgmL^{-1} papain, vortexing the tube. 1mL of the papain digest solution was then pipetted

into Eppendorf tubes each containing a tissue sample. Digests were set up in a 60°C water bath (Grant Sub Aqua 26 Plus), vortexing the samples every 30 minutes of the first 2 hours to assist initial digestion. Pellets required a 4 hour digestion vortexing every hour, all soft tissue was digested following the 4 hours. Explants required overnight digestion (16 hours) at 60°C, after digestion the samples were spun at 2500rcf for 1.5min to pellet the undigested subchondral and calcified cartilage residue. The supernatant was then transferred to sterile Eppendorfs and stored at -20°C to prevent any further digestion. Old tubes containing the undigested calcified cartilage were dehydrated for reweighing to calculate the dry weights of the residual tissue.

2.7.2 Glycosaminoglycan (GAG) quantification using dimethylmethylene blue (DMMB) assays

Dimethylmethylene blue (DMMB) stock was prepared from 16mg DMMB dissolved in 1L of distilled water containing: 3g polyvinyl alcohol (Sigma #P8136-250G), 3.04g glycine (Sigma #G-7403), 2.37g NaCl (Sigma-Aldrich #S7653-1KG), 95mL 0.1M HCL (Merk #HC6067563).

A set of standards was created using bovine chondroitin-sulphate (Sigma #C4383-1G) from 0-40μgmL^{-1} at 10μgmL^{-1} intervals. Dilutions of the digests were necessary so that measurements could be made within the linear range of sensitivity of the assay. Explants required a 1/200 dilution. Pellets required a range of dilutions dependent on the culture. Dilutions of 1/7 for immature and mature control pellets or a 1/40 dilution for immature and mature BMP9 cultured pellets were used. Optimum concentrations were determined through preliminary trial and error experimentation until all the tissue samples of a given culture set fell within a linear range.

25μL of each papain digested sample was pipetted into duplicate wells of a 96-well flat-bottom microassay plate (Thermo Scientific #167008). 200μL of DMMB stock was pipetted into the wells containing duplicate samples. Once all the wells were filled the plate was immediately placed into a microassay plate reader (BMG LABTECH FLUOstar Omega), measuring absorbances at 520nm (540nm – 575nm is optimum) at a 750 gain (optimal conditions found via trial and error).

2.7.3 Hydroxyproline analysis – collagen quantification

500mL of Stock buffer was prepared using 28.5g sodium acetate trihydrate (VWR #27652.298), 18.75g tri-sodium citrate dihydrate (Sigma-Aldrich #S1804-500G), 2.75g citric acid (Sigma #C1857-100G) dissolved in 200mL double distilled water. Mixed with 200mL propan-2-ol (Fischer #P/7500/21) and made up to 500mL with double distilled water. **150mL Diluent** was prepared using 100mL propan-2-ol (Fischer #P/7500/21) and 50mL double distilled water. **Oxidant** was prepared from 0.7g chloramine-T (Aldrich #857319-100G) dissolved in 10mL of water, diluted using 50mL of stock buffer. **The colour reagent** was prepared using 7.5g dimethylamine benzaldehyde (Sigma #D2004-25G) dissolved in 11.25mL (60%) - perchloric acid 70% (Sigma-Aldrich #244252) and 62.5mL propan-2-ol (Fischer #P/7500/21). The colour reagent was prepared in a fume cupboard due to the hazardous reagents.

100μL of 4M sodium hydroxide (Sigma-Aldrich #320221) and 100μL of the papain digested samples were pipetted into a screw top microcentrifuge tube with an o-ring seal (VWR #525-0547). All samples were hydrolysed in the autoclave at 121°C, 15psi, for 30 minutes. After autoclaving samples were cooled to room temperature using a water bath. 100μL of 4M

hydrochloric acid (Sigma-Aldrich #320331) was used to neutralise the reaction mixture completing the process. Neutralised samples were stored at -20°C until use (Cissell et al., 2017).

Hydroxyproline standards were produced by diluting hydroxyproline in the papain digest buffer at concentrations from 0-200µg mL^{-1} in 25µg mL^{-1} increments. Hydrolysed tissue samples were removed from storage and warmed to 37°C to defrost, vortexed and spun before use. 30µL of the hydrolysed sample was added to each well of a micro-assay plate (Thermo Scientific #167008) (BIOFIL #011096) followed by 70µL of diluent and 50µL of oxidant. The microplates were shaken by hand for 5 minutes (plate shaker was too aggressive and caused spillage). Post shaking 125µL of the colour reagent was added to each well and an adhesive film (Thermo #AB-0558) was applied to seal the well plate. Shaken for 30 seconds on the plate shaker at 100rpm and incubate at 65°C for 12 minutes. The film was removed, and plates were analysed immediately after incubation, absorbance readings were taken at 540nm (absorbance peak at 560nm) (da Silva et al., 2015).

Mean absorbances from the hydroxyproline sample duplicates were calculated and then multiplied by 3 as 100µL of the samples were hydrolysed in 100µL of sodium hydroxide and 100µL of hydrochloric acid to find the true concentration of hydroxyproline in the assayed samples. The hydroxyproline concentrations were converted to content values as concentrations were measured as µgmL^{-1} and the total volume of each sample digest was only 1mL. Because hydroxyproline only composes 13% of collagen content on average hydroxyproline readings needed to be converted to collagen by multiplying by 8.

2.8 Bacterial culture of pGEM-T plasmids for generating qPCR standards

2.8.1 Bacterial transfection

Super optimal broth (SOB) was created in stocks for culturing bacterial transfections in 0.186gL^{-1} KCl (Sigma-Aldrich #P5405-250G), 2.4gL^{-1} MgSO$_4$ (Sigma-Aldrich #208094-500G), 0.5gL^{-1} NaCl (Sigma-Aldrich #S7653-1KG), 20gL^{-1} tryptone, 5gL^{-1} yeast extract, (Sigma #Y-1625 250g) adjusted to a pH range 6.8 - 7.2 (2.8% solution).

E.coli XL1-Blue frozen competent cells (FCCs) were used for bacterial transfections. Cells were removed from -80°C storage, placed on ice, and kept partially frozen to prevent cells from losing their competency. When the FCC solution reached a slushy consistency 100µL of cells were pipetted into individual 1.5mL Eppendorfs on ice. 1µL of DTT was added per 100µl of FCC to increase susceptibility. 2µL of 0.5ngµL^{-1} pGEM-T plasmid containing a gene insert was added to the 100µL of cells in the Eppendorf, triturating with the tip to mix the plasmid and cells. The Eppendorf was placed back on ice for 20 minutes, then placed in a water bath at 45°C for 35 seconds, and back on ice for a final 2 minutes. After the transfection process was complete 100µL of Super optimal broth was added to the Eppendorfs and triturated for 10 seconds to suspend the cells. The transfected cells were left in a water bath at 37°C for 10 minutes to ensure that the cells had started to express their antibiotic-resistant genes before plating. Eppendorfs were removed from the water bath and the cells were pipetted straight onto the centre of an agar plate (amp), and spread

evenly across the surface with an inoculating needle. Plates were left to incubate overnight at 37°C. After the incubation period cells were inspected for growth and stored at 4°C.

Plasmids used for bacterial transfections contained bovine sequences required to produce the standards for qPCR. The sequences are therefore the same sequences listed for qPCR use (Chapter 2.11). pGEM-T plasmids were used as they contain 3'T overhangs at the gene insertion sites that are compatible with DreamTaq PCR-generated inserts.

2.8.2   Overnight culture

Prior to setting up a bacterial overnight culture the incubator was prewarmed up to the temperature of 37°C. Sterile 25mL universal tubes were used for overnight cultures, 2.5µL of 100µgµL^{-1} ampicillin (amp) was pipetted into the bottom of each tube followed by 2.5mL of sterile LB broth (Sigma #L3022) diluting amp to its working concentration of 286µm. An individual colony was isolated from a bacterial plate using an inoculating needle and placed in the universal tubes containing the LB broth, swirling for 5 seconds by hand. Lids were partially screwed closed ensuring they were loose enough to allow airflow. Autoclave tape was used to hold the lid securely in place. Cells were left to culture in the incubator overnight at 37°C, with shaking at 290rpm to increase air diffusion.

2.8.3   Mini-Prep plasmid isolation

Mini-prep plasmid isolations were performed using a QAIPREP spin mini-prep kit (QAIGEN #27104) following the manufacturer's instructions. Overnight bacterial culture tubes were removed directly from incubation. 2.5mL of the overnight was pipetted into a 1mL sterile Eppendorf, and centrifuged at 20,000 x g for 1 minute to pellet the bacteria. The supernatant was removed via pipette and disposed of into a container of virkon. The remaining bacterial pellet was resuspended in 250µL P1 buffer. Subsequently, 250µL P2 buffer was added to the Eppendorf, inverted 4-6 times to mix and left for 5 minutes to allow the cells to lyse. Lastly, 350µL of N3 buffer was added and triturated using the tip, inverting 4-6 times to neutralise the enzyme before centrifuging at 20,000 x g for 10 minutes.

After the neutralisation steps were complete the DNA needed to be isolated. The supernatant was transferred into a QAIprep spin-column. The column was centrifuged for 30 - seconds at 20,000 x g to pull supernatant through and bind the DNA to the column, discarding the Flowthrough. After the column was washed with 0.5mL PB buffer and centrifuged for 30 seconds at 20,000 x g, discarding the flow-through. The column was washed one last time with 0.75mL PE buffer, centrifuged for 30 seconds at 20,000 x g, and flow-through was discarded. After having discarded the flow-through the empty column was centrifuged again for an extra 30 seconds to remove any residual buffer contained within the tube for disposal.

The spin column containing the isolated DNA was transferred into a clean aliquot to elute the DNA. DNA was eluted with 60µL EB buffer applied to the column and left to stand for 1 minute before centrifuging for 1 minute at 20,000 x g. DNA concentrations were quantified using a Nanodrop 2000 spectrophotometer (Thermo Fisher Scientific). 1µL of elution was measured.

2.9   Polymerase chain reactions (PCR)

	50µL reaction	50µL reaction master mix
5x Gotaq buffer green	10	10
MgCl$_2$	3	3
DNTP	0.5	0.5
Forward primer	5	5
Reverse primer	5	5
DNA Polymerase	0.25	0.25
Target	2	-
Double distilled water	24.25	24.25
Total	50	48

2.9.1 PCR components

Polymerase chain reactions (PCR) reactions were conducted to screen for upregulated genes to be investigated further using quantitative PCR analysis. 50µL reactions were conducted following the supplier's instructions. All components, 5x Gotaq buffer green (Promega #M891A), MgCl$_2$ (Promega #A351B), DNTP, forward primers, reverse primers, target, and G2 Flexi DNA Polymerase (Promega #A351B) were removed from storage at -20°C, defrosted and vortexed before use. The DNA Polymerase and 5x Buffer were kept on ice until needed. First, a reaction master mix was prepared by combining all the components in a PCR tube, DNA polymerase and the target DNA were added last to prevent contamination. Once all components were added the PCR tubes were placed into the centre of a BioRad C1000 Thermal cycler.

The PCR protocol consisted of 35 cycles of (95°C for 1 minute, 95°C for 30 seconds, 55°C for 30 seconds, 72°C for 30 seconds), and a final incubation phase at 72°C for 5 minutes. Reactions were cooled to 4°C and held at that temperature until removal from the machine. PCR products were run on 1% agarose gel.

2.9.2 Pouring gels

Gels were prepared fresh prior to running. 50mL of 0.5x TBE was measured into a beaker. 0.5g of agarose powder (Invitrogen #16500-1000) was added to the TBE (1% agarose solution concentration). A microwave set to 600W was used to heat the agarose for 2 minutess until the agarose fully dissolved. Cooling the molten agarose in a larger beaker of water to a reasonable temperature to handle. 2.5µL SYBR Safe DNA dye (Invitrogen #2123950) was pipetted into the agarose solution and stirred for 30 seconds by hand before pouring the gel into a gel run holder (Cambridge Electrophoresis) with an appropriate well comb insert and left to set in the fridge at 4°C for 1 hour.

2.9.3 Loading and running PCR gels

End slips and well comb inserts were removed before pouring 50mL of 0.5x TBE into the run tray, covering the gel completely. The first well of each gel run was loaded with 10µL of a 50bp gene ruler (Thermo Scientific #SM0371). The rest of the wells were loaded with 10µL of the PCR products, loaded as groups of three control, FGF2 and TGFβ1, and BMP9, leaving no gaps between loaded wells to help improve the run quality. When using 5x Green Gotaq flexi buffer no loading dye was required as the buffer contains a running dye, however, if the colourless buffer was used a 6x purple loading dye (Biolabs, #B7024S) was added. Gels were run at 70mV for a period of 1 hour or until the running band had reached the end of the gel. Gels were imaged using a BIORAD Chemidoc MP, selecting for SYBR

Safe imaging on a mini gel. The images captured were analysed using the built-in software to identify differences in band intensities between Control, BMP9, and FT samples to identify gene targets worthy of further analysis using quantitative PCR (qPCR) to identify increases in gene expression.

2.9.4 PCR primer Sequences

All the primers used for PCR reactions were provided by Eurogentec unless specified otherwise.

Gene	Forward primer	Reverse primer
bMMP3	CCATGGAGCTTGTTCAGCAATA	GTCACCTCCAACCCAGAAA
bMMP7	GGCAGCTGGCTCAGGACTAT	ATCCTTCCATCCGCTTGAGTC
bMMP8	AGCTGACCTACAGGATTGTGA	TGCTTCTTCGTCCAAGGTCC
bMMP11	TGGTTCTTCCAAGGAGCTCAG	GTTCTTCTCGGAGCCCCAC
bMMP12	ATTCTTTGGGCTTCCCCTCC	TCTCCTCTCGTCATACCTCCA
bMMP14	TAAGATGCCCCCTCAACCCA	AGAACCAACGCTCCTTGAAGA
bMMP16	CCAGAAGATATACGGTCCGCC	CAAGGATACGAAGGTCTGCC
bADAMTS1	TGCCCGGAGAATAACGGAAA	CTCCCGCGTACTTGGGTATC
bADAMTS8	TACGGAGAGGCCTAGAGAACC	AGTATCAGCCCGCTGTTGTC
bADAMTS9	GCACCCGAGGCAAGTGAAAT	TGTACGTTCGTGGGAAAGGG
bADAMTS15	CCAACAAGTACCGGGTGGAC	AGCGGTATTTCACCCTCACG

2.10 cDNA reactions

Components	50µL reaction	50µL reaction master mix
5x RT buffer	10	10
DNTP	1	1
RNase inhibitor	1	1
Random primers	1	1
Reverse transcriptase	0.5	0.5
Target	500ng RNA – volume dependent on concentrations	
Double distilled water	Makeup to 50µL	
Total	50	13.5

RNA isolated from 10.5-day and 21-day cultured control and BMP9 explants was used to synthesise cDNA for qPCR analysis. All chemicals used for cDNA reactions were provided by Promega along with the random primers. cDNA synthesis was conducted following the manufacturers protocol. 5x RT buffer (Promega #M531A), DNTPs, random primers (Promega #C118A), reverse transcriptase (Promega #M170A), RNA target, and RNase inhibitor (Promega #N251A) were removed from -20°C storage mixed, centrifuged and kept on ice. A "reaction mixture" was created for each reaction by combining the 5x RT buffer, DNTPs, RNase, reverse transcriptase, and the random primers for all the reactions in an Eppendorf, vortexing the components.

For the reactions 500ng of the target RNA solutions were added to the PCR reaction tubes (variations in volumes used dependent on RNA concentration) along with the random primers, heated to 70°C for 5 minutes, and then cooled on ice for 5 minutes to form a annealed primer-RNA template. After which 13.5μL of the reaction mixture was added to each PCR tube, triturating with the pipette tip to mix the reaction solutions. Reactions were run in a T100 Thermal cycler (BioRad), following a protocol of 25°C for 10 minutes (annealing), 42°C for 1 hour (extension), 95°C for 5 minutes to inactive reverse transcriptase, before cooling to 4°C until collection from the machine. After removal from the thermal cycler an additional 50μL of distilled water was added to the cDNA products to reduce the concentrations to 5ngμl^{-1} before freezing for storage at -20°C.

2.11 qPCR

2.11.1 Primer preparation
 All primers were supplied by Eurogentec in stock concentrations of 100μm. Primers were diluted to working concentrations of 3μm and stored at -20°C as stocks ready for direct use when required.

Gene	Forward primer	Reverse primer
bMMP1	CAAATGCTGGAGGTATGATGA	AATTCCGGGAAAGTCTTCTG
bMMP2	CTGGTGTCCAGAAGGTGGAT	TAGGCGCCCTTGAAGAAGAAGTA
bMMP3	CCATGGAGCTTGTTCAGCAATA	GTCACCTCCAACCCCAGAAA
bMMP9	GGAGATTAGGAACCGCTTGC	GAACAGCAGCACCTTACCCTC
bMMP13	TGGTGATGAAACCTGGACAA	GGCGTTTTGGGATGTTTAGA
bADAMTS4	CTCCATGACAACTCGAAGCA	CTAGGAGACAGTGCCCGAAG
bADAMTS5	CACCTCAGCCACCATCACAG	AGTACTCTGGCCCGAAGGTC
18SRNA	CACTGGAGGCCTACACGCCG	AGGCAATTTTCCGCCGCCCA
TIMP1	CACCCACAGACGGCCTTCT	CTGGTATAAGGCAGTTTCATTGACTT
TIMP2	GCTGGACATTGGAGGAAAGA	CGTCCGGAGAGGAGATGTAG
TIMP3	GCCGGATGCAAGCGTAGT	GATGTACCGAGGATTCACCAAGAT

2.11.2 Making qPCR standards
Target genes were replicated in XL1-blue bacterial cells and isolated to create DNA stocks at concentrations of 0.5ngμl^{-1} (Chapter 2.8). The stocks were used to create serial dilutions for each target gene at concentrations 1ngmL^{-1}, 100pgmL^{-1}, 10pgmL^{-1}, 1pgmL^{-1}, 100fgmL^{-1}, 10fgmL^{-1}, 1fgmL^{-1}. Serial dilutions were completed as 1:10 dilutions making up each concentration to a total volume of 1mL. 2μL of DNA stock (0.5nguL^{-1}) was added to 998μL of double distilled water. Proceeding to remove 100μL and pipette it into the next dilution tube containing 900μL double distilled water until all dilutions were complete.

2.11.3 qPCR of explant cDNA

	1x (μL)	18x reaction master mix (μL)

2x SYBR green	7.5	135
Forward primer	1.5	27
Reverse primer	1.5	27
Target	2	-
Double distilled water	2.5	45
Total	15	234

A "Reaction master mixture" was prepared for each gene tested, constructed from 2x SYBR green master mix (Promega #A600A), forward primers, reverse primers, target DNA and double distilled water. cDNA produced from 21-day cultured explants was used as the target for qPCR runs (Chapter 2.10). 15μL qPCR reactions were used to reduce pipetting errors that were prominent when using smaller reaction mixtures. The master mix, primers, and sample were removed from storage at -20°C, vortexing and centrifuging each. Master mix, primers and distilled water for all the PCR reactions were all mixed in an Eppendorf to create a "reaction mixture". 13μL of the reaction mixture was pipetted into wells of a 96-well qPCR plate. 2μL of the samples was pipetted in duplicate into the wells that contained the reaction mixture. 2μL of the standards (2.11.2) and 2μL of double distilled water used as the NTC (non template control) were pipetted in duplicate into the final two columns of the plate. An adhesive film was used to seal the plate before centrifuging to mix samples with the reaction mixture and remove air bubbles. Plates were placed in the qPCR machine CFX96 Real-Time System C1000 Thermal cycler, and a rubber card was used to ensure the film had formed a good seal.

The qPCR thermal cycler followed a protocol of 40 cycles of (95°C for 10 minutes to denature any active enzymes RNase or DNase, 95°C for 10 seconds DNA melt, 60°C for 10 seconds DNA annealing and 10 seconds for extension, Fluorescence plate read, 72°C for 30 seconds). Finishing with a melt curve from 65°C to 95°C at 0.5°C increments.

2.11.4 qPCR analysis

CFX96 Real-Time System C1000 Thermal cycler output the qPCR data as the values of the starting concentration based on the number of cycles required to surpass the threshold. Using this data absolute values were used for comparison between control and BMP9 explants at day 10.5 and day 21. Relative gene expressions were also found by normalising BMP9 expression levels to control explant expressions at the same time point for a direct comparison of the relative changes in BMP9 expression at the two different time points.

2.12 DreamTaq PCR and TA cloning for DNA standards

2.12.1 DreamTaq PCR components

Recombinant DreamTaq polymerase (Thermofisher #EP0401) was used to produce DNA strands for insertion into vectors. DreamTaq PCR was completed with primers for *bMMP1*, *bMMP13* and *COL2A1* which we had struggled to replicate using pGEM-T plasmids transfected in XL-1 Blue FCC cells. The primers used were the same used for PCR reactions supplied by Eurogentec. The DreamTaq enzyme was used as it doesn't cleave the A-tails at the ends of amplified DNA sequences, unlike most Taq polymerases. Therefore, the amplified DNA strands produce overhangs used as inserts for recombinant vectors to be cloned in FCC cells. DreamTaq reactions were completed following the manufactures instructions provided.

2.12.2 DreamTaq PCR amplification and gel run

All components were stored at -20°C. On removal from storage, components were defrosted in a 37°C water bath. The target cDNA used was from a BMP9 21-day cultured 4mm diameter bovine explant previously used to genetic screening (Chapter 2.9), known to express the genes of interest at a high level. The reaction mixture was prepared by adding all the components into a PCR tube that was kept on ice. Taq polymerase and the DNA target were the last two components to be added to the reaction. Reactions were run immediately on a BioRad C1000 Thermal cycler PCR machine for 35 cycles. The protocol consisted of initial denaturing at 95°C for 1 minute, then 35 cycles of: 95°C denaturing for 30 seconds, 53°C annealing for 30 seconds, and a 72°C extension for 30 seconds. Reactions were held at 12°C after all the cycles were completed. PCR products were loaded into 0.1% agarose Gel using a 6x loading dye (Biolabs, #B7024S) following the standard PCR gel preparation and electrophoresis procedures previously stated (Chapter 2.9). 20μL of PCR product and 3.5μL 6x loading dye were mixed in a PCR tube before loading. The gel was run at 70v for 1hr or until the running dye reached the end of the gel .

	100μL reaction	100μL reaction master mix
10x Dream Taq Buffer	10	10
MgCl$_2$ 25mM (Promega)	6	6
DNTP	1	1
Forward primer	10	10
Reverse primer	10	10
DreamTaq polymerase	0.5	0.5
Target DNA	2	-
DDW	78.5	78.5
Total	100	98

2.12.3 PCR DNA purification

PCR purification was completed using a QAIquick PCR purification kit (QIAGEN #28104) following the manufacturer's instructions. 400μL of PB buffer was added to 80μL of the DreamTaq PCR product and vortexed until yellow (5:1, Buffer: Product). The solution was poured into a QAI Quick spin column and centrifuged for 30 seconds at 10,000rpm. After centrifuging 750μL PE buffer was added to the QAI Quick column and centrifuged for 30 seconds at 10,000rpm. Residual waste was removed from the column by centrifuging for an

additional 1 minute then each column was placed in a clean centrifuge tube and the DNA was eluted with 60μL EB buffer. Purified PCR products were stored at -20°C.

2.12.4 Purified DreamTaq DNA insert and vector ligation

	15μL reaction	10μL reaction master mix
10x T4 ligation buffer	1	1
T4 ligase	1	1
Vector pBluescript SK+	1	1
DNA Insert	5	-
Double distilled water	2	2
Total	10	5

T4 ligase and T4 ligation buffer were removed from -20°C storage and kept on ice. All the reaction components were added to a sterile Eppendorf in the order listed, 1μL T4 ligation buffer (Promega #C126A), 1μL T4 DNA Ligase (Promega #M1808), 1μL pBluescript SK+ vector (stratagene #XB-VEC-1221267), 5μL DreamTaq purified PCR DNA insert, 2μL double distilled water. Reaction tubes were left overnight at room temperature to allow for the ligation process to occur.

2.12.5 Vector transfection of pBSTA

Vector transfection of pBSTA cells followed the same procedure as specified for XL1-Blue cells (Chapter 2.8.1). The only adjustments were the addition of 10μL of 1M IPTG (Sigma #16758-1G) and 20μL of 50μgmL^{-1} XGal (Molecular Probes, #B-1690) to the transfection tubes before being placed into the water baths for 10 mininutes prior to plating. Amp plates were used to plate the cells. With the addition of IPTG and XGal recombinant bacteria remain colourless as the lac gene was disrupted, providing easy identification of successful colonies. Plates were incubated at 37°C in a 4.0% carbon dioxide atmosphere.

2.12.6 Overnight culture and miniprep

Colourless colonies were isolated from the XGal plates and cultured following the previously stated bacterial overnight culture and miniprep procedure to isolate the cloned DNA vectors from the cells (Chapters 2.8.2-2.8.3).

2.12.7 pBSTA restriction

pBSTA restrictions were conducted to check if the recombinant cells did indeed contain the DreamTaq PCR inserts.

	15μL reaction	5μL reaction master mix
10X buffer C (Promega, #R003A)	1.5	1.5
Pst1	1	1
HindIII	1	1
Spermidine	1.5	1.5
DNA sample	10	-
Double distilled water	0	0
Total	15μL	5μL

All reaction components were removed from -20°C storage, defrosted in a water bath, vortexed, and centrifuged before use. A "reaction mixture" was created in a fresh Eppendorf by pipetting all the components into a DNase and RNase-free Eppenorf. 10μL of DreamTaq cloned and purified plasmids were the last component to be added to the tube, incubated at 37°C for 1.5 hours in a water bath (Grant sub aqua 26 plus). Restriction enzymes Pst1 (Promega, #R611B) and HindIII (Promega, #R604A) were chosen to excise the gene inserts as they flanked the EcoRV insert region containing our DNA inserts. Restriction products were removed from the water bath after 1.5 hours and loaded into 0.1% agarose gels. 6x loading dye was added to the restriction product before loading. Two gene rulers were used, a 50bp ruler and a larger DNA fragment ladder OX174 RF DNA Hae III fragments (Gibco #15611-015). 10μL of each sample or ruler was pipetted into individual consecutive wells. Gel runs were completed at -70mv until run dye reached the end. The gels were imaged with a BIORAD ChemiDoc MP.

Recombinant vectors containing the gene insert were sent for sequencing after confirming the presence of inserts via restriction and 5μL of plasmid (3.7nM) was pipetted into an Eppendorf along with 5μL M13 F/R primer (5μm). M13 sequence: GTA AAA CGA CGG CCA GTG.

2.13 Statistical analysis

Statistical testing was performed using GraphPad (Prism), tests were assumed to be significant if p-values < 0.05. Initially data was tested for normality using Shapiro-wilks statistical test for normality as it has a higher power than its common competitor the Kolmorgorov-Smirnov even with lilliefors corrections. A p-value < 0.05 indicated that the data was normally distributed. Using this information and based on the other parameters of the data being analysed the appropriate tests were selected.

T-test were used to test for the significance between two groups of parametric data with categorical input variables. Alternatively, if the data was non-parametric but satisfied the same conditions a Mann-Whitney U test was used. It is less accurate than the T-test as additional assumptions have to be made as with all non-parametric tests.

One-Way ANOVAs were completed for normally distributed data with two or more groups with categorical input variables. If results were significant then it would be followed up by conducting a Post-Hoc test. Tukeys HSD Post-Hoc test was used to identify which of the groups were significant from each other. For non-parametric data with two or more categorical input variables the Kruskal-Wallis non-parametric test was the best option, it was used as an alternative to an ANOVA as parametric tests make certain assumptions which cannot be applied to non-parametric data. It is also important to note that due to the lack of these assumptions non-parametric tests are not as powerful. With regards to Post-Hoc testing of non-parametric data there are many options to choose from, however, there is not one specific test that excels above the rest each comes with its positives and negatives. Therefore, DUNN non-parametric Post-Hoc was used as it is one of the more common methods used.

For some data sets Two-way ANOVAs were used alongside T-tests. Where T-tests can provide significance between two groups of data focusing on one set of independent variables. Two-way ANOVAs test groups of data with multiple independent variables. e.g. when testing for significance between 1. the effects of BMP9 on 2. mature and Immature pellets. The benefit of the Two-way ANOVA is its ability to measure variance between the

effects of BMP9 and the variance between the mature and immature data simultaneously and individually instead of having to conduct multiple tests for the different variables.

Chapter 3: Results

3 Immature bovine explants cultured with BMP9

3.1.1 Introduction

Postnatal maturation during puberty is critical to cartilage development, as it undergoes reorganisation of the extracellular matrix (ECM), allowing for life-long cyclical weight-bearing performance. Following maturation, collagen fibrils of the ECM form arcade-like patterns which are hallmarks of the transition through maturation. There is limited knowledge regarding the processes involved in maturation, but a recent paper has identified that BMP9 growth factor induces fingertip regeneration in mice, including reconstitution of an intact synovial joint with histologically mature articular cartilage. Additionally, chondrocytes cultured *in vitro* with BMP9 have been shown to differentiate, producing cartilage with collagen fibrils aligned perpendicularly to the surface. Therefore, we hypothesise that BMP9 induces postnatal-like maturation of articular cartilage, causing the reorganisation of collagen fibrils into an adult-like configuration. To study maturation *in situ*, we used 4mm explant cultures of immature bovine articular cartilage.

The hypothesis was tested in 3 ways:

1. Histological, immunological, and biochemical analysis of BMP9 treated immature bovine cartilage explants were conducted to identify changes in tissue structure and morphology. The latter was supported by image analysis to quantify any changes observed.
2. qPCR studies were performed to determine which genes were key to BMP9-induced articular cartilage maturation.
3. Using the data collected, inhibitor assays of BMP9 induced cultures were completed to identify the participating enzymes.

3.1.2 Method of immature explant culture with BMP9

4mm bovine explants were collected from immature bovine metacarpophalangeal joints. Adjacent explants were collected from the same joint to be used as control and BMP9 samples. A third explant was taken as a Day 0 control. After collection the explants were washed once in DMEM, their initial wet weights were measured in bijou tubes containing 1mL of DMEM and then the explants were placed into well plates. 1.5mL of chondrogenic media was added to each well, 3.7nM BMP9 was added fresh to the chondrogenic medium before every feed. Culture media was changed every three days, and 0.5mL of the waste medium was collected at every feed for biochemical analysis. Explants were cultured for 21 days, at the end of the culture period they were reweighed and processed for either histological, biochemical, or genetic analysis.

3.1.3 Changes in collagen organisation observed using polarised light

Figure 2 shows histological images captured of immature control and BMP9 explants cultured for 21 days, embedded for wax sectioning, and stained with picrosirius red (PSR). Picrosirius red selectively stains collagen fibrils of the ECM network which can be visualised using light or polarised light microscopy (PLM). When viewed using PLM aligned collagen fibrils cause the light to refract adopting bifringent properties. Control explants stained with picrosirius red and visualised under normal light microscopy displayed relatively uniform levels of staining across the tissue weakening slightly just below the surface at the start of the midzone of the section (Figure 4A). In comparison, BMP9 explants displayed a varied pattern of staining across the sections in all three zones (Figure 4B). The inconsistencies in the staining viewed under normal light conditions indicate a variation in the density of the collagen network in BMP9 cultured explants. It is important to note that the sectioning process introduced some artefacts affecting the clarity of the stains as can be seen in the bottom left corner of the control section (Figure 4A). Under polarised light the difference between control and BMP9 sections was abundantly clear (Figure 4C-D). In the superficial layer there was intense birefringence parallel to the surface caused by highly aligned fibres running parallel to the surface. Below this region there is a darker blue/green region where the collagen fibres are oriented transversely to the surface. The reason for this change in colour is likely due to a reduction in aligned collagen fibres. Further down in the deep zones, fibres resumed parallel orientations to the surface. The intensity of birefringence in the controls corresponded to the fibril alignment parallel to the surface. In comparison to controls the PLM images captured of BMP9 treated explants showed a significant change in the collagen organisation. The superficial regions retain a bright fluorescence where the fibres are still aligned parallel to the surface. But in the midzone of the sections there was an intense fluorescence of fibres perpendicular to the surface which extended down into the deep zones of the cartilage tissue, a significant change compared to what was visualised in control explants. The reorientation of collagen fibres in BMP9 explants to adopt a perpendicular alignment is an organisational feature commonly observed in mature cartilage.

Some of the explants cultured in control chondrogenic medium and viewed under PLM contained collagen fibres aligned perpendicular to the surface within the mid zones of the tissue (Figure 5A). In the explants where limited amounts of collagen reorganisation was visible in controls the BMP9 treated adjacent explants had undergone significantly greater depths of collagen reorganisation (Figure 3B).
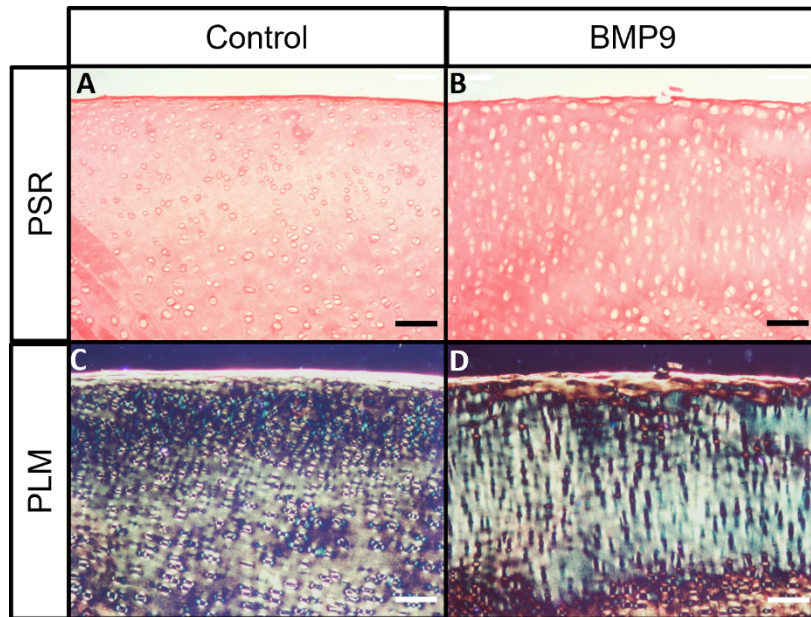
Figure 4. Picrosirius red staining of BMP9 cultured explants revealed collagen matrix organisational changes. 4mm immature bovine explants were cultured for a period of 21 days in control chondrogenic media or with 3.7nM BMP9. Explants were fixed post culture for wax sectioning and stained with picrosirius red. Sections were viewed under normal light (PSR) or using polarised light microscopy (PLM). Control and BMP9 explants were collected from adjacent locations of the joint to neutralise any site-specific effects of tissue maturity. Figures show the top 500μm of the explants tissue, representative of 4 independent samples. Scale bar = 100μm
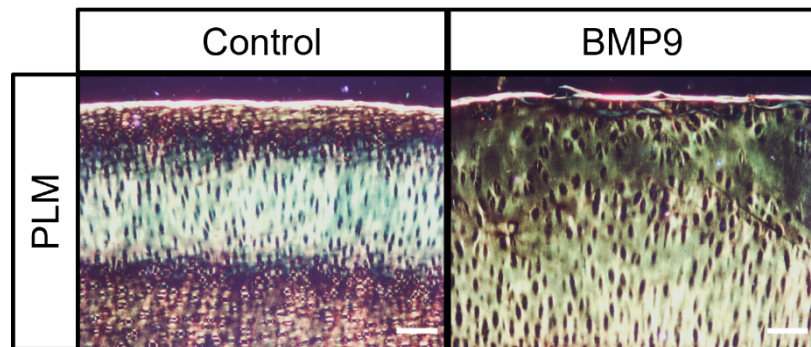
Figure 5. PLM imaging of PSR stained sections reveals some control samples undergo limited amounts of collagen reorganisation. Immature bovine explants were cultured for 21 days in control chondrogenic medium or with 3.7nM BMP9. Explants were fixed post culture for wax sectioning, stained with picrosirius red and viewed using polarised light microscopy (PLM). Figures show the first 500μm from the tissue surface of the sections, representative of 4 independent samples, Scale bar = 100μm

3.1.4 Quantification of collagen reorganisation in BMP9 cultured explants

Immature bovine explants were cultured for 21 days in chonrogenic media with or without BMP9, fixed, sectioned, stained with picrosirius red, and viewed using PLM. Under PLM collagen fibres aligned perpendicular to the surface of the explants appeared darker in colour due to a combination of their orientation and alignment relative to the light source. The extent of collagen reorganisation in the stained sections perpendicular to the surface of the explants was quantified using FibrilJ, an ImageJ plug-in (Figure 6). The mean depth of perpendicular fibres significantly increased between control and BMP9 cultured explants ($P<0.01$) from 304µm±133µm to 662µm±183µm respectively. This indicates BMP9s ability to promote collagen reorientation within immature articular cartilage explants. Some control explants also exhibited a degree of reorganisation of the collagen network. These changes suggest that the chondrocytes of immature explants can induce some reorganisation without additional external stimuli. To account for differences in cartilage maturity of the explants at the time of collection, the depths of collagen reorganisation were compared in pairs with controls to provide a ratio for the change in depth of collagen reorganisation over the culture period. When compared in a pairwise manner BMP9 cultured explants had a 2.4-fold increase in the depth of perpendicularly aligned collagen fibres relative to controls.
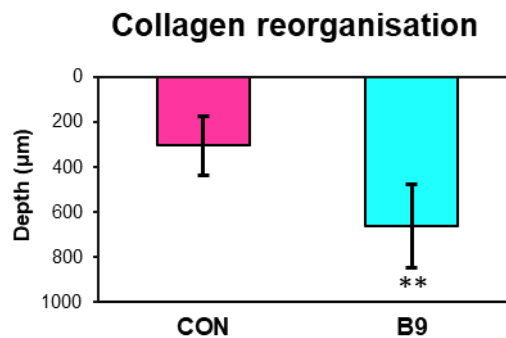

Figure 6. Quantitative image analysis of perpendicular collagen fibre depths in BMP9 cultured explants. 4mm immature bovine explants were cultured for a period of 21 days in control chondrogenic media or with 3.7nM BMP9. Growth medium was changed every 3 days. Explants were fixed, sectioned, and stained with picrosirius red. Image analysis was conducted using ImageJ to determine the mean depths of collagen reorganisation identified by a shift in picrosirius red staining to a blue/green colour indicating the presence of vertically aligned fibres. The thinnest and thickest depths were measured for each explant to find a mean. An overall mean value for each set of four explants cultured in the same conditions was calculated. Measurements were compared in a pairwise manner with controls to calculate the relative increase in collagen reorganisation. The means for 4 independent samples were plotted, error bars represent the standard deviations. ** P <0.01 versus controls, T-Test.

3.1.5 Changes in collagen orientation in BMP9 cultured explants

Variations in collagen orientation with depth were measured in top 500μm of 21-day cultured explants in which changes in collagen organisation were observed using polarised light microscopy (PLM). Using FibrilJ an ImageJ plug-in, PLM images were analysed in 5 regions, 100μm in depth and of equal width (Figure 7A). Collagen fibre orientations were measured from 0°-90° relative to the tissue surface. Collagen fibrils present in the regions 1-5 of controls (increasing with depth) were orientated at 5.3°, 69.3°,44.2°,46.3°, and 24.9° to the tissue surface. In BMP9 treated explants the fibres measured in regions 1-5 were orientated at, 28.5°, 85.9°,86.8°, 86.5°, and 86.3° (Figure 7B).

The superficial fibres found within the first 100μm of control and BMP9 explants were almost parallel to the surface at 6° and 28.5° orientations to the surface respectively. At depths of 200μm the collagen fibres in control explants were orientated at 60° to the surface, almost perpendicular. However, with increasing depth the fibres became less perpendicular and returned to an almost horizontal orientation at 500μm. Whereas, in BMP9 treated explants fibres retained perpendicular orientations throughout the mid and deep zones, where they remained orientated at 86° to the surface. This demonstrates an increase in the abundance of perpendicularly aligned fibres within the top 500μm of BMP9 treated explants (Figure 7C).
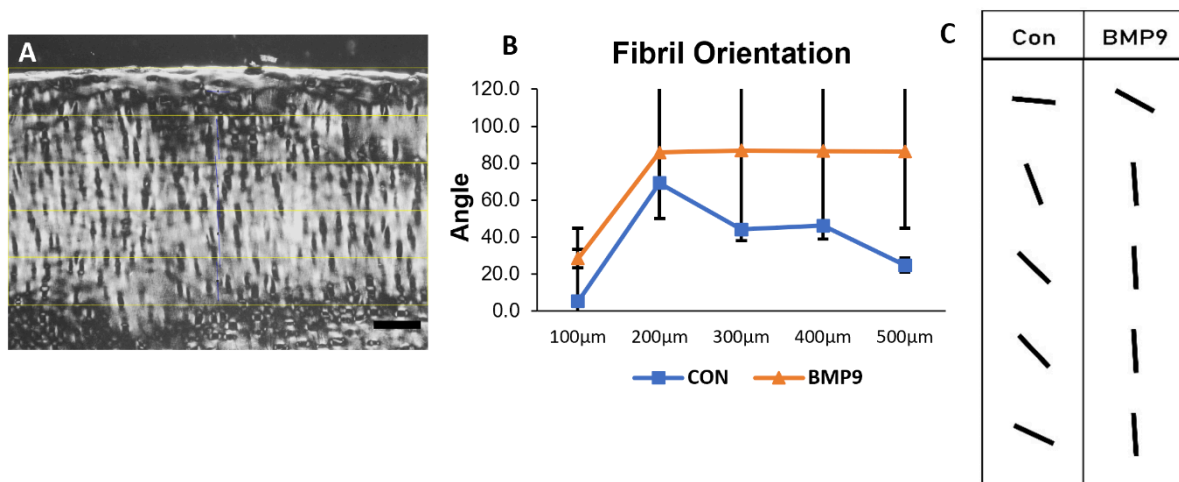

Figure 7. Collagen fibril orientation is altered by culture with BMP9. Explants cultured for 21 days in control chondrogenic medium or with 3.7nM BMP9, stained with picrosirius red and viewed using polarised light microscopy, were analysed using ImageJ plug-in FibrilJ to determine the orientations of the collagen fibres. **A** Explants were measured in 5 regions of 100μm depth, **B** the mean collagen orientations of each region were plotted. **C** Mean fibril orientations from the 5 regions were recreated with the correct angles to the x-axis. Data is representative of 4 independent samples, scale bar = 100μm.

3.1.6 Changes in collagen anisotropy in BMP9 cultured explants

Using FibrilJ changes in collagen anisotropy were measured within the same 5 x 100μm regions used to measure fibril orientations (Figure 8). Anisotropy was measured as a value from 0-1, 0 being isotropic and 1 being anisotropic. In control explants the collagen within the first 100μm of explant tissue was isotropic in nature, with a value of only 0.07. Within the deep zones the fibres were still very isotropic, 0.05 at 500μm. The highest levels of collagen

anisotropy in controls was 0.15 in the 3rd region from 200-300μm deep. In comparison anisotropy of BMP9 treated explant sections increased in an almost linear fashion from the superficial to deep zones. In the superficial region BMP9 fibres had an anisotropic value of 0.09 which increased to 0.27 in the 5th region. Collagen fibres of BMP9 cultured explants increased in anisotropy with depth in association with the observed changes in orientation. In control explants there was no clear link between collagen orientation and collagen anisotropy the tissue remained highly isotropic throughout most of its depth.
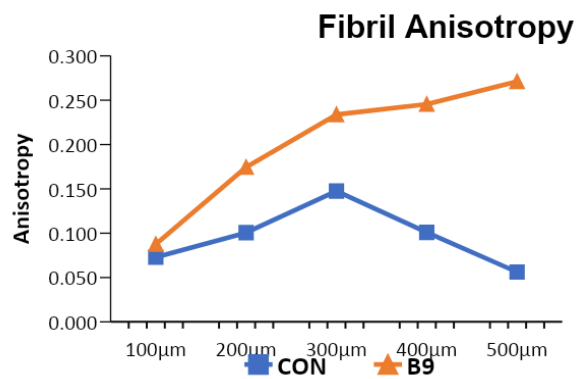

Figure 8. Explants cultured with BMP9 have increased anisotropic collagen organisation. Explants cultured for 21 days with or without 3.7nM BMP9 were fixed, stained with Picrosirius red stained, imaged with polarised light, and analysed using FibrilJ to determine the anisotropy of the collagen fibres. Explants were measured in 5 regions of 100μm depth. Mean fibril anisotropy data is displayed in the graph. Anisotropy is measured as arbitrary units from 0-1, where 0 represents an isotropic organisation and 1 is anisotropic. Data plotted shows the mean values of 4 independent samples.

3.1.7 Remodelling of the collagen network observed using immunofluorescent detection of COL2-3/4m antibody labelling

To detect if the collagen network was being actively degraded in immature treated explants, sections were processed for fluorescent antibody staining of denatured type II collagen fragments using COL2-3/4m antibodies (Figure 9). At days 10.5 and 21 the surface regions of both BMP9 treated, and control explants had negligible fluorescent labelling (Figure 9A-D). However, intense fluorescent labelling was observed at the bottom surface of all the explants, indicating high levels of type II collagen degradation (Figure 9E-D). In histological sections there were clear signs of tissue degradation (*data not shown*) along the bottom surface in all explants, confirmed by COL2-3/4m staining. Thus, the deep zone provides a positive control for each explant validating that BMP9 treatment of immature explants has no effect on collagen degradation in the surface regions of the tissue othwerwise we would expect to see some lablelling as seen within the deeper sections. Day 10.5 control and BMP9 explants were used for no primary controls to dectect the levels of autofluorescence (Figure 10). Within both control and BMP9 treated explants there was no autofluorescence visible within the surface regions, mininmal levels of autoflourescnce were visible in the deep zones, the likely cause of this is the calcified cartilage layer present at the bottom. Therefore the enhanced labelling seen in the deep zones of control and BMP9 teated explants in figure

7 compared to no primary controls is due to active collagen degradation, of which none is present in the surface regions.

Overall, the collagen data shows that BMP9 can induce an organisational change in the collagen matrix of immature bovine explants relative to controls. Inducing an orientational shift in the collagen fibres from mostly horizontal isotropic fibres to partially anisotropic fibres with perpendicular orientations. Interestingly the changes observed in collagen orientations do not require the breakdown of the existing collagen network and thus likely is a reorganisation of the existing collagen fibrils within the tissue.
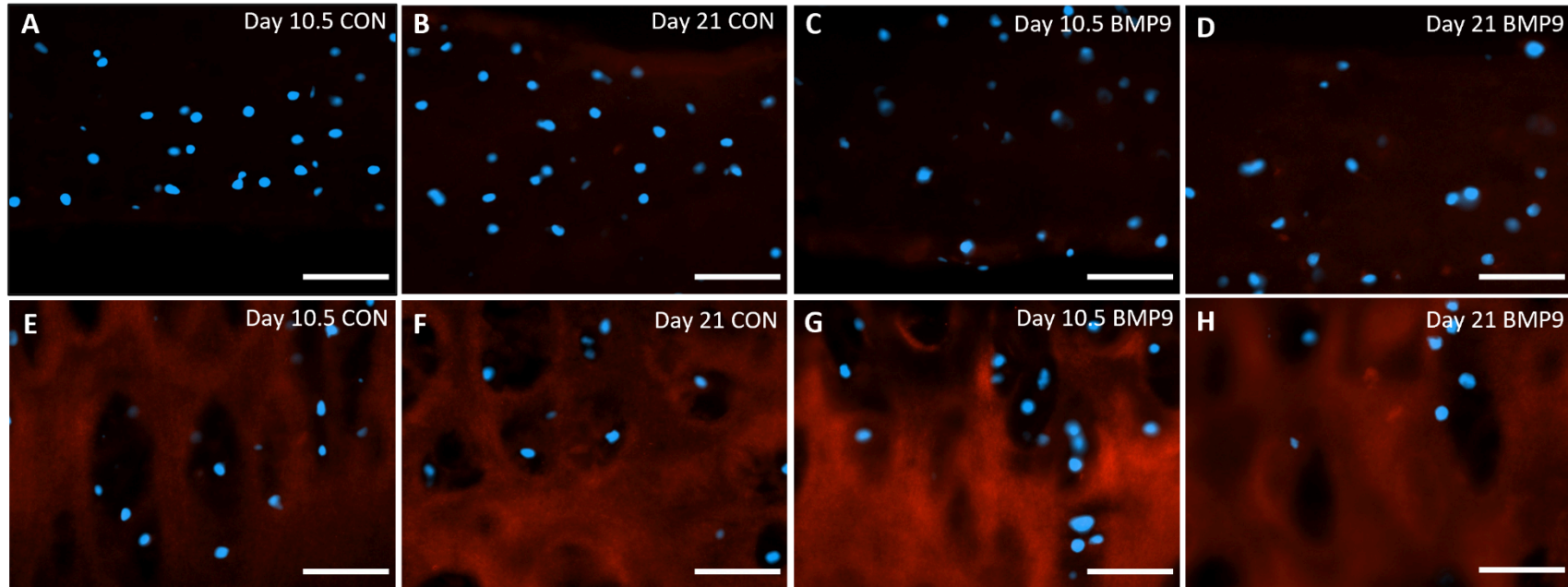
Figure 9. Explants cultured with BMP9 showed no signs of collagen breakdown in the upper zones Explants cultured for 10.5 and 21 days in chondrogenic medium with or without 3.7nM BMP9 were fixed, sectioned, stained with anti-COL2-3/4m antibodies, and imaged via fluorescence microscopy. **A-D** Shows the top 500µm of the control **A-B** and BMP9 **C-D** cultured explants. **E-H** Show the bottom of the control **E-F** and BMP9 **G-H** cultured explants, where tissue degradation was visible, to be used as positive controls for comparison to the surface zones. Counter staining of sections was achieved using a Vectorshield fluorescent mountant containing DAPI. Scale bars = 100µm.
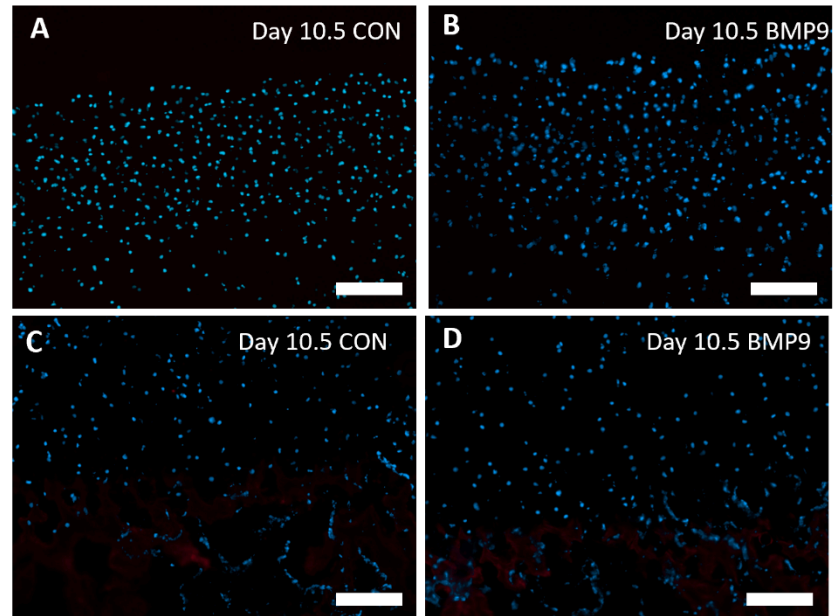
Figure 10. Explants cultured with BMP9 without primary antibody show weak autoflourescnece in the deep zones and Explants cultured for 10.5 and 21 days in chondrogenic medium with or without 3.7nM BMP9 were fixed, sectioned, stained following with anti-COL2-3/4m antibodies, without the primary antibody, and imaged via fluorescence microscopy to idenfiy if any autofluorescence was present. **A** Shows the top superficial 500µm of control and **B** BMP9 cultured explants. **C** Shows the bottom surface of control and BMP9 cultured explants, where weak levels of autofluorescence were visible, counter stained using Vectorshield fluorescent DAPI mountant. Scale bars = 100µm

3.2 Biochemical analysis of BMP9 cultured immature explants

3.2.1 Wet weights and water content of BMP9 cultured explants

Wet and dry weights of immature explants cultured for 21-days were measured to calculate changes in wet weight, dry weight, and water content (Figure 11). BMP9 cultured explants had significantly increased wet weights compared to controls (P<0.05) and both were significantly increased relative to day 0 explants (P<0.05 and P<0.01) respectively (Figure 11B). The dry weights of control and BMP9 treated explants were also significantly increased relative to day 0 explants, however, they were not significant from each other (P=0.13), and thus both must be producing new ECM over the 21-day culture period (Figure 8A). Interestingly the water content of BMP9 treated explants was significantly increased relative to controls (P<0.05). Therefore the increase observed in BMP9 treated explant wet weights is likely to be due to changes in water content and not insoluable components (Figure 11A-D).
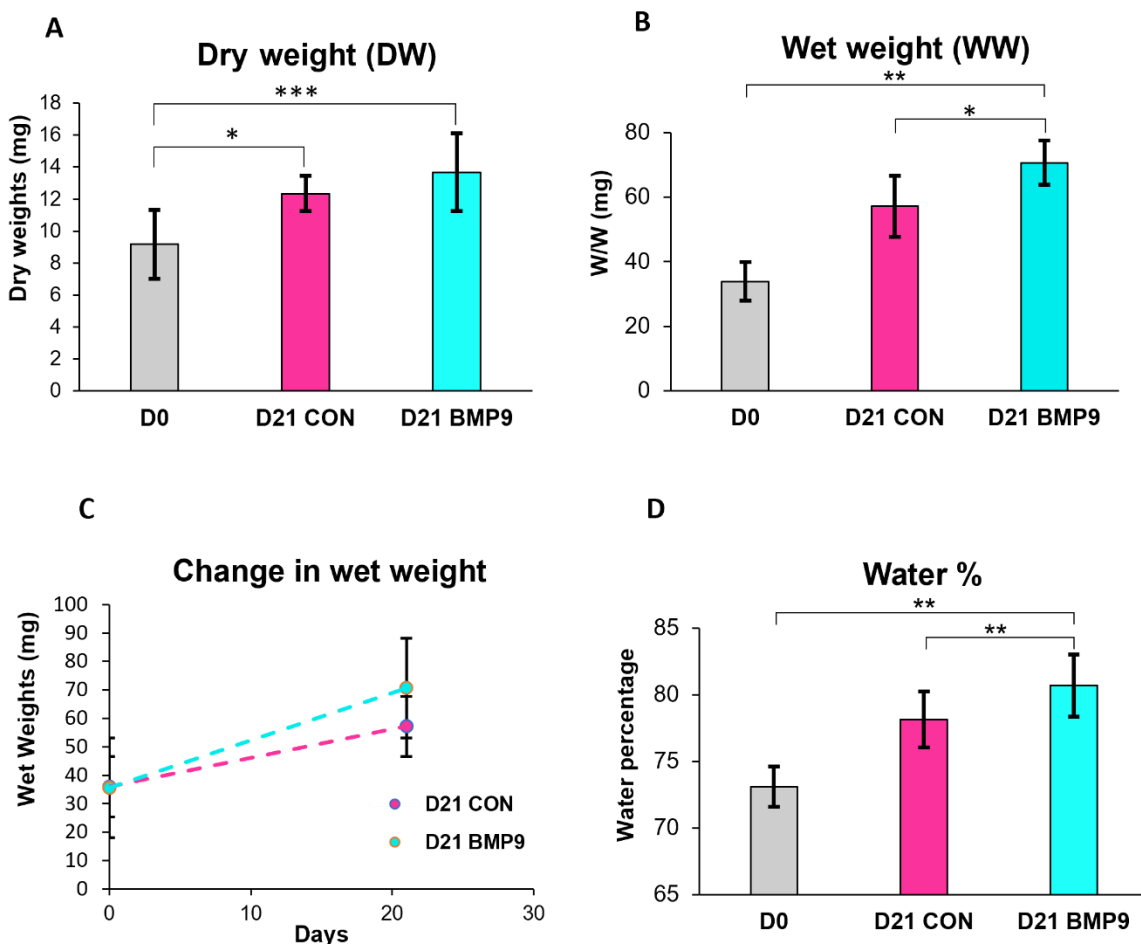
Figure 11. Increases in the Wet and Dry weights of BMP9 cultured explants indicates an increase in ECM and water content. Immature bovine explants were cultured for 21 days in control chondrogenic media (D21 CON) or with 3.7nM BMP9 (D21 B9). Explant wet weights were measured before and after culture. Explants were then dehydrated at 50°C for 24 hours and the dry weights were measured. From the data collected the change in wet weight for each explant was calculated along with the water content of the explants. The mean values of 6 independent samples were plotted in each graph, error bars represent the standard deviations. Data was tested for normality, then either oneway-ANOVA and Tukeys HSD post hoc tests, or Kruskal-Wallis and Dunn post hoc tests were conducted. *P<0.05, **P<0.01, ***P<0.001.

3.2.2 Changes in proteoglycan content of BMP9 cultured immature explants

Immature bovine explants cultured for 21 days in chondrogenic medium with or without BMP9 were dehydrated post-culture, digested with papain, and used for DMMB assays to determine the concentrations of glycosaminoglycans (GAG) (Figure 12). Raw GAG content of BMP9 cultured explants significantly increased over the 21-day culture period relative to the day-0 and day-21 controls 1.4-fold ($P<0.05$) and 2.0-fold ($P<0.01$) respectively (Figure 12A). However, when GAG content was normalised to the wet or dry weights there were no significant differences between BMP9 cultured explants and day 21 controls ($P=0.23$) (Figure 12B).

Waste medium was collected during the culture period to be analysed using DMMB assays to determine the concentration of GAGs lost from the explants (Figure 12C). GAGs lost was calculated as the accumulative loss over the 21-day culture period for comparison between control and BMP9 explants. The concentration of GAGs lost were normalised to the initial explant wet weights to negate any differences that the starting size of the explants might have. Based on the normalised results there was a 1.37-fold increase in the GAGs lost in BMP9 explants relative to day 21 controls ($P<0.01$).

The data shows that compared to day 0 explants there is an increase in the raw GAG content of control and BMP9 explants which are negated when normalised to the wet weights of the explants. The significant difference induced by BMP9 relative to controls was an increase in the loss of GAGs from the explants (Figure 12C). Interestingly normalising the data to the wet weights reduced the increases observed in the GAG content of BMP9 explants suggesting that the increase in GAGs is proportional to the increase in explant weight. As the region of tissue being reorganised is small compared to the tissue as a whole, changes in proteoglycan content may be too small to be reliable indicators of extracellular remodelling.
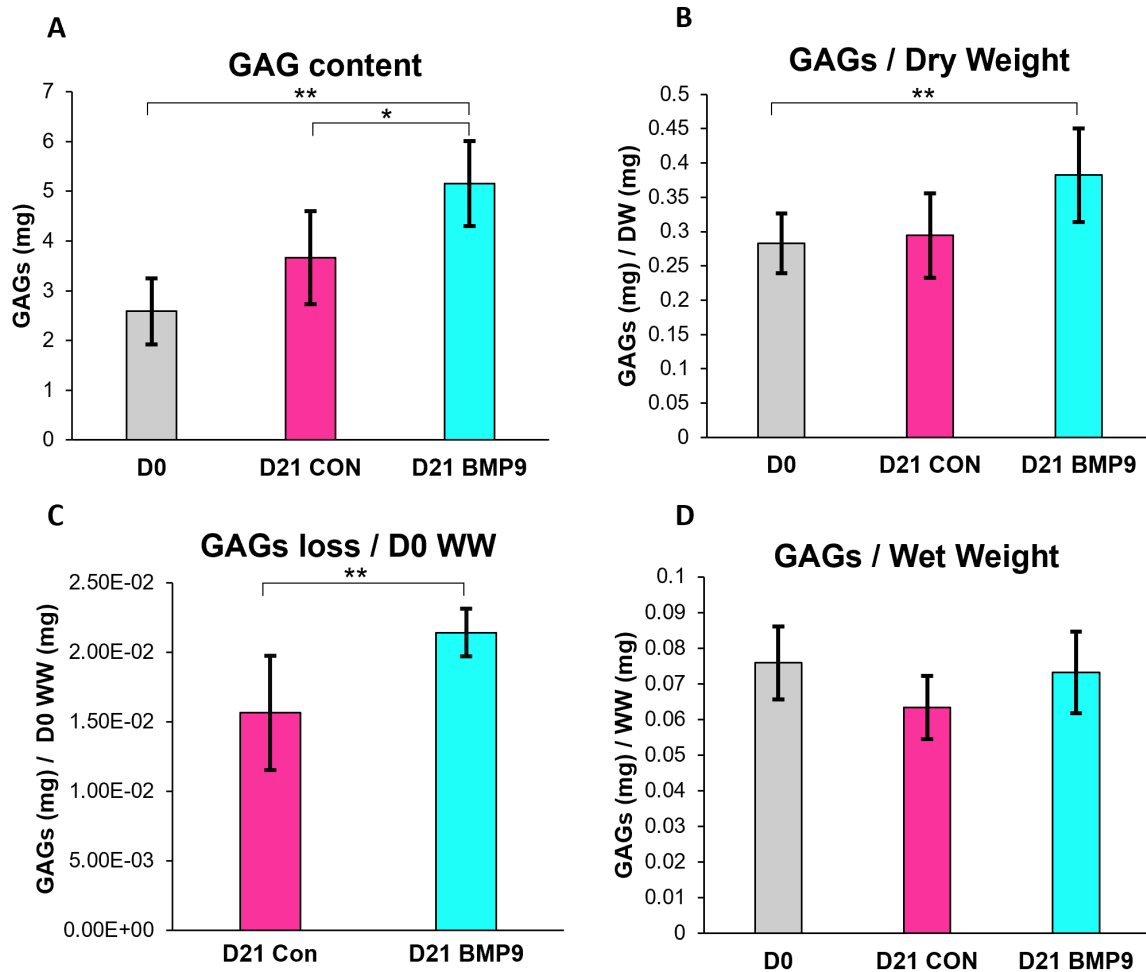
Figure 12. GAG content of cultured explants increases with BMP9 exposure, increases in GAGs is consistent with the increase in water content. Immature bovine explants were cultured for 21 days in control chondrogenic medium (D21 CON) with or without 3.7nM BMP9 (D21 B9). Post-culture explants were dehydrated at 50°C for 24hrs, and digested with papain for use in dimethylmethylene blue (DMMB) assays. GAG content was normalised to the wet and dry weights of each explant. The mean values of 6 independent samples are plotted on the graphs, error bars represent the standard deviation. Data was tested for normality, followed by oneway-ANOVAs and Tukeys HSD post hoc test. *P<0.05, **P<0.01.

3.2.3 Changes in collagen content of explants cultured with BMP9

Immature bovine explants cultured for 21 days in chondrogenic medium with or without 3.7nM BMP9 were dehydrated, digested in papain and used for hydroxyproline assays. Raw hydroxyproline data was converted into collagen content and normalised to the wet or dry weights (Figure 13). Raw collagen content was not significantly different between day 0, and day-21 controls (P=0.49) or BMP9 (P=0.62) treated explants (Figure 13A). However, when collagen content was normalised to explant dry and wet weights both day-21 control and BMP9 treated explants had a 0.7-fold reduction in collagen content compared to day-0 explants (P<0.05) and (P<0.01) for both explants respectively (Figure 13B-C). This data indicates that there was very little or no change in collagen content in BMP9 and control explants over the duration of the 21-day culture period. (Figure 13).
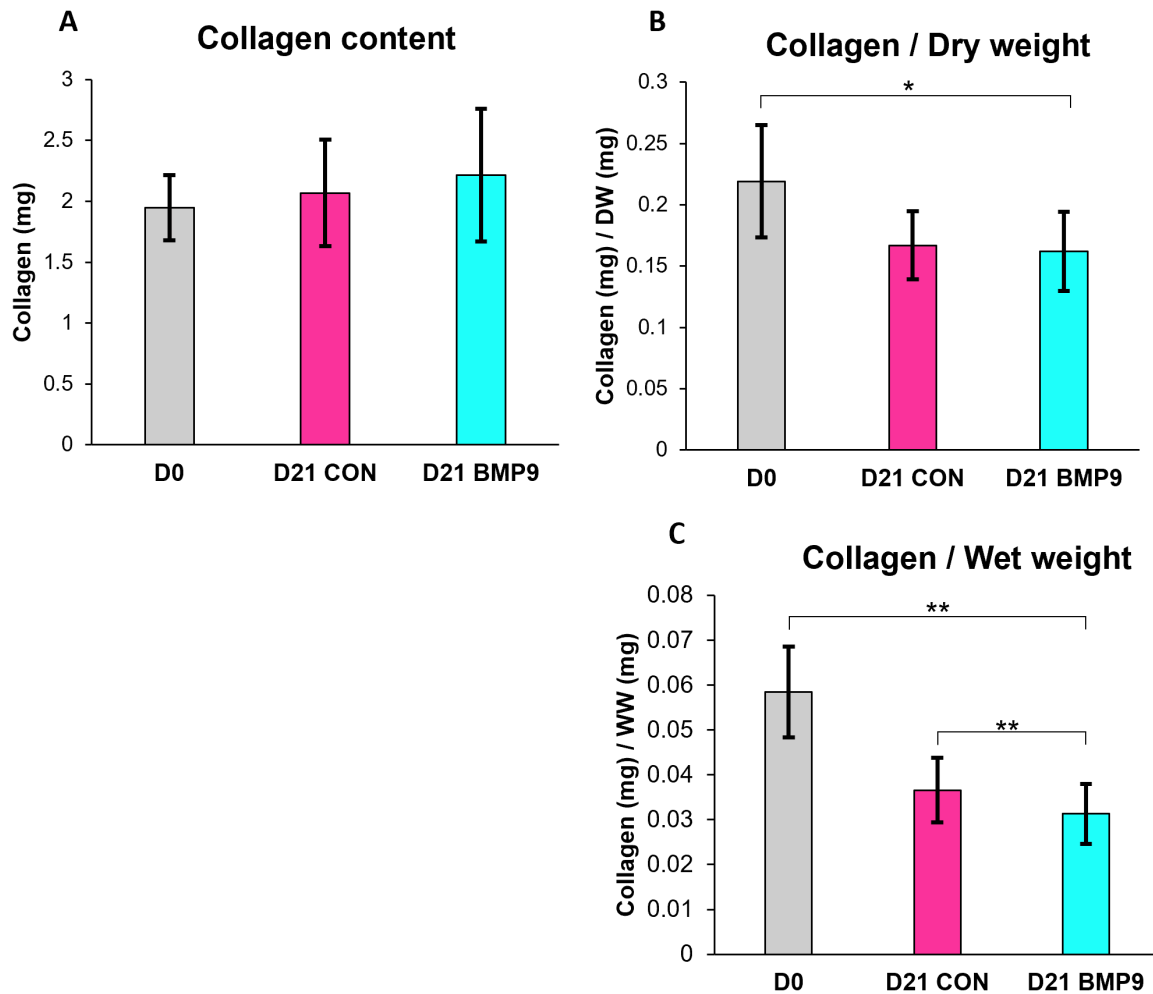
Figure 13. Collagen content of BMP9 explants decreases relative to wet and dry weight. Immature bovine explants were cultured for 21 days in control chondrogenic medium with 3.7nM BMP9 (D21 B9) or without (D21 CON). Post-culture explants were dehydrated for 24 hours at 50°C and digested with papain for use in hydroxyproline assays. Additional to the cultured explants fresh explants (D0) were collected for comparison. Raw hydroxyproline data was converted into collagen content and normalised to the wet and dry weights of each explant. The mean values of 6 independent samples are plotted on the graphs, error bars represent the standard deviations. Data was tested for normality, followed by oneway-ANOVAs and Tukeys HSD post hoc test. *P<0.05, **P<0.01.

3.3 Changes in chondrocyte organisation and morphology of BMP9 cultured immature bovine explants

3.3.1 Changes in chondrocyte densities observed using DAPI nuclear staining

Immature explants cultured for 21 days in chondrogenic medium either with or without 3.7nM BMP9 were fixed, sectioned, and stained using a DAPI mountant. DAPI stained sections were viewed using fluorescent microscopy to observe any differences in nuclei densities (Figure 14. A-B). DAPI stained sections were analysed using ImageJ particle analyser to

count the number of stained nuclei within the first 500μm of tissue, sections were measured in 5 regions 100μm deep. Across the top 500μm of control and BMP9 cultured explants there was no significant difference in the average nuclei density within any of the zones, likely due to the low sample number, n=4. However, within the upper zones from 200-300μm the reduction observed in nuclei density of BMP9 explants relative to controls was almost significant P=0.06, 581 ± 377 cells/mm^2 and 1275 ± 151cells/mm^2 respectively. In the deeper zones from 300-500μm the opposite was found, explants cultured with BMP9 media had higher nuclei densities than controls 1346 ± 222cells/mm^2 and 768 ± 358cells/mm^2 respectively (P=0.27).
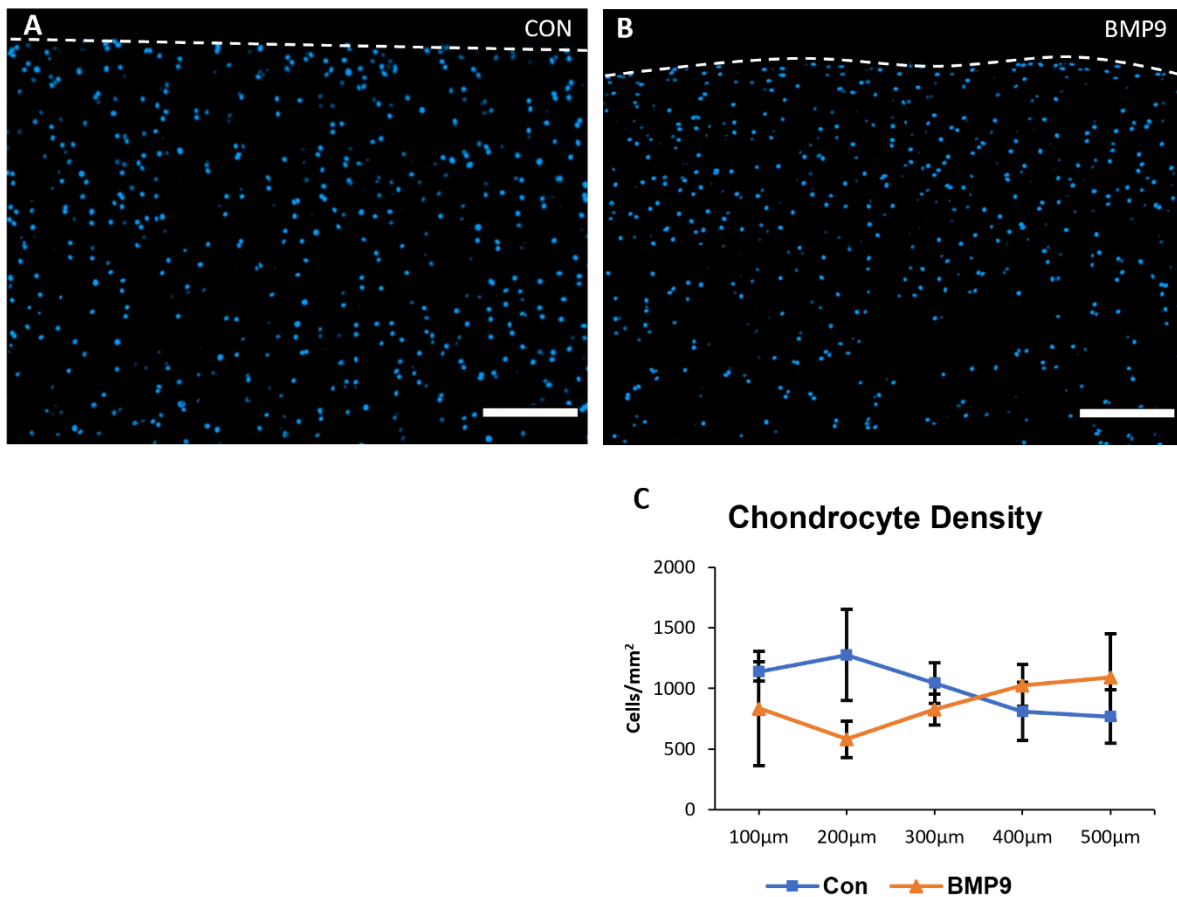
Figure 14. Cartilage explant chondrocyte density is reduced by exposure to BMP9. Explants were cultured for 21 days in control (**A**) or BMP9 (**B**) chondrogenic media. After the culture period explants were fixed and stained with DAPI. (**C**) DAPI stained sections were imaged using fluorescent microscopy and chondrocyte densities were calculated using ImageJ's particle analyser. The data shown in the graph is representative of 4 independent samples. Scale bar = 150μm. Chondrocyte density data was tested for normality and Two-tailed T-tests were used to calculate significance. No significant data.

3.3.2 Cell proliferation of the surface and deep zones in explants cultured with BMP9 observed via BrdU antibody staining

Immature bovine explants were cultured for 21 days with or without 3.7nM BMP9. To detect whether BMP9 induces cellular proliferactionn bromodeoxyuridine (BrdU) was added on the last feed 3 days prior to the end of the culture period. Explants were fixed, sectioned, stained with alexafluor 594 anti-BrdU antibodies, counterstaining with DAPI (Figure 15). Sections were observed using fluorescent microscopy to identify proliferating cells labelled with anti-BrdU antibodies. BMP9 treated explants had labelling in the mid and deep zones (Figure 15C – arrows) in comparison to control explants which had no labelling (Figure 15A). Explants cultured for 21 days with TGFβ1 and FGF2 (FT) were also treated with BrdU and stained with anti-BrdU antibodies to be used as positive controls for cell proliferation (Figure 15B). FT treated explants contained greater amounts of labelling within the surface regions compared BMP9 treated explants, but no labelling was visible in the deeper zones. Thus, cell proliferation of the deep zones is a feature unique to BMP9 treated explants.
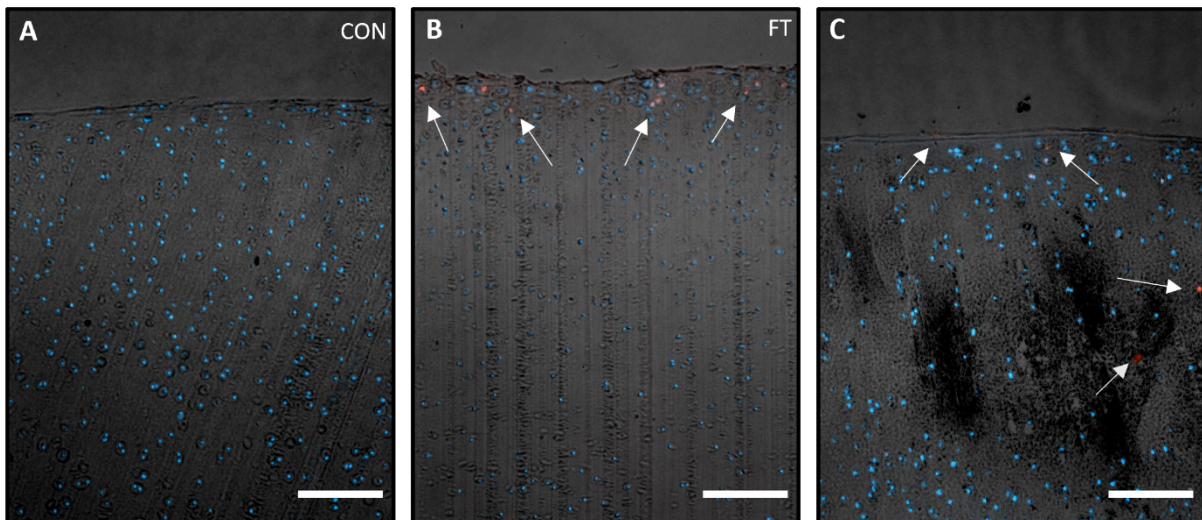
Figure 15. Cell proliferation in the surface and deep zones of immature explants cultured with BMP9 observed via BrdU anti-body staining. Explants were cultured for 21 days in (**A**) control, (**B**) FGF2 and TGFβ1, (**C**) or 3.7nM BMP9 chondrogenic media. After the culture period explants were fixed, sectioned and stained with DAPI and anti-BrdU AF593 fluorophores. Sections were observed using fluorescent microscopy to visualise proliferating cells (**B-C** arrows). Images are representative of 4 independent samples. Scale bar = 150μm

3.3.3 BMP9 induced changes in chondrocyte morphology of immature explants

Immature explants cultured for 21 days in chondrogenic medium with or without 3.7nM BMP9 were fixed, sectioned, and stained with toluidine blue. Toluidine blue stained sections were analysed in 5 regions 100μm in depth using FibrilJ to measure changes in chondrocyte morphology (Figure 16). Chondrocyte area increased with depth in both control and BMP9 explants, on average BMP9 chondrocytes were slightly larger than controls however these differences were negligible (Figure 16A). The greatest difference in chondrocyte area

between control and BMP9 treated explants was in the first 100μm of tissue, where cells measured on average $88\mu m^2 \pm 28\mu m^2$ and $115\mu m^2 \pm 34\mu m^2$ (P<0.01), increasing in area to $149\mu m^2 \pm 28\mu m^2$ and $152\mu m^2 \pm 20\mu m^2$ (P<0.01) within the deepest regions measured.

Chondrocyte orientation was measured in ImageJ by calculating the angle of the cells longest axis relative to the surface (Figure 16B). Chondrocytes within BMP9 treated explants were more vertically orientated relative to controls throughout the top 500μm of tissue 33° ± 19° and 53° ± 15° respectively . Within the first 100μm of tissue cells were orientated at an average angle of 16°± 9.7° and 34°± 9.5° in control and BMP9 explants (P<0.01), these cells were the most parallel to the surface of any depth measured. With increasing depth chondrocytes became rounder and more axially rotated compared to surface cells. Within the deepest region measured chondrocytes were orientated at an average angle of 40°±19° and 60°±20° to the x-axis in control and BMP9 explants (P<0.01). A common hallmark of mature cartilage is the transition of planar cells at the surface to larger, rounder cells of the deep zone rotated axially to the surface.

Finally chondrocyte circularity was measured in arbitrary values from 0-1, where 1 is a perfect circle (Figure 16C). In control and BMP9 treated explants average circularity was lowest within the 1st 100μm where cells were orientated parallel to the surface and thus are elongated parallel to the surface. Average circularity increased with depth from the surface to the deep zones both in control and BMP9 cultured explants 0.79 ± 0.04 - 0.84 ± 0.08 and 0.74 ± 0.04 – 0.79 ± 0.12 respectively (P<0.01). Over the 500μm of tissue measured BMP9 chondrocytes were less circular than controls 0.83 ± 0.15 and 0.77 ± 0.04 respectively (P<0.0001).

A Area

B Orientation

C Circularity
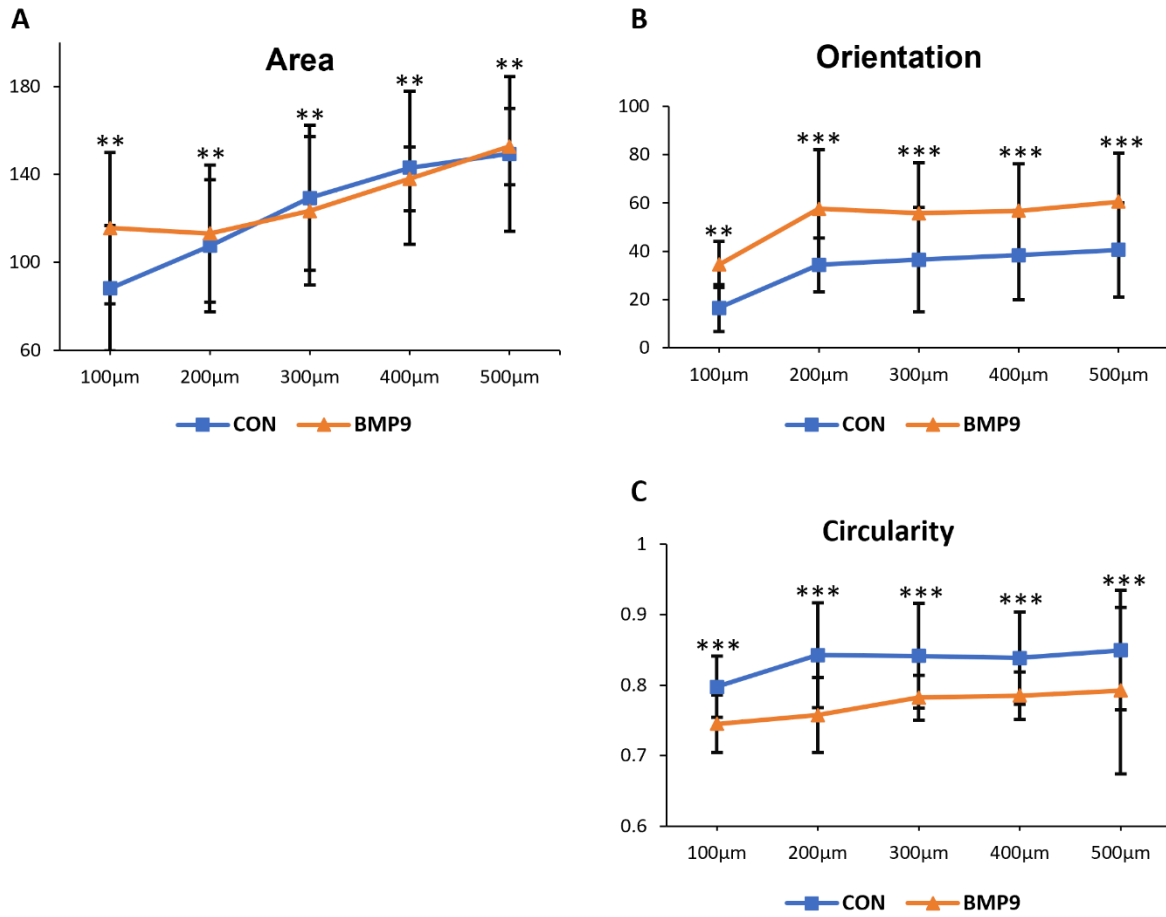
Figure 16. BMP9 induces changes in chondrocyte morphology increasing in size with depth. 21-day cultured explants were fixed and stained with toluidine blue. Stained sections were measured in 5 regions of 100µm depth. ImageJ was used to hand draw around 15 cells of each region for a total of 75 cells per section, roughly 1/4 of the total cells present. ImageJ was used to measure (**A**) chondrocyte area, (**B**) orientation, and (**C**) circularity. Mean data plotted in the graphs is representative of 4 independent samples. Data was tested for normality, then either T-tests or Mann and Whitney U tests were used to calculate the significance, *$P<0.05$ **$P<0.01$, ***$P<0.001$ of BMP9 treated explants compared to controls.

3.3.4 Formation of cell columns in immature explants cultured with BMP9

Explants cultured for 21 days in 3.7nM BMP9 chondrogenic media were stained with DAPI fluorescent nuclear staining and viewed using fluorescent microscopy (Figure 17). Images viewed via fluorescent microscopy clearly showed the organisation of cells stacked columns within the deep zones of the cartilage tissue. Chondrocytes are normally only found organised as columns in the deep zones of mature cartilage. However, there was variability in BMP9 treated explants, not all explants contained obvious formation of chondrocyte columns.
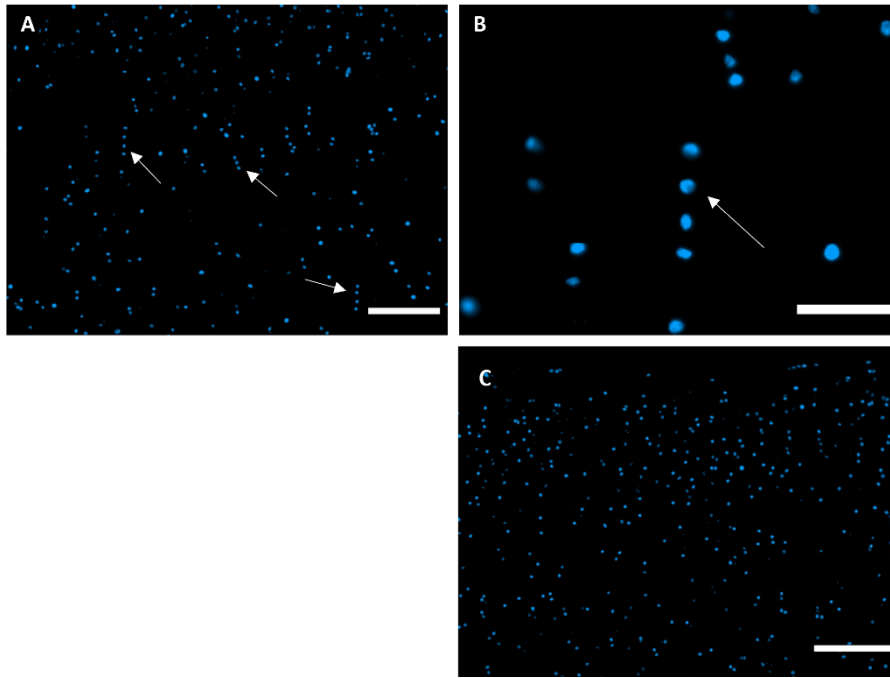
Figure 17. BMP9 cultured explants produced chondrocytes organised into columns. Explants cultured in chondrogenic media for 21 days with or without 3.7nM BMP9 were fixed and stained with DAPI. DAPI sections were visualised using fluorescent microscopy left and right images are of the same region in a BMP9 section at (**A**) 10X and (**B**) 40X magnification. **(C)** control section at 10x magnification. **A** and **C** Scale bar = 100µm, **B** Scale bar = 50µm. Representative of 4 independent samples.

3.4 BMP9s effect on gene expression in immature bovine explants

3.4.1 Effect of BMP9 on aggrecan expression in immature explants

QPCR analysis was conducted on cDNA synthesised from the RNA of 21-day cultured explants to identify BMP9s effect on aggrecan (*ACAN*) gene expression (Figure 18). At day 10.5 *ACAN* gene expression levels were very similar (P=0.96) in control and BMP9 treated explants. At day 21 gene expression of *ACAN* in BMP9 treated explants dropped significantly in comparison to day 10.5. and day 21 controls 0.5-fold (P>0.05). The marked decrease in aggrecan expression suggests it is not required for the organisational changes BMP9 induces in the explants. It hints towards the opposite fact, that lower expression levels at day 21 may be responsible for the other changes observed, and thus a reduction in aggrecan.

ACAN

Figure 18. Expression of ACAN in BMP9 cultured explants is downregulated relative to controls. qPCR was used to analyse the levels of mRNA expression of immature control and 3.7nM BMP9 cultured explants. Explants were cultured for a period of either 10.5 or 21 days. cDNA was synthesised from RNA. Expression was normalised to 18SRNA expression profiles for the explants, identified in a previous experiment. Data is presented as the means and the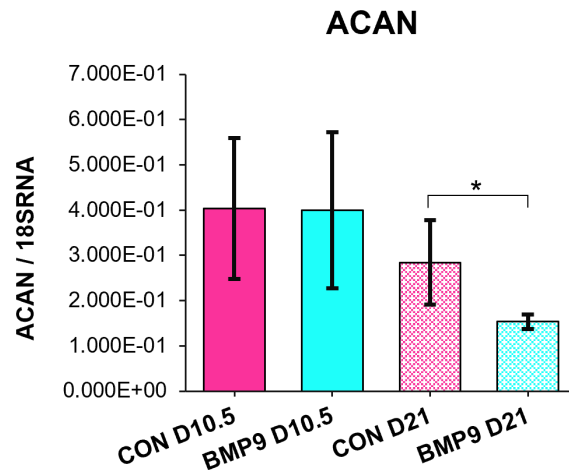 error bars represent the standard deviations. Significance values were calculated between Control (CON) and BMP9 explants cultured for the same length of time. All qPCR reactions were completed in duplicate with 4 independent samples.*P<0.05, first testing for normality, then Mann-Whitney U tests were used to test the significance between explants treated for the same period of time.

3.4.2 Effect of BMP9 on matrix metalloproteinase gene expression

Matrix metalloproteinases (MMPs) and ADAMTs are essential enzymes involved in tissue turnover and matrix remodelling during skeletal development. Therefore, qPCR was used to changes in MMP gene expression in immature explants cultured for 10.5 or 21 days, either with or without 3.7nM BMP9 (Figure 19). At day 10.5 no genes were found to be significantly upregulated in BMP9 cultured explants. At day 21 *MMP3* was the only gene to be significantly upregulated (P<0.05) in BMP9 treated explants, exhibiting a 1.5-fold increase in gene expression (Figure 19D). On a side note, *ADAMTS5* expression was significantly downregulated 0.6-fold in BMP9 treated explants at day 10.5 (P<0.05), and at day 21 both *ADAMTS5* 0.75-fold and *MMP9* 0.53-fold were significantly downregulated compared to controls (P<0.05) (Figure19B and E). This indicates that control explants have elevated *ADAMTS5* and *MMP-9* expression compared to BMP9 samples and may be undergoing tissue degradation due to a lack of stimulation.

Figure 19. qPCR analysis of immature explants cultured with BMP9 reveals an increase in MMP expression. Immature explants cultured in control chondrogenic media with or without 3.7nM BMP9 for 10.5 days (C10.5 or B10.5) or 21 days (C21 or B21). qPCR was used to analyse the actual levels of mRNA expression for each explant. Expression of *ADAMTS4, ADAMTS5, MMP2, MMP3, MMP9, MMP13* mRNA was measured. Expression was normalised to the *18SRNA* of the explants. Data is presented as means and error bars represent the standard deviations. Significance values were calculated between corresponding control and BMP9 Explants. All qPCR reactions were completed in duplicate for 4 independent samples. Data was tested for normality, then either Mann-Whitney U tests or T-Tests were used to calculate the significance between the gene expression of explants treated for the same time period. *P<0.05, **P<0.01

3.4.3 TIMP gene expression

Tissue inhibitors of metalloproteinases are responsible for regulating MMP activity during the development of the musculoskeletal system, known to be expressed within native cartilage during different phases of the tissues maturation. Therefore, we used qPCR to measure differences in the gene expression of tissue inhibitors of metalloproteinases (TIMPs) in BMP9 treated explants immature explants cultured for 10.5 or 21 days, in chondrogenic medium either with or without 3.7nM BMP9. In immature explants cultured for 10.5 days with BMP9 media *TIMP-1* was the only gene to be significantly downregulated 0.36-fold compared to controls (P<0.001) (Figure 20A). At day 21 *TIMP2* expression was significantly downregulated 0.36-fold (P<0.001) (Figure 20D). Down regulation of *TIMP*s at both time points is indicative of increased MMP activity within BMP9 cultured explants relative to controls, as we detected (Figure 19).
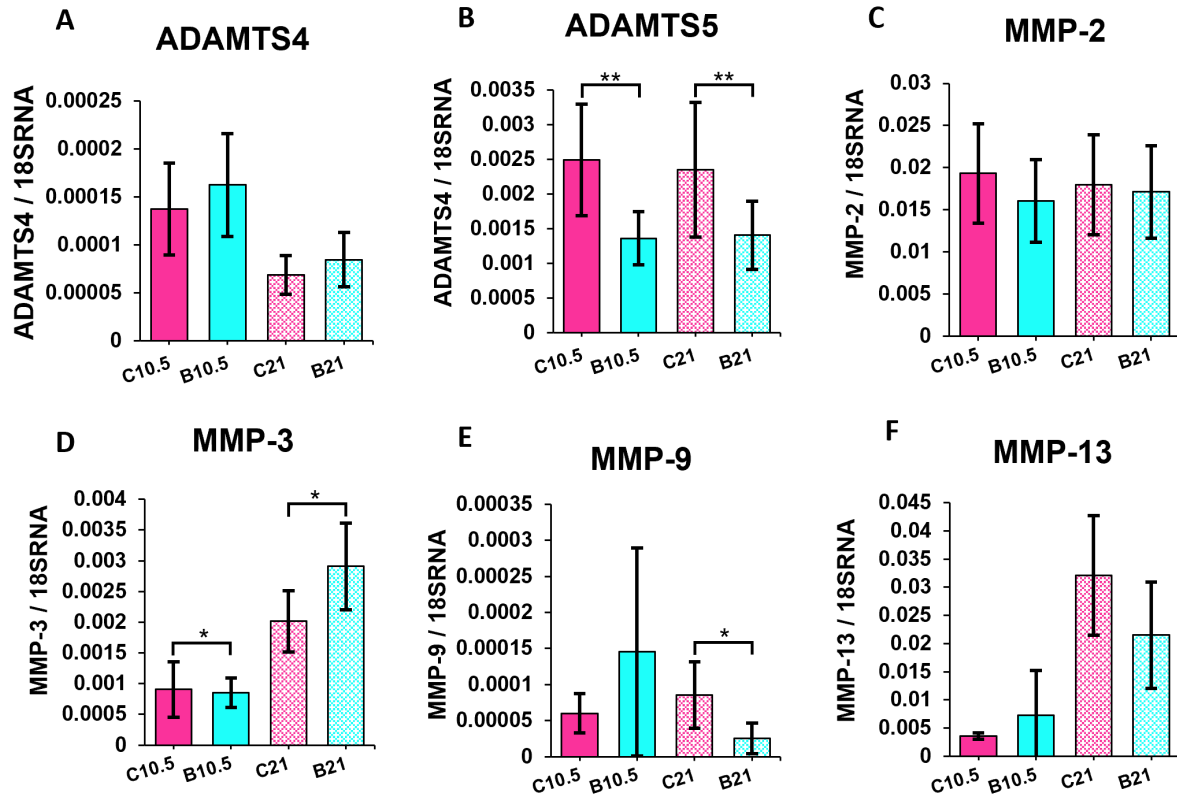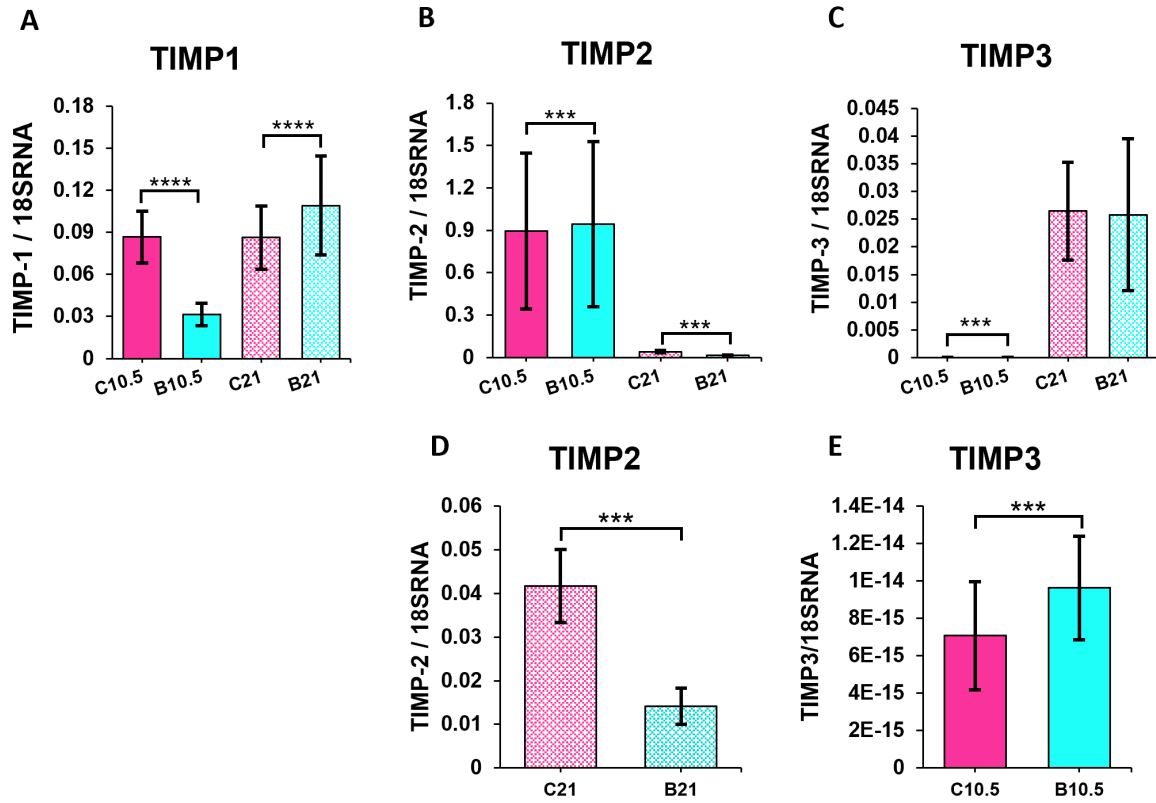
Figure 20. qPCR analysis of immature explants cultured with BMP9 reveals a reduction in TIMP-1 expression. Immature explants were cultured in control chondrogenic media with or without 3.7nM BMP9 for a period of either 10.5 days (C10.5 or B10.5) or 21 days (C21 or B21). qPCR was used to analyse the actual levels of mRNA expression for each explant. Expression of *TIMP1*, *TIMP2* and *TIMP3* mRNA was measured. Expression was normalised to the 18SRNA of the explants. Data is presented as means and error bars represent the standard deviations. Significance values were calculated between corresponding control and BMP9 Explants. (**D-E**) Enlarged versions of figures **B-C** so the smaller bars can be seen. All qPCR reactions were completed in duplicate for 4 independent samples. Data was tested for normality, then either Mann-Whitney U tests or T-Tests were used to calculate the significance between the gene expression of explants treated for the same period of time. *P<0.05, **P<0.01, ***P<0.001, ****P<0.0001

3.4.4 PCR screening of genes

PCR amplification combined with gel electrophoresis was used to screen for alternaitve genes that may be upregulated in explants by BMP9 treatment. Relative expression was compared between 21-day control and BMP9 cultured bovine immature explants. RNA isolated from explants was converted into cDNA for PCR amplification. Genes selected for screening were chosen due to their ability to degrade cartilage ECM and specific remodelling properties relevant to articular cartilage. *COL2A1* was also screened to detect the levels of type II collagen expression in BMP9 treated explants. The amplified products were run on gels and imaged using a BIORAD chemidoc, band intensities were measured to identify gene expression levels relative to control explants. We were able to identify that the expression of *bMMP3* was upregulated the most in BMP9 explants (1.51-fold), identical to what was found in qPCR (Figure 17). All other genes had negligible levels of upregulation, none surpassing *bMMP3*. Of the genes that had downregulated expression in the cultured explants *COL2A1* was the most downregulated 0.4-fold in BMP9 treated samples, over a 2-fold decrease in expression between BMP9 and control explants.

Gene	Presence	BMP9 Relative Ab.
bMMP3	Strong	1.51-fold
bMMP7	No clear Bands	N/A
bMMP8	No clear Bands	N/A
bMMP11	No clear Bands	N/A
bMMP12	Weak	N/A
bMMP14	Strong	1.26-fold
bMMP16	Strong	0.90-fold
ADAMTS1	Weak	1.27-fold
ADAMTS8	No Bands	N/A
ADAMTS9	Weak	1.13-fold
ADAMTS15	No Bands	N/A
Col2A1	Strong	0.40-fold

Table 1. PCR screening of immature explants cultured with BMP9. Immature explants cultured in chondrogenic media with or without 3.7nM BMP9 for 21 days. cDNA was produced from explant RNA was amplified using PCR and run on a 1% agarose gel. Relative band intensities were measured using a BIORAD chemidoc to screen the levels of mRNA expression. All PCR reactions were completed in duplicate for 4 independent samples.

3.5 Effect of MMP inhibitor doxycycline on immature bovine explants cultured with BMP9

3.5.1 Changes in collagen organisation observed via polarised light microscopy

To understand the process of collagen reorganisation induced by BMP9, explants were cultured with doxycycline (dox), a broad-spectrum inhibitor of MMPs, to determine their role in the remodelling process. Dox cultured explants were sectioned after 21 days of culture, stained with picrosirius red and viewed using polarised light microscopy (PLM) to view changes in the structural organisation of the collagen network (Figure 21). BMP9 treated explants cultured with dox, stained with picrosirius red, and viewed under PLM contained a considerably thinner region of perpendicularly aligned fibres than normal BMP9 treated explants (Figure 21 B and D). Dox exhibited similar effects in control explants preventing the spontaneous formation of perpendicularly aligned collagen fibres (Figure 21 A and C) that had been observed within normal control explants (Figure 5). Of note, BMP9 doxycycline treated sections were very similar in organisation to control doxycycline sections, within the deeper zones there was intense birefringence parallel to the surface with a darker region just below the surface, corresponding to the mid/transitional zone in cartilage. The increase in birefringence of the dox cultured explants is likely a result of increase collagen alignment, an outcome of inhibiting MMP functionality. The lack of perpendicularly aligned fibres in BMP9 dox cultured explants indicates that inhibition of MMPs prevents reorganisation of the collagen network. Secondly, dox inhibits the formation of perpendicular fibres in control explants meaning that collagen reorganisation must be an active process requiring MMP activity for tissue remodelling.
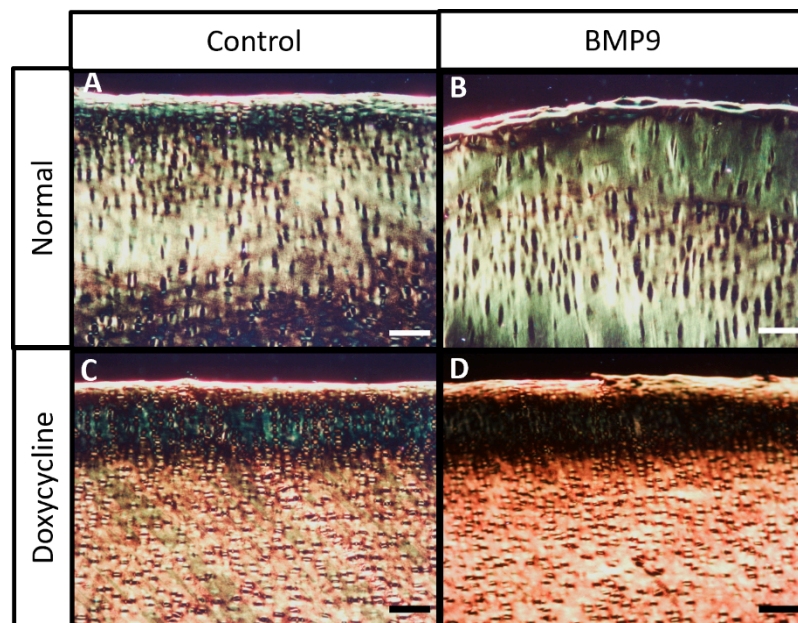
Figure 21. Polarised light microscope images of immature explants cultured with BMP9 and doxycycline show its ability to inhibit collagen reorganisation. A-B 4mm immature bovine explants were cultured for 21 days in (**A**) control chondrogenic media or (**B**) with 3.7nM BMP9. (**C-D**) An additional set of (**C**) control and (**D**) BMP9 explants were cultured with the addition of 100μm doxycycline (dox). Explants were fixed post-culture for wax sectioning, stained with picrosirius red and viewed using polarised light microscopy (PLM). Sections **A-D** show the first

500μm of the explants from the surface. Doxycycline explants were part of the same culture set as shown in Chapter 3.1. Scale bar = 100μm, figures are representative of 4 independent samples.

3.5.2 Extent of collagen reorganisation in picrosirius red sections

Immature bovine explants were cultured for 21 days with BMP9, sectioned, stained with picrosirius red, and viewed using PLM. Under PLM perpendicularly arranged fibres within the explants appear darker in colour due to a combination of their orientation and alignment relative to the light source (Rieppo et al., 2008). The extent of collagen reorganisation perpendicular to the surface of the explants was quantified using FibrilJ, an ImageJ plug-in (Figure 22A). The mean depth of perpendicular fibres was significantly increased in BMP9 cultured explants relative to controls (P<0.01) 662μm±183μm and 304μm±133μm respectively (explants were part of the same culture set as show in Chapter 3.1, hence the replication of control and BMP9 data for comparison). Reorganisation of the collagen network in BMP9 treated explants was significantly reduced by the addition of dox (P>0.01) from 662μm±183μm to 226μm±76. BMP9 dox and control dox explants displayed similar depths of collagen reorganisation (P=0.21) 226μm±76 and 174μm±40μm respectively. Both control and BMP9 cultured dox explants had less collagen reorganisation than standard controls, though an insignificant difference. Dox is therefore an effective inhibitor of induced collagen reorganisation in BMP9 induced immature explants. It also means that some of the reorganisation is already present within the explants upon collection if we assume dox inhibits any changes in collagen organisation after collection.

To negate the affect differences in cartilage maturity of the explants at the time of collection have on the results I compared the depths of collagen reorganisation in a pairwise manner with controls to find a ratio for the change in depth of collagen reorganisation over the culture period (Figure 22B). BMP9 cultured explants had significantly more reorganisation than both control dox and BMP9 treated dox explants (P<0.01) and (P<0.05) respectively. Additionally, there was no significant difference between the relative collagen reorganisation of the dox cultured explants. Therefore, dox inhibits reorganisation of collagen in BMP9 treated and control explants with the same effectiveness.
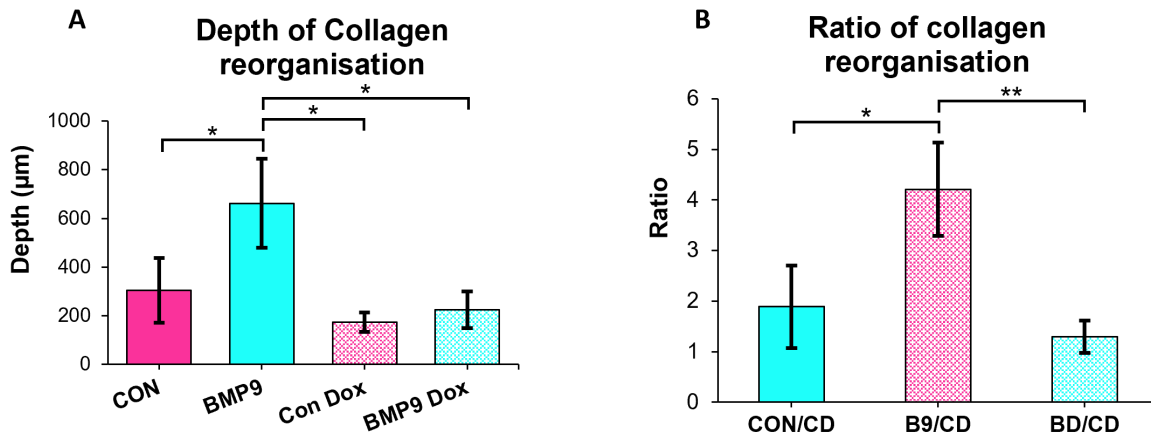
Figure 22. Quantitative image analysis of perpendicular collagen depths in BMP9 and dox cultured explants using PLM. 4mm immature bovine explants were cultured for 21 days in control chondrogenic media or with 3.7nM BMP9. An additional set of control and BMP9 explants were cultured with the addition of 100μm doxycycline (Con Dox or BMP9 Dox). Explants were fixed, sectioned, stained with picrosirius red, and viewed under polarised light. (**A**) Image analysis was conducted using ImageJ to determine the mean depths of collagen reorganisation identified by a shift in collagen fibril alignment to perpendicularly orientated fibres. Doxycycline explants were part of the same culture set as shown in Chapter 3.1, hence the replication of control and BMP9 data for comparison to doxycycline treated explants. The thinnest and thickest depths were measured for each explant to find a mean. (**B**) Measurements were compared in a pairwise manner to doxycycline treated controls to calculate the relative increase in collagen reorganisation, control/control dox (Con/CD), BMP9/control dox (B9/CD), and BMP9 dox/Control dox (BD/CD). Data is presented as the means of 4 independent samples, error bars represent standard deviations. Data sets were tested for normality and statistical signficance was calculated using oneway-ANOVAs combined with Tukeys HSD post hoc test *P<0.05, **P<0.01.

3.5.3 Changes in collagen orientation in dox cultured explants

Variation in collagen orientation with depth was measured in the top 500μm of tissue of 21-day cultured explants where the changes in collagen organisation were observed using polarised light microscopy (PLM). PLM images were analysed in 5 regions of 100μm in depth and equal width using FibrilJ an ImageJ plug-in (Figure 23B). Orientations of the collagen fibres were measured as values from 0°-90° relative to the tissue surface. Collagen fibrils present in the regions 1-5 of controls (increasing with depth) were orientated at 5.3°, 69.3°, 44.2°, 46.3°, and 24.9° to the tissue surface. In BMP9 explants the fibres found in regions 1-5 were orientated at, 28.5°, 85.9°,86.8°, 86.5°, and 86.3° (explants were part of the same culture set as show in Chapter 3.1, hence the replication of control and BMP9 data for comparison).

Orientational changes in the collagen fibril network of 21-day cultured control and BMP9 explants with 100μm dox were analysed to determine doxdoxycycline's effect on BMP9 treated explants (Figure 23). Both control and BMP9 cultured dox explants had similar collagen orientations with depth. Within the superficial 100μm both explants had fibrils aligned parallel to the surface at angles of 7.3° and 2° similar to the orientation of fibres in the normal control explants. At 100-200μm dox cultured explants both had an increase in orientation relative to the surface reaching a mean of 32° in controls and 26° in BMP9 explants, this was a reduction in the perpendicular orientation compared to the normal control 69°and BMP9 86° (P<0.001) treated explants, which at 200μm were measured at 69° and 86° angles to the surface. With increasing depth from 300μm to 500μm collagen

fibres in control dox and BMP9 dox explants retainedained orientations parallel to the surface, neither surpassing a 5° angle to the surface. WhereasWhereas in normal BMP9 explants collagen fibres retained a perpendicular orientations consistently with increasing depth up to 500μm where they were still found at an 86° angle to the surface, signifying doxycyclines effective ability to inhibit changes in collagen organisation.

3.5.4 Changes in collagen anisotropy in dox cultured explants

Using FibrilJ changes in collagen anisotropy were measured using the same 5 x 100μm regions used for measuring orientation (Figure 23C). Anisotropy of the fibres was measured as a value from 0-1, 0 being isotropic and 1 being anisotropic. In control explants collagen within the first 100μm of explant tissue was isotropic in nature, with a value of only 0.07. Within the deepest zone the anisotropy of control fibres was still very low, 0.05 at 500μm, the highest levels of collagen anisotropy measured was 0.15 in the 3rd region from 200-300μm.

BMP9 explant fibril anisotropic values increased from the superficial zone with depth in almost a linear fashion. In the superficial region BMP9 explants had an anisotropic value of 0.09 and in the 5th region the value had increased to 0.27. This shows that the collagen fibres of BMP9 cultured explants increased in anisotropy with depth in association with the observed changes in orientation (explants were part of the same culture set as show in Chapter 3.1, hence the replication of control and BMP9 data for comparison).

Anisotropy values of the dox cultured explants varied greatly over the 5 regions measured. The anisotropy values for both control and BMP9 dox cultured explants dipped at 100-200μm coinciding with the peak in collagen reorientation in both explants. This may be due to the transitional change in collagen orientation reducing anisotropy values within the region. From 200μm onward the anisotropy values for both dox explants increased with depth. At 500μm control dox and BMP9 dox had isotropic values of 0.12 and 0.18 that are both lower than in the first region but greater than the isotropic values of normal control explants at 500um. Dox cultured explants are therefore more isotopically organised compared to normal BMP9 treated explants.

Overall, the collagen data shows BMP9 can induce an organisational change in the collagen matrix of immature bovine explants relative to controls. Inducing an orientational shift in the collagen fibres from mostly horizontal isotropic fibres to partially anisotropic fibres with perpendicular alignment. The application of dox to these cultures prevents changes in collagen orientation bar a sub-surface region which was present in all explants, coinciding with the lowest anisotropic values in dox explants. Suggesting that slight maturational features were already present in some explants before culture. Doxs ability to inhibit the changes induced in control and BMP9 treated explants proves collagen reorganisation is an active process.
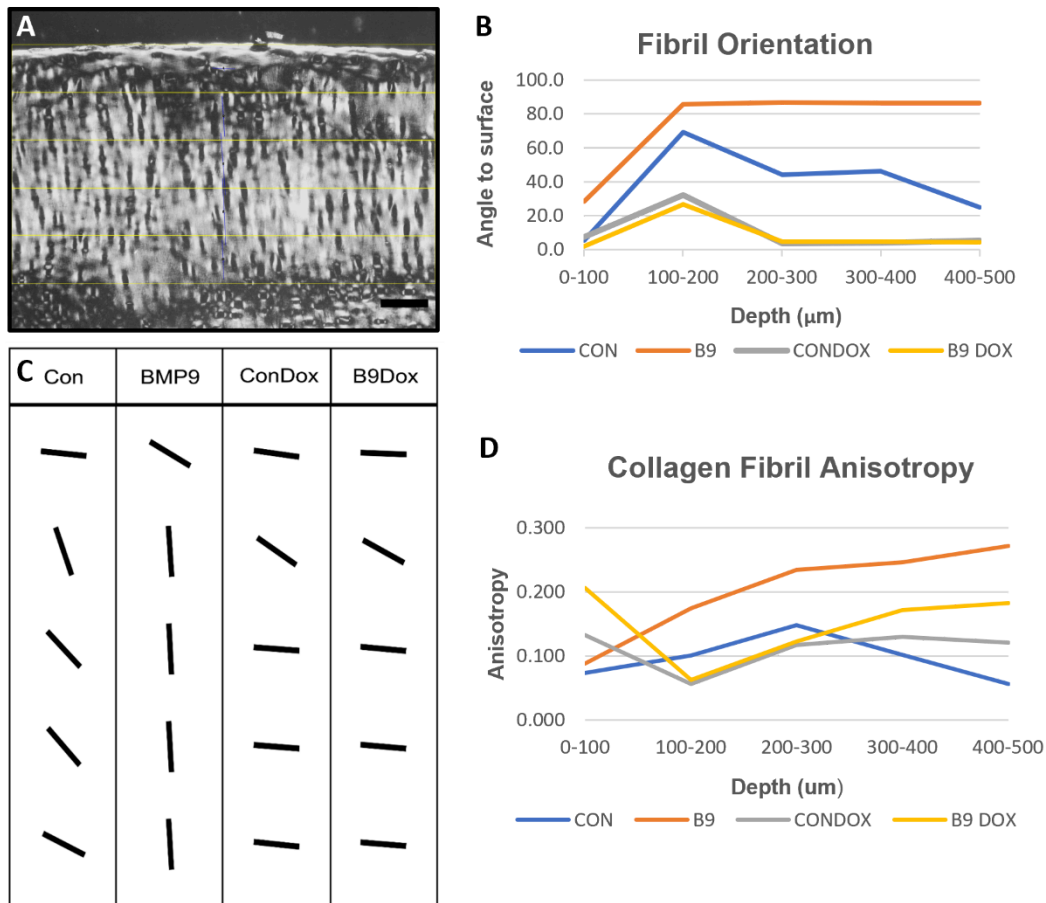
Figure 23. Quantitative image analysis of collagen orientation and anisotropy varies with depth, BMP9, and inhibition by doxycycline. 4mm immature bovine explants were cultured for a period of 21 days in control serum free DMEM or with 3.7nM BMP9 (Con or BMP9). An additional set of explants were cultured in serum free DMEM with or without 3.7nM BMP9, with the addition of 100μm doxycycline (ConDox or B9Dox). Explants sectioned and stained with picrosirius red, sections were viewed using polarised light microscopy (PLM). Image analysis was conducted using FibrilJ, to determine the orientation and anisotropy of collagen fibres within the top 500μm of tissue. **A** Explant sections were analysed in 100μm deep regions. **B** Fibril orientations were measured from 0° – 90° relative to the surface. **C** Mean collagen fibril orientations were drawn to represent the variation in orientation with depth between explants. **D** Collagen fibril anisotropy was measured as arbitrary units from 0-1, 0=isotropic 1=anisotropic. Doxycycline explants were part of the same culture set as show in Chapter 3.1, hence the replication of control and BMP9 data for comparison to doxycycline treated explants. Data is representative of 4 independent samples.

3.6 Changes in collagen organisation of immature explants treated with BMP9 and MMP inhibitor PD166793

Immature bovine explants were cultured for 21 days in chondrogenic medium with or without 3.7nM BMP9. 10μm of PD166793 was added to an additional set of control and BMP9 treated cultures. At the end of the culture period the explants were fixed, section, stained with picrosirius red and viewed under polarised light (Figure 21). Explants cultured with PD166793 exhibited a varied response to the MMP inhibitor. PD166793 was unable to inhibit the changes induced via BMP9 culture. However, it inhibited changes in collagen organisation observed in the control explants. This suggests that the concentrations of PD166793 were high enough to inhibit the changes induced via basal cell activity but were

unable to overcome the tissue remodelling effects activated by BMP9. This corroborates what was found by culturing explants with doxycycline that the changes in control explants over the culture is an active process requiring MMPs.
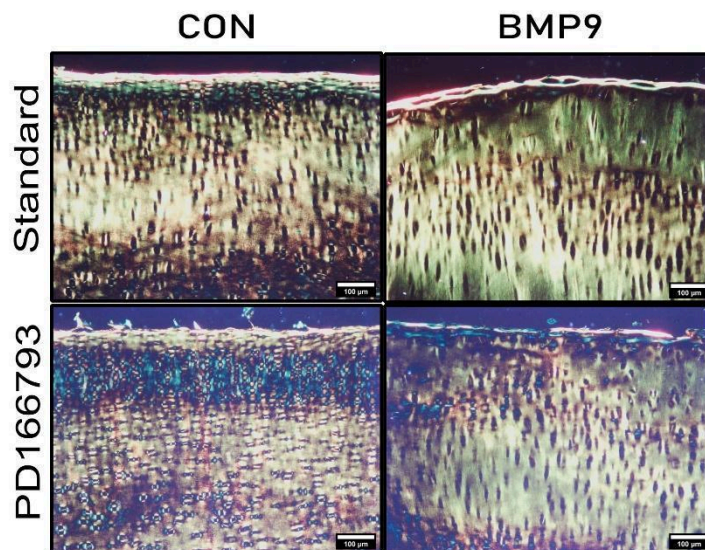
Figure 24. Explants cultured with PD166793 fail to inhibit BMP9 induced changes but does prevent changes observed in controls. Control and BMP9 explants were cultured for 21 days with the addition of MMP inhibitor PD166793. After the culture period explants were fixed, stained with picrosirius red and viewed using PLM. PD166793 explants were part of the same culture set as shown in (Chapter 3.1 and 3.5), hence the replication of control and BMP9 figures for comparison to PD166793 treated explants. Figures are representative of 4 independent samples.

3.7 Summary of explant data

Using polarised light microscopy, we observed changes in the collagen organisation of immature cartilage explants cultured in chondrogenic media with 3.7nM of BMP9 up to a mean depth of 0.66mm±183μm (P<0.01) (Figure 2). A significant increase (P<0.01) compared to explants cultured in control medium 0.3mm±0.13μm. Within this region of reorganisation, the collagen fibres formed columnar structures, orientated parallel to the articular cartilage surface in the superficial zones (25°) transitioning to perpendicular orientations (86°) within the first 100μm of tissue. These perpendicular fibres persisted throughout the mid and deep zones of the cartilage explants. Whereas we observed consistently parallel fibres throughout the zones in control explants. Additional to the changes in collagen orientation, we observed an increase in collagen fibre anisotropy in explants treated with BMP9 media compared with controls (Figure 8). Levels of anisotropy were lowest within the superficial and transitional zones of the tissue increasing in anisotropy with depth as fibres became more perpendicularly aligned.

In BMP9 treated explants changes in cell morphology and organisation were observed. Within the superficial regions of the BMP9 explants chondrocytes were orientated at 35° parallel to the surface with no distinct organisation, transitioning to a more perpendicular orientation of 60° within deep zones of cartilage, in which chondrocytes could be found

arranged into columns (Figure 17). Chondrocyte area and circularity also increased from the superficial to the deep zones compared to controls. Increasing in area from $115\mu m^2$ to $152\mu m^2$ and circularity from 0.74 – 0.79 respectively (Figure 16). The changes observed in chondrocyte morphology mirrored the changes in the organisation of collagen fibres within the tissue.

Explants treated with BMP9 had no significant change in the overall collagen content (Figure 13). This was supported by PCR analysis which showed there was no increase in type II collagen (*COL2a1)* gene expression in BMP9 cultured immature explants relative to controls (Table 10). Additionally, BMP9-treated explants lacked the same intensity of picrosirius red staining of the collagen network relative to controls (Figure 4). The areas of tissue with reduced staining were localised to regions of cartilage that had undergone changes in fibril orientation, containing perpendicular fibres. However, COL2-3/4m antibody staining showed that no breakdown in collagen was occurring within the surface zones of cartilage tissue where changes in collagen orientation occurred (Figure 9). Suggesting that the changes observed in collagen organisation are due to transformation of the existing collagen network not enzymatic cleavage of fibres.

Gene expression analysis revealed that *MMP3* was the only MMP to be significantly upregulated at day 10.5 by BMP9 relative to control explants (Figure 19). In explants cultured with BMP9 media there was a significant reduction in *TIMP1*, and *TIMP2* gene expression compared to controls (Figure 20). Thus, an upregulation in *MMP3* and a downregulation in its inhibitor could result in increased enzyme activity, correlating with the significant increases in PG loss observed in BMP9 treated explants (Figure 12). Inhibition of MMPs via doxycycline (dox) prevented reorganisation of the collagen matrix in explants treated with BMP9, preventing the formation of perpendicular fibres, supporting the findings that BMP9 induces upregulation of MMPs (Figure 21).

Biochemical assays of explants cultured with BMP9 revealed that there was no significant difference in proteoglycan normalised to wet weight compared to controls (Figure 12). However, there was a significant increase in the turnover of proteoglycans from within BMP9 cultured explants normalised to day 0 wet wights combined with a loss in staining of the mid and deep zones of BMP9 cartilage explants. Supporting this finding was a reduction in aggrecan (*ACAN*) gene expression and upregulation of *MMP3* expression measured at day 21 in BMP9 explants indicating an increase in tissue degradation (Figure 18-19). In BMP9 treated explants increases in proteoglycan turnover correlated with an observed increase in water content (Figure 13). Therefore, BMP9 induced degradation of proteoglycan may induce increases in water content. Increased water content correlates with the reductions observed in picrosirius red staining of explants and the reduction in collagen content in proportion to wet weight.

Inconsistencies observed in explant cultures that resulted in spontaneous maturation, may be due to several uncontrollable factors inherent to explant cultures. For example, differences in cartilage maturity or damage to explant surfaces. Therefore, it would be useful to replicate the experiment *in-vitro* using chondrocytes in an environment where we have more control over the culture system. This will allow us to prove unequivocally that BMP9 induces maturational effects.

Chapter 4: Analysis of BMP9s effects on immature and mature bovine chondrocyte pellet cultures

4.1 Introduction to chondrocyte pellet cultures

Using bovine cartilage explants we have shown that BMP9 induces changes in immature cartilage tissue that recapitulate certain structural and morphological aspects of mature cartilage. The changes identified included organisation of the collagen matrix, chondrocyte morphology and the biochemical composition of the tissue. However, when using explant cultures we identified spontaneous maturational changes taking place. The cause of spontaneous reorientation of collagen fibrils could be attributed to one of many factors including; proteoglycan loss, the developmental stage of the tissue on collection, or swelling of the tissue. Finding a more unequivocal model is important to validate the role of BMP9 in inducing maturational changes. Therefore, we used chondrocytes isolated from bovine articular cartilage grown as pellet cultures to investigate the role of BMP9 in inducing collagen reorganisation.

Additionally, it has not been shown whether BMP9 can induce similar organisational changes in chondrocytes derived from mature articular cartilage. This latter experimental study will show whether chondrocytes retain the phenotypic characteristics that produce the extracellular matrix typical of adult mature articular cartilage.

This chapter aimed to investigate if BMP9 was able to induce maturational effects using a more stringent model system using pellet culture of isolated chondrocytes. This aim was achieved in three phases:

1) Histological staining of immature and mature chondrocyte cultured pellets to identify differences in tissue structure and morphology, supplemented with Image analysis to quantify any differences.
2) Biochemical analysis of the pellets to determine differences in water, collagen, and proteoglycan content of immature and mature pellets
3) Addition of BMP receptor inhibitors to cultures to determine if potential changes induced by BMP9 could be inhibited, providing insight into the underlying mechanisms responsible.

4.2   Chondrocyte pellet culture methods
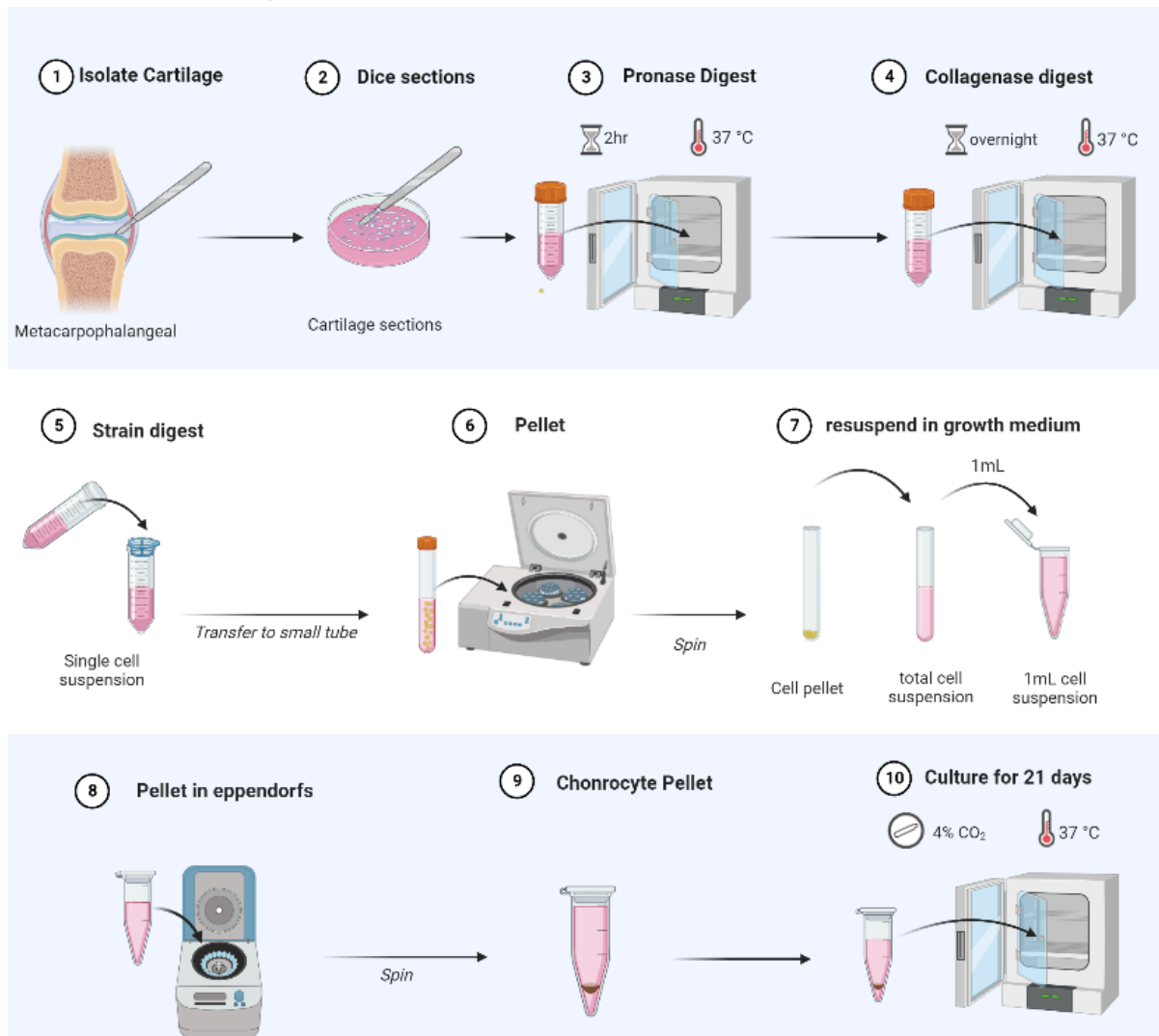
Figure 25. Work scheme for producing chondrocyte pellets for culture with control or BMP9 chondrogenic media. (**1**) Cartilage sections were collected from immature and mature metacarpophalangeal joints. (**2**) Cartilage sections were diced in a petri dish prior to (**3**) digestion in 0.2% pronase for two hours followed by (**4**) 0.06% collagenase overnight. (**5**) Cartilage digests were strained to create single-cell suspensions (**6**) before transferring the required volume to make all the pellets into smaller tubes. (**7**) Pelleted cells were resuspended in expansion medium and 1mL of the final suspensions were pipetted into Eppendorfs. (**8**) Eppendorfs were spun for 5 minutes to pellet the cells and transferred to incubators. (**10**) Pellets were cultured for 21 days exchanging the media every 3 days.

4.2.1   Cartilage collection

Immature and mature bovine feet were collected from local abattoirs and prepared for dissection and cartilage collection from the metacarpophalangeal joints following the procedures in the general methods (2.1.1-2.1.2). Pellets were created by collecting cartilage explants from a single mature or immature bovine joint surface and digesting the tissue to isolate the chondrocytes as single-cell suspensions. To collect cartilage from the joints a scalpel was used to score along the edges of the condyle head, cutting slices of full-depth cartilage starting with the ridges of the joint followed by the planes. The slices of cartilage were directly placed into a sterile petri dish containing a small volume of DMEM-high glucose (HG).

4.2.2 Cartilage digest

40mL of 0.2% pronase digest medium was prepared containing, 80mgs pronase (Roche Diagnostics #11459643001), 40µL gentamicin (gibco #15750-037), 40µL ascorbate (Sigma #A4034-100G), 40mL DMEM – HG glucose (Corning #10-013-CVR)

40mLs of 0.06% collagen digest medium was prepared with 24mgs of collagenase from Clostridium histolyticum (Sigma #C130-1G), 40µL gentamicin, 40µL ascorbate, 0.4mL FBS (foetal bovine serum) 10% by volume, and 40mL DMEM-HG (Corning #10-013-CVR).

Once the cartilage from a joint had been removed and collected in a petri dish the cartilage slices were diced into smaller pieces~1mm^3 to reduce the time needed for digestion. Waste DMEM-HG was decanted, and cartilage sections were transferred to 50mL Falcon tubes containing 20mL of the 0.2% pronase digest media. The tubes were sealed with parafilm around the lids to ensure the tubes were air and watertight and incubated for 2 hours at 37°C on rollers to agitate the samples, assisting with digestion.

After the pronase digest step was complete the digest medium was decanted and replaced with 20mL of the 0.06% collagenase medium, sealing the tubes again with parafilm around the lids. The collagenase medium contained 10% v/v FBS to inhibit any pronase that may remain in the medium. The collagenase digests were incubated overnight at 37°C on rollers to agitate and help break up the samples.

4.2.3 Pellet formation

Cartilage digests were removed from overnight incubations and decanted into 50mL fresh Falcon tubes, straining the medium through 40µm cell strainers (Corning #431750) to create single-cell suspensions. Cell suspensions were quantified to determine the cell concentrations using trypan blue (Sigma, #RNBJ4985) measured on counting slides (BIORAD) in a BIORAD TC10 Automated cell counter.

$$\frac{No.\ of\ pellets\ \times 0.5 \times 10^6}{Concentration\ of\ cells/ml} = Volume\ Required$$

To create one pellet 500,000 cells were required. The volume of cell suspension needed to produce all the pellets was pipetted into a fresh 50mL Falcon tube, creating separate control and BMP9 pellet suspensions. Cell suspensions were centrifuged at 1500 x g for 5 minutes to pellet the cells, disposing of the waste digest medium and resuspending in chondrogenic growth medium with or without 3.7nM. 1mL of the resuspended cell solutions were pipetted into sterile Eppendorfs (Thermo Scientific #3451) and pelleted at 800 x g for 5 minutes in a microfuge. Eppendorfs containing the chondrocyte pellets were then placed directly into incubators for culture at 36°C and 4% carbon dioxide. Immature and mature pellets were formed following the same protocol.

4.2.4 Pellet culture

Mature chondrocytes cultured as pellets require foetal bovine serum (FBS) to survive the initial culture period. Therefore, all pellets including immatures were fed with 1mL chondrogenic medium containing 5% v/v FBS for the first feed. After the first feed pellets were fed with 1mL of normal chondrogenic medium with or without BMP9 3.7nM every 3 days for 21 days. 0.5mL of waste medium from each feed was collected for biochemical analysis. At the end of the culture period pellets were fixed in 10% neutral buffered formyl

saline (NBFS) prior to embedding and sectioning, or snap frozen in liquid nitrogen and stored at -80°C prior to papain digestion for biochemical analysis.

4.2.5 Dorsomorphin inhibitor cultures

Cartilage collected from immature and mature bovine metacarpophalangeal joints were processed in a series digest of pronase and collagenase to create single-cell suspensions. The cell suspensions were used to form pellets containing 0.5 million cells per pellet (4.1.1 – 4.1.3). Pellets were formed in chondrogenic medium containing 5% FBS for the first feed to allow the cells to acclimate and adhere to each other. After initial formation pellets were fed with 1mL chondrogenic medium containing dorsomorphin (Tocris #3093) at concentrations of either 0µm, 2µm, or 20µm. Control and BMP9 pellets were cultured for 21 days at each of the concentrations. After culture pellets were fixed in 10% NBFS for histological staining.

4.1.8 Histological staining of pellet

Pellets were fixed in 10% NBFS at 4°C overnight and loaded into cassettes for embedding in paraffin wax. Dehydrated by immersion in a series of graded ethanol baths from 30%-100% to remove water, cleared using xylene (Sigma #534056-5L) before infiltration with paraffin wax at 65°C – 70°C and embedding back onto the wax cassettes (Embedding services were kindly provided by Singleton Hospital Pathology Department). Embedded pellets were sectioned to a depth of 100µm before collection of samples. Samples were cut using a microtome at a 7µm thickness. Wax sections were placed in 45°C water baths and adhered to positively charged lysine-coated slides (Thermo Scientific #J2800AMNZ), left on 60°C hot plates for 20 minutes to melt the wax and complete adhesion. Pellet sections were stained with haematoxylin and eosin, toluidine blue, safranin-O and picrosirius red following the same protocols used for explants (see Chapter 2.3)

4.1.9 Image analysis of histological sections

Histological sections stained with toluidine blue were processed using ImageJ analysis software to find the mean cross-sectional areas of cultured pellets by overlaying a grid at set intervals, measuring the depth and width of each line to calculate an average across the whole pellet. ImageJ plugin tool FibrilJ was used to measure the orientation and anisotropy of collagen fibrils in cultured pellets. Collagen orientations were measured in 5 regions of 100µm depth and equal width starting from the surface of the cartilage tissue, fibre orientations were measured from 0°- 90° relative to the tissue surface. Collagen anisotropy was measured as arbitrary values between 0 and 1 with the value 1 represents anisotropic collagen directionality and 0 represents isotropic directionality.

4.1.10 Biochemical analysis

Immature and mature cultured pellets were snap frozen in liquid nitrogen post-culture to inhibit biological activity and stored at -20°C until needed. Pellets were digested using papain following the same protocols as explants (see Chapter 2.7.1), pellets only required a 4 hour digestion period vortexing the digests lightly every hour to aid completion. There was no residual undigested tissue remaining at the end of the incubation.

Dimethylmethylene blue assay (DMMB) assays were conducted on digested pellets following the same protocols used for explants (see Chapter 2.7.2). Dilutions of the pellet

digests were necessary so that measurements could be made within the linear range of sensitivity of the assay. Dilutions of 1 in 7 for immature and mature control pellets, or 1 in 40 for immature and mature BMP9 cultured pellets were determined as optimal.

Hydroxyproline assays of papain digested pellets followed the same protocols as used for explants without requiring any adaptation (see Chapter 2.7.4).

4.3 Chondrocyte pellet results

4.3.1 Macroscopic changes in pellet morphology

Immature and mature chondrocyte pellets were cultured for 21 days in chondrogenic growth media either with or without 3.7nM BMP9. At the end of the 21-day culture period there was an observable increase in BMP9-treated pellet sizes compared to controls for both mature and immature chondrocytes (Figure 26). Of note, there was a distinct increase in the size of immature pellets compared to mature pellets cultured in BMP9 media, suggesting that immature chondrocytes are more responsive to BMP9 exposure than mature chondrocytes. Immature cultured pellets shown in Figure 26 A-B had greatly distorted pellet morphologies, this in likelihood was due to their orientation within the Eppendorf tubes restricting regular pellet growth as a disc. However, most pellets cultured in this set and following sets retained a disc-like morphology as seen in Figure 4.2D.
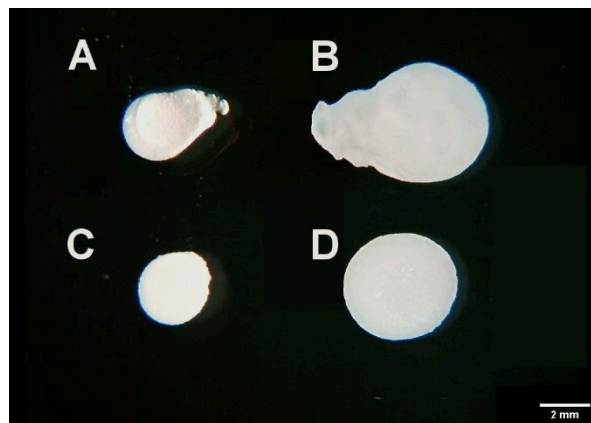
Figure 26. BMP9 induced an increase in the size of mature and immature cultured pellets. Immature and mature chondrocyte pellet constructs were cultured for 21 days in control chondrogenic medium with or without 3.7nM BMP9. A visible increase in pellet size was observed between pellets cultured in chondrogenic medium with BMP9 (**A-B**) or without (**C-D**). **(A)** Immature control, **(B)** immature BMP9, and **(C)** mature control, **(D)** mature BMP9 pellets. Images are representative of 3 independent samples.

4.3.2 Changes in collagen organisation observed using polarised light

Immature and mature pellets were cultured for 21 days in chondrogenic growth medium with or without 3.7nM BMP9. At the end of the culture period the pellets were fixed, sectioned, and stained with picrosirius red (Figure 27). Stained sections were viewed using either normal light microscopy or polarised light microscopy (PLM) to visualise changes in collagen composition and organisation. Picrosirius red sections viewed with PLM cause the stained collagen fibres to refract the light viewed as bifringence varying in intensity dependent on collagen fibril size, alignment, and orientation.

Immature pellets cultured in chondrogenic medium containing BMP9 (Figure 27E), stained with picrosirius red and viewed using PLM contained collagen fibres aligned in perpendicular orientations to the cartilage surface within the mid and deep zones, in respect to immature

control pellets (Figure 27B) which contained uniformly crisscrossing fibres in oblique orientations to the surface. The collage fibres present in immature control pellets appeared to be limited to the pericellular region of the tissue, however, in immature pellets cultured with BMP9 media the fibres extended throughout the interterritorial regions of the tissue (Figure 27E). Immature pellets cultured in control media also lacked any birefringence of collagen fibres parallel to the surface of the tissue, treatment with BMP9 restored the presence of these fibres which are key hallmarks of mature cartilage.

Mature chondrocyte pellets cultured with control chondrogenic medium, stained with picrosirius red and viewed using PLM contained perpendicular fibres relative to the tissue surface (Figure 27H). However, the perpendicular fibres were intersected by horizontal fibres running parallel to the surface. Culturing mature chondrocyte pellets with BMP9 medium (Figure 27I) reduced the abundance of the intersecting fibres within the upper zones of the pellets, in which the collagen fibres remained perpendicularly orientated with a remarkable resemblance to mature cartilage.

Notably, both chondrocyte pellet maturities cultured with BMP9 medium had reductions in PSR staining when viewed using normal light microscopy in comparison to their respective controls, indicating a reduction in the collagen content of the tissues. In immature pellets cultured with BMP9 the reduction in picrosirius red staining was also reflected by a decrease in fibril birefringence when viewed using PLM, fibres appear more dispersed compared to control immature pellets.
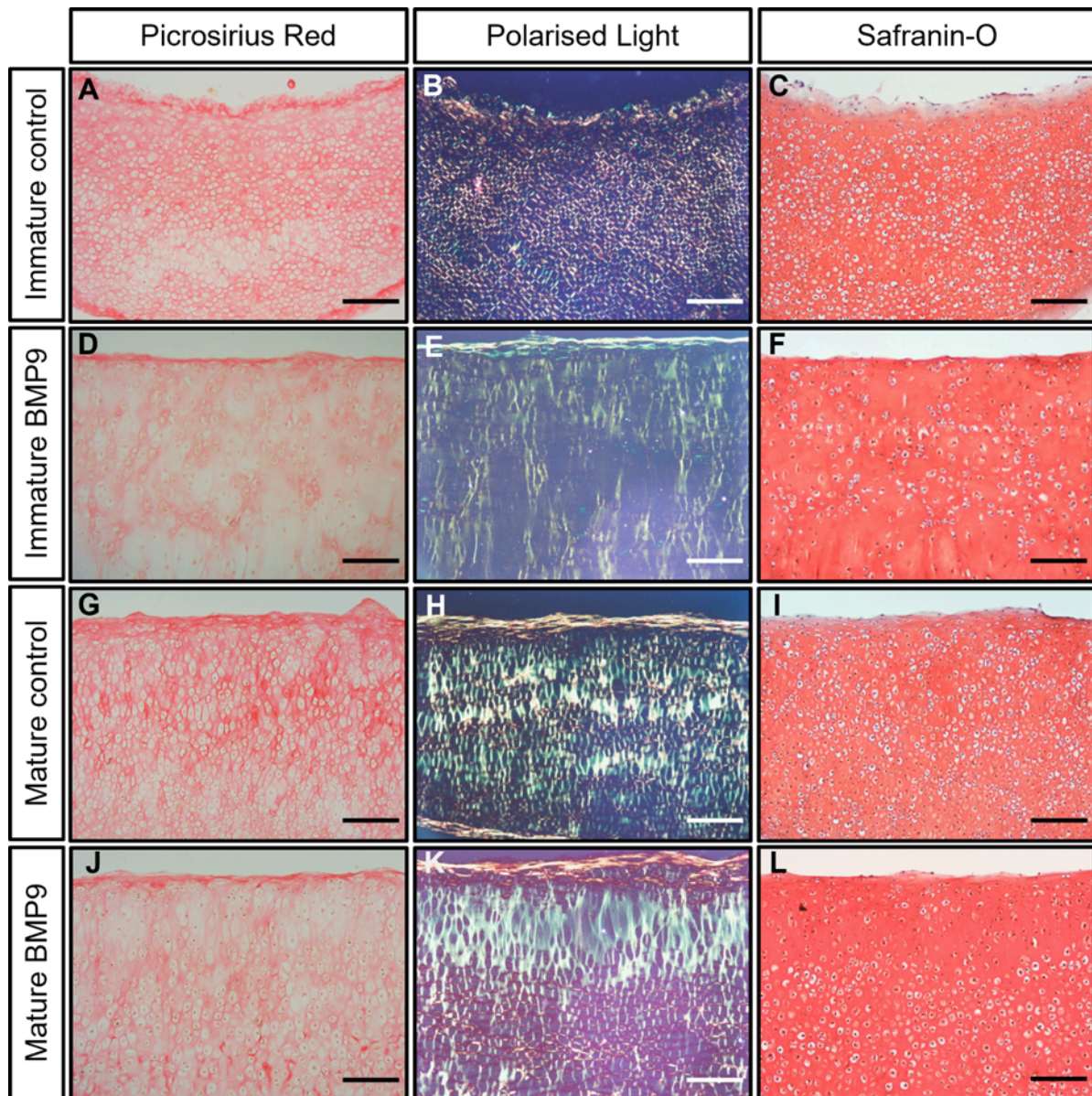
Figure 27. Picrosirius red staining of BMP9 cultured pellets indicates collagen reorganisation is inducible with mature chondrocytes. Immature and mature bovine chondrocyte pellet constructs were cultured for 21 days in control and BMP9 (3.7nM) chondrogenic medium, fixed in 10% NBFS, sectioned, and stained with picrosirius red or safranin-O (SAF-O). Safranin-O sections were viewed using normal light microscopy. Picrosirius red sections were viewed under either normal or polarised light. Figures are representative of 3 independent samples. Scale bar = 150μm

4.3.3   Quantification of collagen orientation and anisotropy

FibrilJ, an ImageJ plugin, was used to quantify changes in collagen fibril orientation observed in cultured pellets. Orientations were measured in 5 regions 100μm in depth from the surface of the cartilage tissue (Figure 28). Orientations were measured from 0°- 90° relative to the tissue surface (Figure 28A). Collagen orientation data shows that immature pellets cultured in BMP9 chondrogenic medium had increasingly perpendicular fibres in comparison to immature pellets cultured in control media, the change in orientation was

most observable from a depth of 100-300μm where the average collagen fibre orientations were 89° and 67° respectively (Figure 28C). Mature pellets cultured with BMP9 contained similarly perpendicular fibres to that observed in immatures from 100μm-500μm deep, maintaining an average angle of 83° relative to the surface. Interestingly, mature control pellets also contained perpendicularly aligned fibres similar to what was found in BMP9-treated mature and immature pellets. Therefore, mature chondrocytes have an innate ability to produce collagen fibres orientated perpendicular to the surface without BMP9 stimulation.
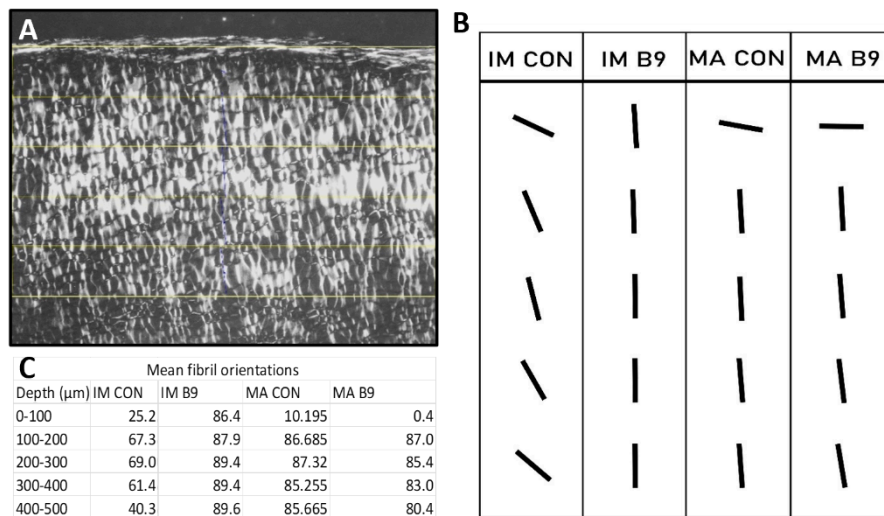

C Mean fibril orientations

Depth (μm)	IM CON	IM B9	MA CON	MA B9
0-100	25.2	86.4	10.195	0.4
100-200	67.3	87.9	86.685	87.0
200-300	69.0	89.4	87.32	85.4
300-400	61.4	89.4	85.255	83.0
400-500	40.3	89.6	85.665	80.4

Figure 28. BMP9 induces significant changes in the collagen organisation of immature and mature chondrocyte pellets. Immature (IM) and mature (MA) pellets cultured for 21 days in chondrogenic growth media with or without 3.7nM BMP9. Post-culture pellets were fixed, sectioned and stained with picrosirius red. Sections were viewed using polarised light microscopy (PLM). **(A)** Collagen fibril orientation within the top 500μm of picrosirius red stained sections was quantified using ImageJ plugin FibrilJ. Images were measured in 5 regions of 100μm depth. **(C)** Orientations of the collagen fibrils were given as values from 0° – 90° relative to the surface. **(B)** Mean values for fibril orientations were drawn to represent the orientation of the fibres within each region. The figure is representative of 3 independent samples.

Using the ImageJ plugin FibrilJ, anisotropy measurements, the property of collagen being directionally dependent, were obtained for the 5 depths in immature and mature pellets cultured with or without BMP9 (Figure 29). Anisotropy measurements are given as arbitrary values between 0 and 1 with the value 1 representing anisotropic collagen directionality and 0 representing isotropic directionality. The data shows that immature pellets cultured in BMP9 chondrogenic medium display greater level of anisotropy, peaking at a depth of 100-200μm, than in controls. Mature chondrocyte pellets with or without BMP9 display a high level of anisotropy. Importantly the increased anisotropy in BMP9 treated mature pellets was confined to 300μm deep below which there were an abundance of intersecting horizontal fibres.
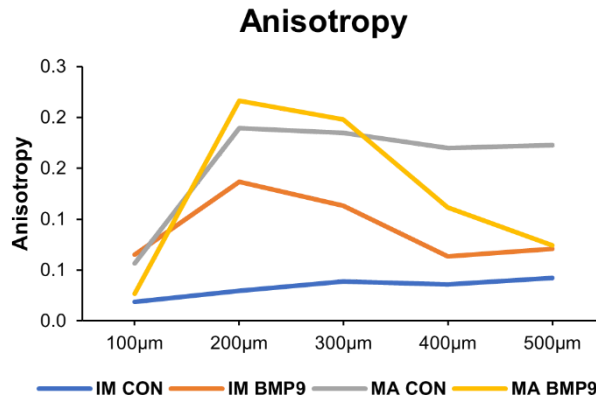
Figure 29. BMP9 induces significant changes in the collagen anisotropy of immature and mature chondrocyte pellets. Immature and mature chondrocytes pellets were cultured for 21 days in control chondrogenic medium with or without 3.7nM BMP9. Pellets were fixed after culture, sectioned and stained with picrosirius red. Sections were viewed using polarised light microscopy (PLM). Image analysis was conducted using FibrilJ to determine the anisotropy of collagen fibres within the top 500µm of tissue. Anisotropy is measured by arbitrary values from 0-1, 0=isotropic 1=anisotropic. Data is representative of 3 independent samples.

4.3.4 Changes in chondrocyte organisation and morphology

Histological staining of immature and mature chondrocyte pellets cultured in chondrogenic growth media with or without 3.7nM of BMP9 was performed to identify changes in ECM composition and chondrocyte organisation. Pellets were stained with haematoxylin and eosin, toluidine blue and safranin-O. Immature pellets cultured in BMP9 media contained visibly hypertrophic cells that were less densely organised, in comparison to immature controls, in-which chondrocytes were more uniform in size and density (Figure 30). Staining of immature pellets was also visibly weaker in BMP9 treated pellets, most deficient within the large interterritorial regions of the pellet, whereas in control pellets staining was much darker and not limited to the pericellular regions.

Mature chondrocyte pellets cultured with BMP9 also exhibited hypertrophic effects, however, reductions in cell density were only obvious within the upper zones of the pellet (Figure 30), where perpendicular fibres had been observed using PLM (Figure 30). Additionally, mature pellets treated with BMP9 appeared to be more strongly stained with haematoxylin and eosin than controls, a direct contrast to the effects observed within immature pellets (Figure 27). Interestingly, when focusing on the mature BMP9 pellets there was a visible reduction of haematoxylin and eosin staining in the upper zones of the pellet where larger interterritorial regions could be seen (Figure 30), relating to the same regions that contained perpendicular fibres in PLM sections (Figure 27).
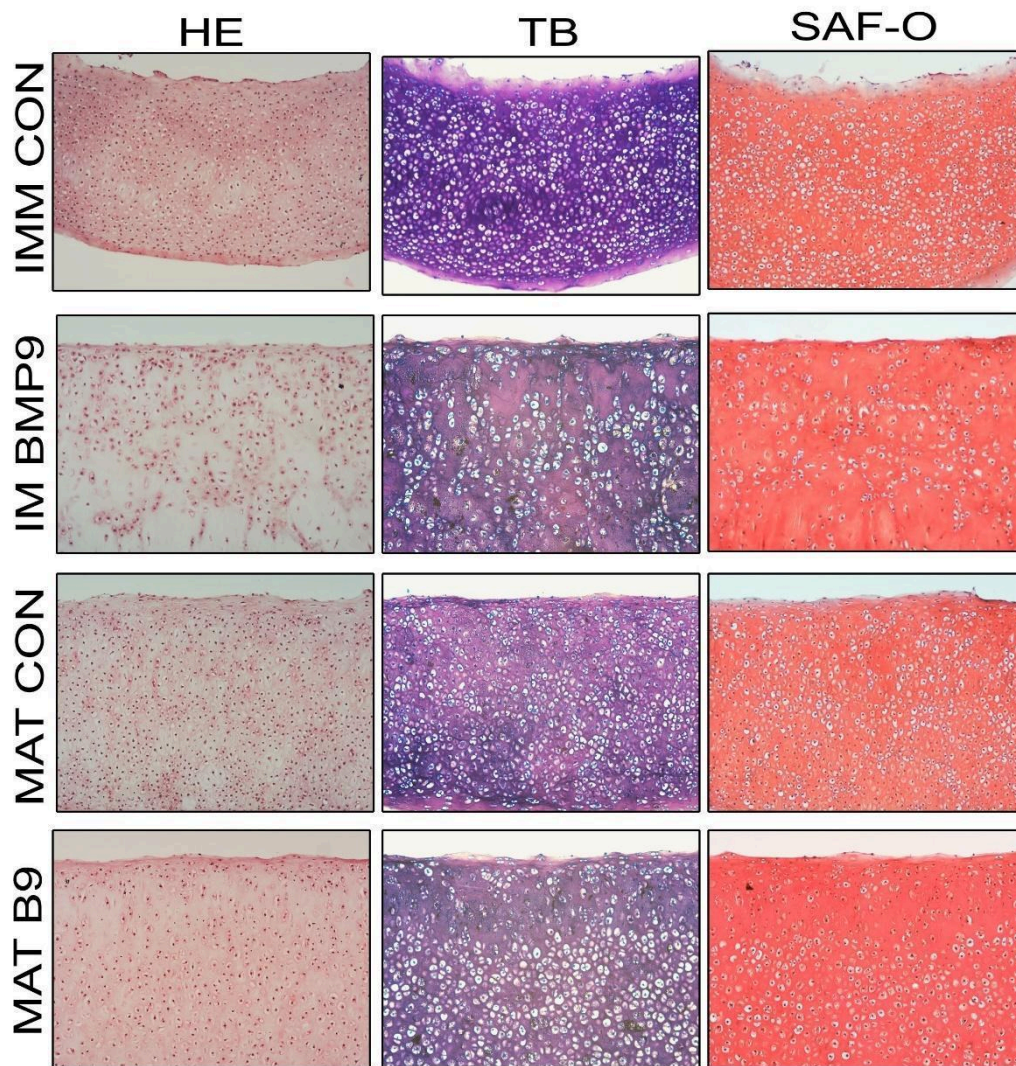
Figure 30. Histological staining of BMP9 cultured pellets reveals a reduction in cell density. Immature and mature chondrocyte pellets were cultured for 21 days in control chondrogenic medium with or without 3.7nM BMP9. Pellets were fixed post-culture, sectioned and stained with either haematoxylin and eosin (HE), toluidine blue (TB), or safranin-O (Saf-O). Stained sections were viewed using light microscopy. Figures are representative of 3 independent samples.

4.3.5 Pellet biochemical data

Wet weights of immature and mature chondrocyte pellets treated with BMP9

Wet and dry weights of immature and mature pellets cultured for 21 days in chondrogenic medium with or without BMP9 were weighed at the end of the culture period. The wet and dry weights were used to determine BMP9s effect on the water content of the pellets (Figure 31). Immature and mature pellets cultured with BMP9 both had increased wet weights (Figure 31B) compared to their respective controls 8.6-fold and 3.2-fold (P<0.001), relating to the increases in size of BMP9 treated pellets (Figure 26B-D). There was a measurable difference between the wet weights of immature and mature controls, but the magnitude was negligible 0.8-fold, associated with the minimal size differences observed between immature and mature control pellets (Figure 26A-C). Additionally, both immature and mature BMP9 pellet dry weights were increased relative to controls 12-fold, and 4.4-fold respectively (P<0.01) contributing to the increases observed in wet weight (Figure 31A).

Of note, immature pellets cultured with BMP9 media had insignificant changes in water percentage compared to immature controls. However, mature pellets treated with BMP9 had significantly lower water percentages (P<0.01) than controls, 88.6% and 91.8% respectively and therefore the composition of mature pellets must contain a higher ratio of insoulabe ECM components relative to water than immature treated pellets.
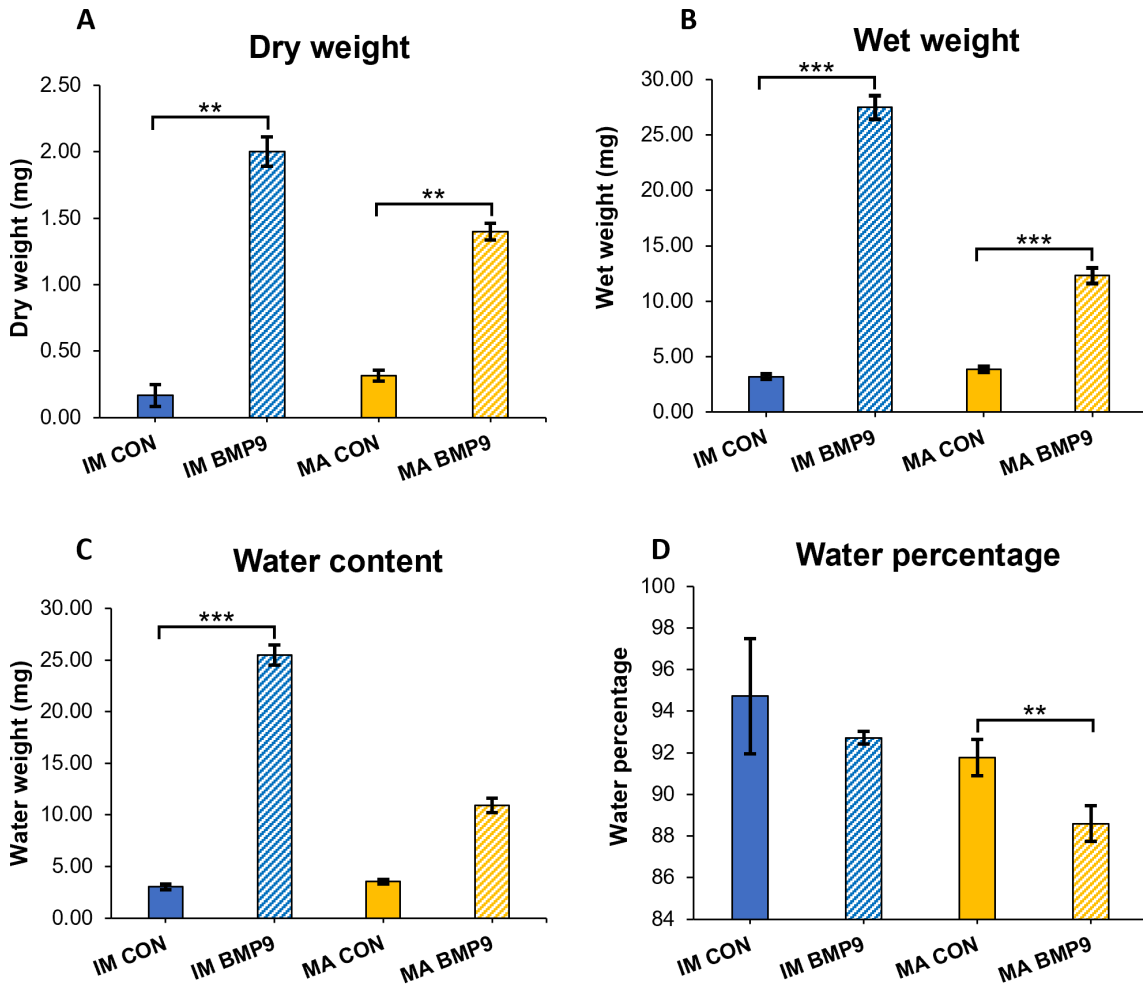
Figure 31. BMP9 induces ECM synthesis and water uptake of immature and mature pellets. Immature and mature chondrocyte pellets were cultured for 21 days in control chondrogenic medium with or without 3.7nM BMP9. At the end of the culture period pellet wet and dry weights were measured and water content calculated. Data is represented as the means of 6 independent samples, error bars represent the standard deviations. Tested for normality then either (**A, C, D**) Kruskal-Wallis and Dunn post hoc tests were used or (**B**) Oneway-Anovas and Tukeys HSD post hoc tests. *P<0.05, **P<0.01, ***P<0.001, ****P<0.0001.

Proteoglycan content of chondrocyte pellets

Immature and Mature chondrocyte pellets were digested with papain and used for DMMB assays to determine the glycosaminoglycan (GAG) content of the pellets and thus an indication of the proteoglycan content. Raw GAG data was normalised to wet and dry weights to find the relative proportions within each pellet (Figure 32). Immature pellets cultured with BMP9 had a 16.4-fold increase in raw GAG content relative to controls (P<0.0001), corresponding to the 12-fold increase observed in dry weight (Figure 32A). Immature pellet GAG content in proportion to wet weight was also significantly increased (P<0.01) in BMP9 cultured pellets by 1.9-fold associated with reductions observed in water percentage (Figure 32D).

In mature pellets treated with BMP9 there was a 5.3-fold increase in raw GAG content compared to controls (P<0.0001), partially accounting for the 3.2-fold increase observed in mature pellet dry weight (Figure 32A). Interestingly GAG content in proportion to wet weight was increased in BMP9 treated mature pellets compared to immature treated pellets (P<0.05), this is consistent with darker staining of the ECM observed in haematoxylin and eosin-stained sections in BMP9 treated mature pellets compared to treated immature pellets (Figure 30).

Of note, mature control pellets in comparison to immature control pellets had a 1.5-fold increase in raw GAG content reflecting the increases in dry weight (Figure 31A). Showing that chondrocyte maturity has some effect on GAG content of the pellets irrelevant of BMP9 stimulation.

Figure 32. BMP9 induces proteoglycan accumulation in immature and mature pellet constructs. Isolated immature bovine chondrocytes were used to develop pellet constructs. Pellets were cultured for 21 days in control chondrogenic medium without 3.7nM BMP9. At the end of the culture period pellets were weighed, flash frozen, air dried, and digested with papain for 4 hours at 60°C. Pellet digests were diluted and used for DMMB assays to determine the glucosaminoglycan (GAG) content of the pellets and thus an indication of the proteoglycan content. Data is represented as the means of 6 independent samples, error bars represent the standard deviations. Tested for normality then either **(A)** Kruskal-Wallis and Dunn post hoc tests were used or **(B, C)** Oneway-Anovas and Tukeys HSD post hoc tests. *P<0.05, **P<0.01, ***P<0.001, ****P<0.0001.

Collagen content

Hydroxyproline assays were conducted on the papain digested pellet material to determine the hydroxyproline content of cultured pellets and hence provide insight into the collagen content of the pellets (Figure 33). Hydroxyproline forms 13% of the chemical composition of collagen so all raw data was multiplied by 8 to convert it to collagen content. Collagen data was normalised to the wet and dry weights of the pellets for comparison.

Immature pellets treated with BMP9 had no significant difference in raw collagen content compared to control pellets (Figure 33A). However, collagen content in proportion to dry weight was decreased 11.2-fold compared to controls ($P<0.0001$) (Figure 33B), This proportional decrease in collagen relates to the 16.4-fold increase observed in GAG content (Figure 32A). Collagen content in immature BMP9 treated pellets was also decreased 7-fold in proportion to pellet wet weights ($P<0.01$), correlating to the reductions observed in picrosirius red staining of BMP9 treated pellets relative to controls (Figure 27), and the 8.4-fold increase observed in pellet water content (Figure 31C).

Mature pellets treated with BMP9 had similar changes in collagen content as observed in immature pellets. No significant difference was observed in raw collagen content but in BMP9 treated mature pellets there was a 2.4-fold decrease in collagen content in proportion to pellet wet weights. This relates to the increases in pellet water content and the reduction of staining observed in mature BMP9 treated pellets compared to controls (Figure 31C). Additionally there was a 3.3-fold decrease in collagen in proportion to pellet dry weight (Figure 32C), relating to 5.3-fold increase in GAG content (Figure 33B).

Interestingly mature BMP9 treated pellets contained higher collagen content in proportion to wet weight than immature treated pellets, this would explain the slight increase in picrosirius red staining observed in mature BMP9 treated pellets compared to immature pellets. (Figure 27)
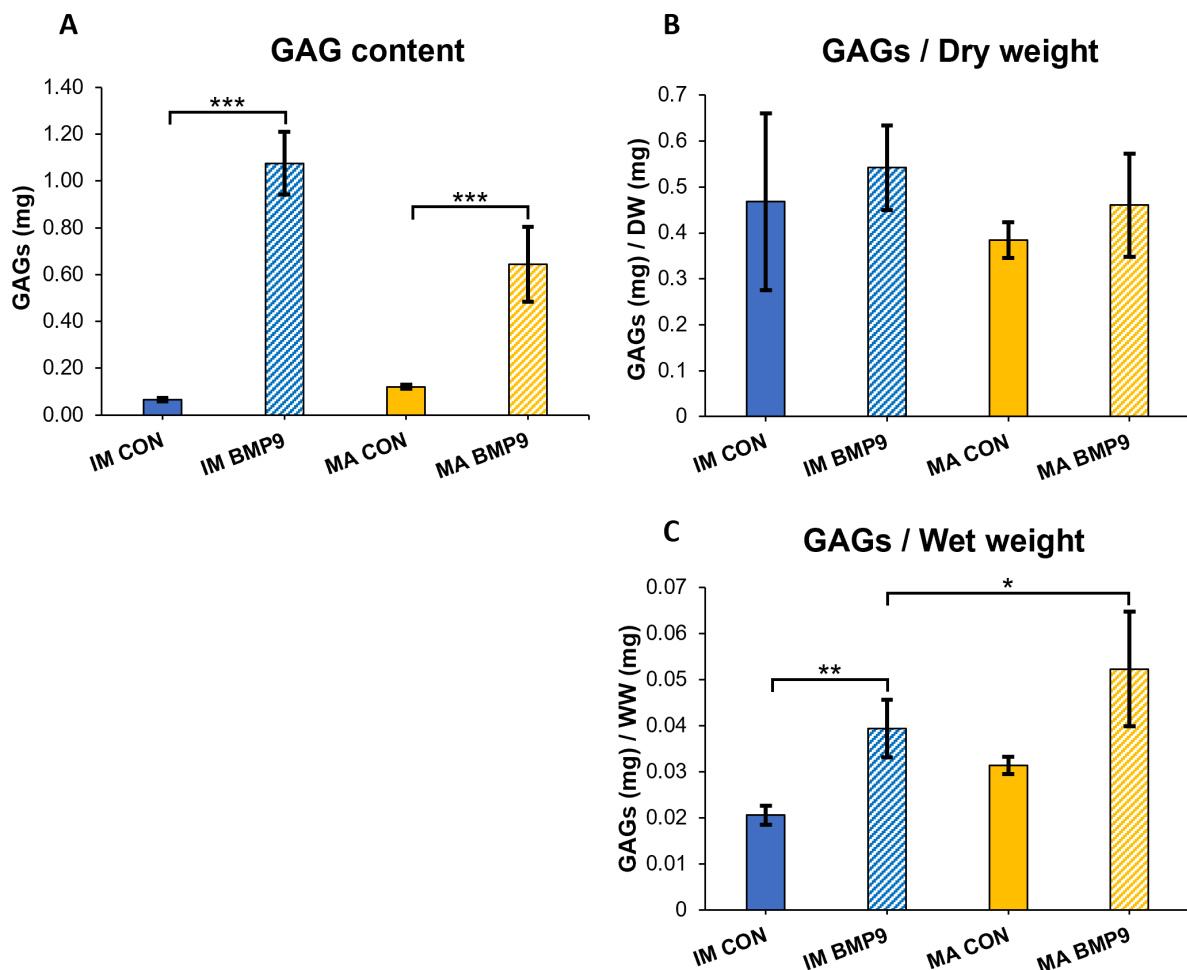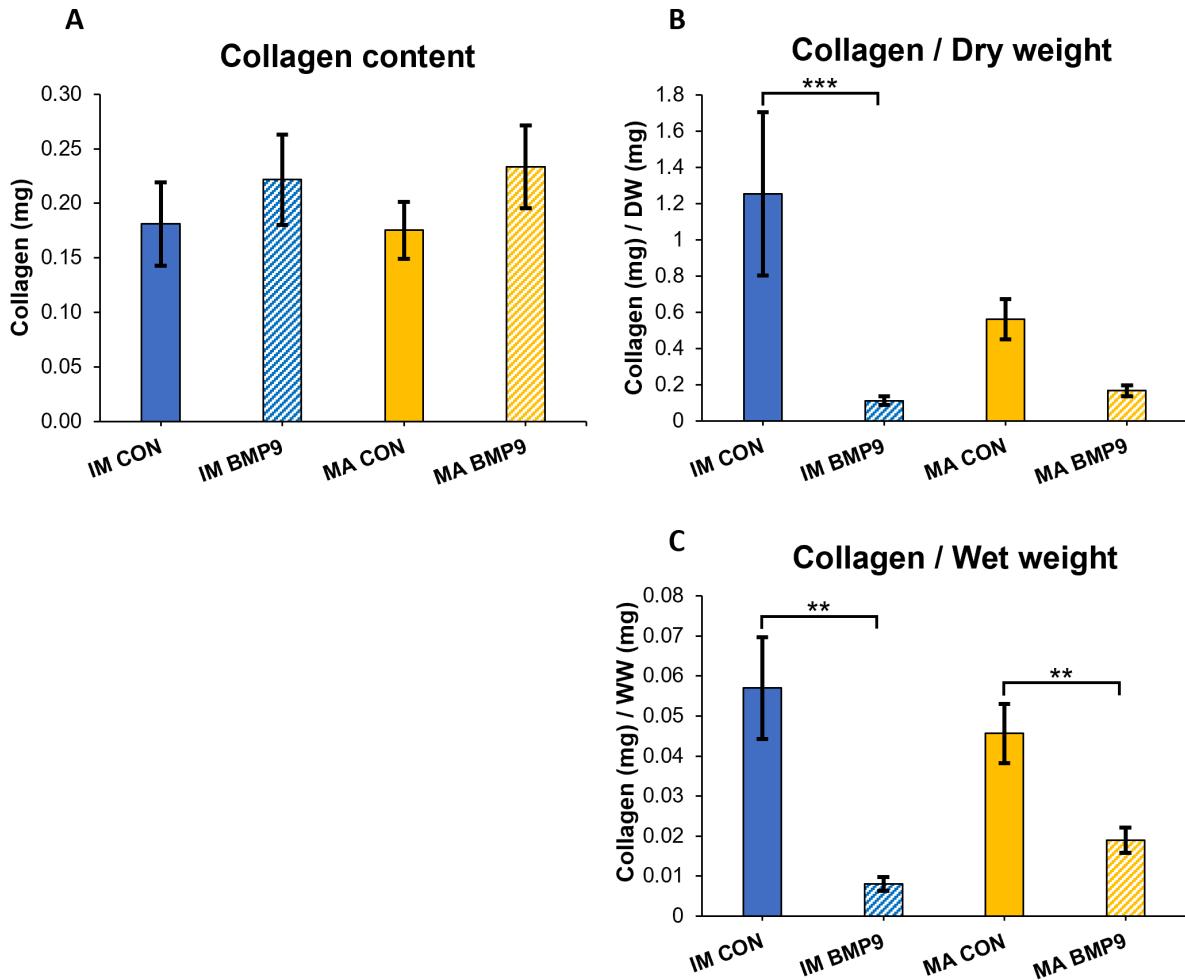
Figure 33. BMP9 induced collagen accumulation in mature and immature pellet constructs. Isolated immature bovine chondrocytes were used to develop pellet constructs. Pellets were cultured for 21 days in control chonrogenic medium or with BMP9. At the end of the culture period pellets were weighed, flash frozen, air dried, and digested with papain for 4hrs at 60°C. Pellet digests were diluted and used for hydroxyproline assays to determine the hydroxyproline content of the pellets and thus an indication of collagen content. Data is represented as the means of 6 independent samples, error bars represent the standard deviations. Tested for normality then either (**B, C**) Kruskal-Wallis and Dunn post hoc tests were used or (**A**) Oneway-Anovas and Tukeys HSD post hoc tests. *P<0.05, **P<0.01, ***P<0.001, ****P<0.0001.

4.4 Analysis of the effects of dorsomorphin on BMP9 treated chondrocytes

4.4.1 Prevention of collagen reorganisation by doxycycline observed using polarised light microscopy

Dorsomorphin is a potent inhibitor of BMP9 signalling, specifically preventing signalling through BMP type 1 receptors via ALK2. Therefore, to further investigate BMP9s role in collagen reorganisation of immature and mature pellets a set of pellets were cultured for 21 days with or without 3.7nM BMP9 with the addition of varying concentrations of dorsomorphin 0μm, 2μm, and 20μm. Post-culture the pellets were fixed, stained with picrosirius red and viewed using PLM to visualise the organisation of collagen within the pellets (Figure 34). When viewed using PLM picrosirius red staining causes aligned collagen fibrils to appear birefringent.

Immature pellets cultured with BMP9 and no dorsomorphin contained brightly bifrigent collagen fibres parallel to the tissue surface. Within the deeper zones of the BMP9 treated pellets collagen fibres were predominately located with the interterritorial matrix aligned perpendicular to the surface, however, the birefringce of these fibres was not as bright as the pericellular fibres observed in immature controls (Figure 34A-B). The lack of birefringence of the perpendicular fibres may be a result of either decreased collagen alignment, fibril width, or density. These features observed in BMP9 treated immature pellets are identical to those seen in the previous cultures (Figure 27). When dorsomorphin was added to the cultures distinct differences in collagen organisation were observed. Immature BMP9 pellets cultured with 2μm dorsomorphin were visibly smaller. Perpendicular fibres were still present within the pellets however they appeared to be more densely packed, intersected by many fibres running parallel to the surface of the pellets (Figure 34C). Fibres present in the pellets were limited to the pericellular and territoral regions of the tissue whereas in normal BMP9 treated pellets most of the fibres spanned across the interterritorial regions uninterrupted. Pellets cultured with 20μm dorsomorphin were greatly reduced in size compared to normal BMP9 samples, collagen fibre fluorescence within the pellet was limited to the pericellular matrix of the tissue crisscrossing around the cells, resembling that of the immature control pellets (Figure 34D).

Dorsomorphin had similar inhibitory effects in mature chondrocyte pellets. Normal mature pellets treated with BMP9 contained collagen fibres parallel to the surface. Within the deep zones of the pellet collagen fibres were located within interterritorial regions, perpendicularly orientated to the surface. Fibres of the deep zone lacked the perpendicular intersecting fibres of the pericellular matrix observed in all depths of normal controls. BMP9 treated mature pellets cultured with 2μm dorsomorphin abolished the appearance of any perpendicularly orientated fibres and collagen fibres were limited to the pericellular regions of the tissue, similar to controls (Figure 34E). Culture with 20μm of dorsomorphin resulted in fragmentation of the pellets during fixation and sectioning. The pellets were much smaller and unable to remain intact. Only very weak birefringence of the fibres was observed in the remaining fragments.

In summary dorsomorphin used at concentrations of 2μm was able to inhibit most of the effects induced by BMP9 signalling preventing collagen reorganisation and pellet growth. When used at 20μm dorsomorphin completely abolishes changes in collagen organisation observed in normal BMP9 treated pellets, preventing any tissue growth, placing the chondrocytes under stress and potentially inducing apoptosis.
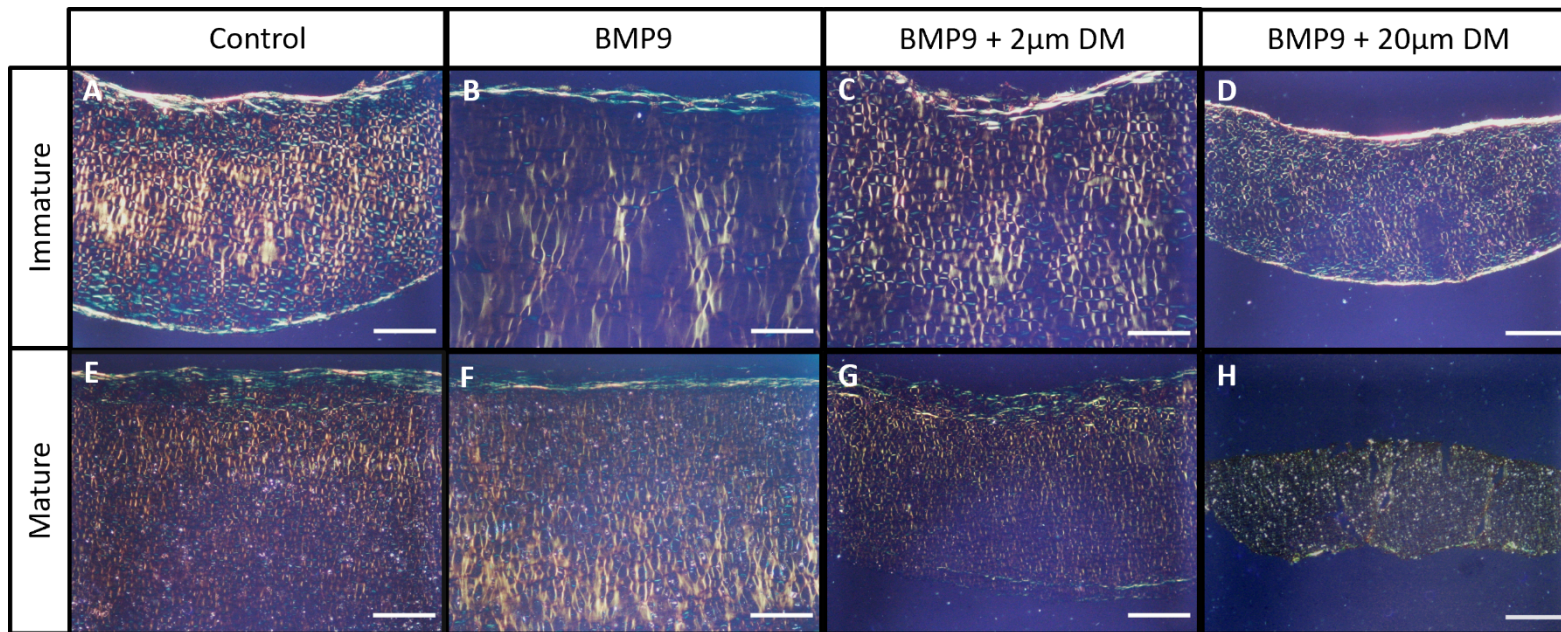
Figure 34. Dorsomorphin prevents collagen organisational changes induced via BMP9 in mature and immature pellet constructs. Isolated immature and mature bovine chondrocytes were used to create pellet constructs. Pellets were cultured for 21 days with BMP9 and varying concentrations of Dorsomorphin 0μm, 2μm, and 20μm. At the end of the culture period pellets were fixed and stained with picrosirius red. Mature Dorsomorphin sections contain white impurities that seem to be a result of the staining process and not an artefact of tissue culture. Mature sections contain increasing background light due to the low levels of staining. Images are representative of 2 independent samples.

4.5 Summary of chondrocyte pellet data

Immature and mature pellets cultured for 21 days in chondrogenic medium underwent significant changes in composition and morphology when treated with BMP9. For both maturities BMP9 induced visible pellet growth (Figure 26). These changes in size were related to increases in the tissues' ECM and water content. Along with the changes in ECM content structural changes were observed within the ECM with regard to the organisation of the collagen matrix.

BMP9 induced changes in the collagen organisation of cultured pellets, with varying effects dependent on cell maturity (Figure 28-29). The collagen organisation in immature chondrocyte control pellets was highly isotropic, mostly orientated at oblique angles to the tissue surface, never exceeding 70° relative to the surface. The collagen matrix became more anisotropic after immature pellets were cultured with BMP9, inducing a shift in collagen fibre orientation from oblique crisscross structures seen in controls to fibres oriented at an angle of 86° perpendicular to the tissue surface. The perpendicularly aligned fibres observed in BMP9-treated immature pellets were found throughout the entire depth of the tissue within the interterritorial matrix of the pellets, in controls fibres were only observed pericellularly around the chondrocytes.

Interestingly mature pellets treated with BMP9 contained higher levels of collagen anisotropy than the immature pellets, as did mature controls, containing perpendicular fibres that were intersected by horizontal fibres within the deep zone (Figure 28-29). In mature pellets stimulated with BMP9 the perpendicular fibres were more apparent than in controls, similar to the changes in organisation observed in immature pellets. However, the transition in collagen organisation was only limited to the upper half of the tissue where fibrils could be found within the interterritorial matrix, the deeper zones remained unchanged and thus BMP9s effect on mature chondrocytes is restricted compared to immatures. This partial change in collagen orientation of mature BMP9-treated pellets was also observed in later cultures, however, the zones in which perpendicular fibres were observed in these cultures seemed to shift between the upper and lower zones of the tissue, always affecting only a portion of the tissue, this may be due to pellets inverting during the feeding process.

Another distinct difference between the two pellet maturities was an increase in collagen fibril birefringence of the mature pellets compared to immatures when viewed using polarised light microscopy PLM. Immature pellets cultured with BMP9 were effected most significantly with the lowest birefringence observed of all the pellets (Figure 27). The reason for the reduction in birefringence between mature and immature pellets is likely due to several factors, PLM birefringence can be effected by collagen fibril alignment, size, or density. The relative decrease in anisotropic values of immature pellets relative to matures, explains in part why the PLM images were less intense as the fibres are not as aligned, but does not explain the decrease between immature control and BMP9 pellets which had higher anisotropic values. Although there was no significant difference in the raw collagen content of the pellets there were significant increases in GAG and water content (Figures 31-33). Therefore, the significant reduction in collagen content normalised to either dry weight or wet weight between BMP9 cultured pellets and controls would explain the decrease in picrosirius red staining and PLM birefringence of immature BMP9 cultured pellets relative to controls and compared to mature pellets.

BMP9 cultured pellets underwent significant biochemical compositional changes in water content, dry weight, and water percentage (Figures 31-33). The raw water content of

immature and mature pellets treated with BMP9 increased significantly compared to controls by 8.6-fold and 3.2-fold respectively, this was accompanied by a 12-fold and 4.4-fold increase in pellet dry weights. However, the water percentages decreased for pellets cultured with BMP9 likely due to the low ECM content of the pellets and high cellularity, of which cells are mostly water, observable from the dry weight data and histological sections.

BMP9 treated immature and mature pellets had no significant change in raw collagen content compared to controls, however, collagen content relative to wet was severely reduced in both mature and immature pellets 3.3-fold and 11.2-fold, as was collagen content relative to dry weight, 2.4-fold and 7-fold respectively. The decreases in collagen content observed must be on account of increases in the GAG and water content of the pellets. In BMP9 cultured pellets, GAG content was increased by 1.7-fold and 1.9-fold for mature and immature pellets respectively. BMP9, therefore, has a greater effect on GAG accumulation within immature pellets compared to matures. Interestingly in control pellets GAG content normalised to wet weight was 0.7-fold higher in mature pellets than in immatures, thus mature chondrocytes maintain higher levels of GAG content without any external stimulation.

Culturing BMP9 pellets with dorsomorphin a BMP type-1 inhibitor obstructed BMP9s effects in mature and immature constructs (Figure 34). In mature pellets, 2μm concentrations of dorsomorphin effectively inhibited the changes observed in collagen orientation in BMP9 cultured mature pellets, resembling mature controls when viewed using PLM. Immature pellets cultured with BMP9 and 2μm dorsomorphin still contained slight changes in the collagen matrix containing fibres perpendicularly orientated fibres, but the size of the interterritorial regions were reduced when compared to immature BMP9 treated pellets. At concentrations of 20μm dorsomorphin prevented any growth in BMP9 treated pellets, immature pellets were smaller than their controls and mature pellets fragmented when sectioning. Thus, BMP9s induced effects on pellet collagen organisation and growth were effectively inhibited by blocking ALK signalling with dorsomorphin.

Chapter 5: Discussion

5.1 BMP9 recapitulates aspects of postnatal cartilage maturation

Critical to the development of structurally mature articular cartilage is the process of postnatal maturation, in which isotopically immature cartilage adopts a highly organised anisotropic arrangement, resulting in a thinner and stiffer tissue. Using tissue engineering to repair or replace damaged or diseased cartilage that does not recapitulate the process of maturation is destined to fail due to its inferior biomechanical properties (Hunziker, 2009). Therefore, the inclusion of processes that can induce features of postnatal maturation in engineered tissues is essential for long-term durability. In this study we have shown that bone morphogenetic protein 9 (BMP9) is capable of inducing tissue remodelling of immature cartilage that mirrors features of postnatal maturation, the most prominent of which is the reorganisation of the collagen network and the formation of fibres perpendicular to the tissue surface in the deep zones.

Bone morphogenetic protein 9 (BMP9) belongs to the TGFβ superfamily, known for its osteogenic and chondrogenic properties in bone formation. It has recently been established in a mouse model of digit tip amputation that BMP9 can induce regeneration of the joint including the formation of histologically mature articular cartilage (Yu et al., 2019). In addition, BMP9 can induce precocious differentiation and morphological changes to the collagen structure of articular chondroprogenitors grown as pellet cultures (B. J. Morgan et al., 2020). In this study we used polarised light microscopy (PLM) to visualise changes in the collagen organisation of immature cartilage explants cultured with BMP9. Changes were observed up to a mean depth of 0.66mm±0.2mm from the surface (Figure 4). Within this region of reorganisation, collagen fibres formed columnar structures similar to the arcades described by Benninghoff (Benninghoff, 1925; Kääb et al., 1998). In the superficial zone, collagen fibres were orientated parallel to the articular cartilage (25°) surface transitioning to perpendicular orientations (86°) within the first 100μm of tissue depth (Figure 5). Perpendicular collagen fibres persisted throughout the mid and deep zones of the cartilage explants. Identical zonal changes in collagen orientation from parallel fibres in the superficial zone to perpendicular fibres within the mid and deep zones of articular cartilage have been documented in many studies of the organisation of native immature and adult cartilages (Kääb et al., 1998; Rieppo et al., 2009). The appearance of these zonal structures only occurs during postnatal maturation, in immature articular cartilage collagen fibres are principally orientated parallel to the surface within all zones (Clark et al., 1997; Cluzel et al., 2013; van Turnhout et al., 2010). We observed similarly parallel-oriented fibres in immature control bovine explants (Figure 4).

This study was able to quantify the anisotropy of the collagen fibril organisation in immature explants cultured with BMP9 (Figure 8). Anisotropy was lowest within the superficial and transitional zones of the tissue increasing with depth as fibres became more perpendicularly aligned. During postnatal maturation of articular cartilage collagen fibres undergo the same organisational transformations from an isotropic organisation in immature cartilage to anisotropic in mature, indicating BMP9s effectiveness at inducing postnatal-like changes to the collagen matrix (Rieppo et al., 2009).

Lewis et al, performed a study using full thickness cartilage from immature bovine metacarpal joints under 2 years of age. In which they found that the total depth of cartilage present was 0.54mm ± 0.08mm (Lewis et al., 1998). We observed changes in the collagen organisation of immature cartilage explants cultured BMP9 up to a mean depth of 0.66mm±0.2mm, implying that the reorganisation of collagen induced by BMP9 affects the

entire depth of permanent cartilage within the immature explant (Figure 6). Interestingly, some explants cultured in control chondrogenic medium also exhibited a degree of spontaneous collagen fibre reorientation perpendicular to the surface. We theorise that these changes are due to breakdown of cartilage and swelling of the tissues caused by localised proteoglycan loss, though in every case the extent of collagen reorientation in the BMP9 treated counterparts were significantly more apparent.

In addition to the changes in collagen structure induced by BMP9 we observed differences in chondrocyte morphology and organisation. In mature cartilage tissue changes in chondrocyte morphology and organisation are defined by the three cartilage zones, superficial, transitional, and radial. The latter zones make up the top 10%, next 10% and the remaining 80% of cartilage tissue respectively (Hunziker et al., 2002). Within the superficial zone chondrocytes are at their highest density and shaped with a disc-like morphology, elongated and parallel to the tissue surface. Chondrocytes of the mid zone are less densely organised and obliquely orientated along their long axis to the surface. With increasing depth chondrocytes continue to decrease in density becoming larger and more circular, forming columns of cells sometimes sharing a singular large chondron and territorial matrix (Hunziker et al., 2002; Jadin et al., 2005). In BMP9 cultured explants we observed similar changes in cell morphology and organisation emulating mature cartilage. Within the superficial regions the long axis of chondrocytes were orientated at 35° parallel to the surface with thick bundles of highly birefringent fibres, transitioning to a more perpendicular orientation, 60° to the surface, within deep zones of cartilage, in which chondrocytes could be found arranged into columns (Figure 16-17). With increasing depth from the superficial to deep zones an increase in chondrocyte area was also observed from $115\mu m^2$ to $152\mu m^2$ (Figure 16). Other *in vitro* studies have demonstrated similar hypertrophic effects on chondrocytes cultured in scaffolds in the presence of BMP9 (Blunk et al., 2003).

The changes observed in chondrocyte morphology and organisation with increasing depth in BMP9 treated immature cartilage explants were coincident with changes in collagen fibre organisation, however, it is not clear which change precedes the other, either rearrangement of collagen causes changes in chondrocyte morphology and organisation, or the opposite occurs and changes in chondrocyte organisation modulate collagen alignment. Previously Decker et al have described that growth in mouse tibial cartilage is caused by chondrocyte hypertrophy and rearrangement of the existing cell population to form columns, proposing that changes in collagen fibril orientation were promoted by 'convergent extension' through deeper zone chondrocytes undergoing hypertrophy during maturation and cellular rearrangement (Decker et al., 2017). Convergent extension has mainly been studied in embryos and is a process whereby an embryo's tissues (cells) are restructured to converge upon a single axis and extend (Wallingford et al., 2002). However, Mankin and Hunziker identified that chondrocytes proliferate in the surface and deep zones, above the subchondral bone plate, theorising that vertical expansion of cartilage is caused by cell proliferation of the deep zone chondrocytes, the outcome of which is the formation of cell columns. The latter changes, Hunziker infers are caused by appositional growth and resorption of underlying epiphyseal tissue including the newly formed deep zone cartilage (Hunziker et al., 2007; Mankin, 1962). We observed cells in BMP9 treated immature cartilage undergoing proliferation and hypertrophy (Figure 14-15). Therefore, a combination of the two theories may be correct, rearrangement of the existing cell population forms distinct zonal organisations which undergo proliferation and hypertrophy in the deep zone driving a vertical expansion of the tissue. It is conceivable that differences between our observation and those showing little or no proliferation in mouse cartilage may be due to

species differences or a difference in the joints analysed (tibial plateau versus metacarpophalangeal joint).

5.2 Changes in collagen reorganisation of immature explants cultured with BMP9 is a result of remodelling and not new synthesis

In bovine articular cartilage maturation, increases in collagen content occur from foetus to calf, however, during the later stages of maturation from calf to adult there is no significant increase in collagen content (Williamson et al., 2001). In immature bovine explants cultured with BMP9 we observed no significant change in raw collagen content (Figure 13). In fact, normalisation of collagen content to explant wet weights indicated a decrease in the proportion of collagen in day 21 BMP9 explants compared to day 0 controls. This was supported by PCR analysis in which there was a decrease (0.4-fold relative to controls) in *COL2A1* expression at day 21 in BMP9 treated explants compared to controls. Previous studies have shown *in vitro* chondrocyte pellet cultures stimulated with BMP9 induce elevated type II collagen expression until day 7, after which expression levels are relatively lower. However, these studies were contextually different in that pellet growth was being studied and therefore may be of little relevance to chondrocyte function with a preformed ECM (Morgan et al., 2020). Immature explants cultured in BMP9 media lacked the same intensity of picrosirius red staining of the collagen network relative to controls (Figure 4). The areas of tissue with reduced staining were localised to regions of cartilage that had undergone changes in fibril orientation, containing perpendicular fibres. However, COL2-3/4m antibody staining showed that no breakdown (denaturation) of type II collagen was occurring within the surface zones of cartilage (Figure 9). Together this data suggests that in BMP9 treated explants there is no deposition of new collagen fibres or remodelling through collagen turnover, therefore the changes observed in collagen organisation must be due to the transformation of the existing collagen network.

5.3 BMP9 induces compositional changes in the ECM content of immature explants

Biochemical assays of immature cartilage explants cultured with BMP9 chondrogenic medium revealed there was no significant difference in proteoglycan content normalised to wet weight compared to controls (Figures 11-13). However, there was a significant increase in the turnover of proteoglycans from within BMP9 cultured explants normalised to day 0 wet weights, combined with a loss in staining of the mid and deep zones of BMP9 cartilage explants. Supporting the latter change, a reduction in aggrecan (*ACAN*) gene expression and upregulation of *MMP3* expression was measured at day 21 in BMP9 explants, indicating an increase in tissue degradation (Figure 18-19). Previous studies in equine cartilage found that decreases in proteoglycan content occur during postnatal maturation and ageing, supporting our findings (Brama et al., 2000; Klein et al., 2007).

In BMP9 cultured explants increases in proteoglycan turnover correlated with an increase in the proportion of water within the tissue (Figure 11). During OA it is well documented that MMP mediated proteoglycan degradation results in an increase in water content and an expansion of cartilage tissue (Horton et al., 2006). Therefore, BMP9 induced degradation of proteoglycans may cause an uptake of water into the tissue promoting expansion of cartilage that ultimately drives collagen reorganisation. Swelling of articular due to water uptake would explain the reductions observed in picrosirius red staining and collagen content (normalised to wet weight). A previous study of collagen orientation in equine tissue found that during the

early months of postnatal maturation there is a decrease in proteoglycan content. This decrease in proteoglycan content corresponded to the initial changes in collagen orientation (Oinas et al., 2018). Therefore, MMP3 mediated proteoglycan loss, water uptake, and swelling of cartilage may be the principal force behind collagen reorganisation in BMP9 cultured explants.

5.4 Matrix metalloproteinase tissue degradation drives tissue remodelling of immature cartilage via an increase in water content

Tissue degradation and remodelling are modulated by proteins such as matrix metalloproteinases. During cartilage maturation MMP9 and MMP13 play crucial roles in the transition of epiphyseal cartilage to bone during the processes of endochondral ossification (Ortega et al., 2004). However, MMP activity within the permanent cartilage, specifically during postnatal maturation, has never been studied, most literature focuses on the changes in MMP expression during cartilage breakdown.

We observed that inhibition of MMPs via doxycycline prevented reorganisation of the collagen matrix in immature cartilage explants cultured with BMP9. Furthermore, gene expression analysis revealed that MMP3 was the only MMP to be significantly upregulated by BMP9 treatment relative to control explants (Figure 19). MMP3 is a stromelysin responsible for the degradation of proteoglycans and other smaller components within tissues. MMP3 can activate other pro-MMP3 enzymes, as well as processing MMP1, -2, and -9 into their active forms, making it a crucial protein in initiating cartilage remodelling (Munhoz et al., 2010). In cartilage, *MMP3* is highly expressed, along with its inhibitor TIMP1 (tissue inhibitor of metalloproteinase) regulating its activity in normal tissue homeostasis (Kevorkian et al., 2004). In immature explants cultured with BMP9 media we also observed a 2.8-fold reduction in *TIMP1* gene expression at day 10.5 and a 2.8-fold reduction in *TIMP2* expression at day 21 relative to controls (Figure 20). Studies have shown that TIMP1 has the highest affinity for MMP3 compared to other TIMPs (Hamze et al., 2007). Thus, upregulation of MMP3 and downregulation of its inhibitor would result in increased enzyme activity, which we suspect occurs in a co-ordinated and localised manner. A previous study identified the colocalization of MMP3 and COL2-3/4m in the surface of OA (Lin et al., 2004). In contrast, we observed no COL2-3/4m activity at the surface or mid zones in BMP9 treated explants (Figure 9). This is unsurprising as MMP3 cannot degrade collagen triple helices due to its catalytic domain but does degrade proteoglycans, thus its activity would explain the increased turnover of proteoglycans and why there is no significant reduction in collagen content (Lin et al., 2004; Murphy et al., 1992).

Studies in mice have shown that *MMP3* expression is low at birth increasing until skeletal maturity is reached (Gepstein et al., 2002). At the same time *TIMP1* expression is very low at birth, increasing up until 2 months of age. At 4 weeks old *TIMP1* expression is mostly localised to the pericellular matrix of proliferating and hypertrophic chondrocytes and osteocytes of the mineralising zone. *TIMP2* expression follows a more varied pattern peaking at 3 months, localised to the surface zone and hypertrophic cells like *TIMP1*. In general TIMP staining was quite low in the articular cartilage relative to epiphysial cartilage. (Joronen et al., 2000). However, at skeletal maturity *TIMP1* and *-2* expression are localised to the permanent cartilage. Changes in localisation suggest that low-level MMP3 activity is permitted by low-level expression or the absence of TIMP1 in permanent cartilage during the early phases of postnatal maturation but as mice mature *TIMP1* expression localises to the permanent cartilage inhibiting MMP3 activity, further maturational changes, and resorption of

the permanent cartilage by the underlying tissues. However, it is important to note that TIMP1 and all other TIMPs have broad MMP inhibitory effects therefore further research would be required to identify the exact locations of *MMP3* and *TIMP1* expression within the cultured explants.

5.5   BMP9 signalling is involved in the early stages of cartilage maturation

MMP3 is also involved in growth factor signalling processes, cleaving perlecan and decorin which releases FGF2 and TGFβ1 from the pericellular regions of cartilage (Imai et al., 1997; Whitelock et al., 1996). Unpublished data from our lab has shown that BMP9 induces upregulation of *TGFβ1* gene expression in chondroprogenitors in pellet culture. FGF2 and TGFβ1 stimulate precocious maturation of articular cartilage upregulating lysyl oxidase-like1 (LOXL1) crosslinking of the collagen fibres which we believe prevents reorganisation of fibres to the extent found in BMP9 treated explants (Khan et al., 2011; Zhang et al., 2017). This combination of growth factors also upregulates the expression of *TIMP1* 64-fold (Khan et al., 2011). We therefore hypothesise that the structural and morphological changes induced by BMP9 precede those changes induced by *FGF2* and *TGFβ1* expression. BMP9 induces reorganisation of the collagen matrix via MMP3 mediated tissue degradation, followed by increases in *TGFβ1* and *FGF2* expression inhibiting further reorganisation of the collagen matrix caused by *TIMP1* upregulation. The final steps of maturation would involve LOXL1 mediated crosslinking of the collagen matrix locking the collagen structure in place by inducing mature collagen crosslink formation preventing further reorganisation.

Quiros et al. have shown that in equine chondrocyte pellet cultures BMP9 and TGFβ1 have synergistic effects, they observed increased *MMP3* expression after 28 days, *COL2A1* expression until day 7, and increases in GAG content (Quiros et al., 2020). Another relevant study showed that in chondrocyte pellets TGFβ1 has an inhibitory effect on BMP9 preventing osteogenic markers osteopontin, osteocalcin, and type X collagen but does not affect type II collagen expression, maintaining an ideal chondrogenic environment (R. D. Li et al., 2021; van Caam et al., 2015). These studies support our theory that together BMP9 and TGFβ1 have complementary effects in cartilage maturation.

5.6   Chondrocyte maturity modulates the structural and organisational effects of BMP9

Studying the maturation-inducing effects of BMP9 in intact immature cartilage proved to be a very useful model to dissect some of the key mechanisms that drive the process forward. However, we noted occasional spontaneous appearance of re-orientated fibres aligned perpendicularly to the surface in control explants (Figure 5). These changes in collagen fibril alignment were often in deeper zones, where prolonged culture induces cartilage catabolism, or where the surface zone was damaged. We also noted that in paired explants the BMP9 sample always had more pronounced changes compared to control explants and they were localised to the surface zone and within the depth from the surface (~0.66mm) where the permanent cartilage is present (Figure 6). To develop a more stringent method to evaluate the role of BMP9 in postnatal maturation we decided to use isolated chondrocytes from immature and mature bovine cartilage grown as pellet cultures to investigate the effects of BMP9 on maturation.

We discovered that BMP9 does in fact have a profound effect on collagen fibril organisation in growing cartilage derived from immature chondrocytes. Fibril organisation was perpendicular to the surface of pellets in BMP9 treated cultures and pericellularly organised in non-treated pellet cultures (Figure 27). When using mature chondrocytes, we found that in the absence of BMP9 they formed thin perpendicularly aligned collagen bundles and the superficial parallel fibres were more pronounced. This appears to show that mature chondrocytes retain the phenotypic properties required to produce and organise an adult-like ECM. This also implies a genetic difference between cells which could be further examined through Next Generation Sequencing. We found that mature chondrocyte pellets cultured with BMP9 caused the enhanced formation of perpendicular interterritorial fibres (Figure 27). Production of the latter fibres was more pronounced within the upper zones of the tissue. In the deeper zones of BMP9 treated mature pellets perpendicular collagen fibres were intersected at right angles by fibres running parallel to the tissue surface. These same intersecting fibres were present throughout the depth of mature chondrocytes cultured in control chondrogenic medium.

In normal articular cartilage maturation, the formation of perpendicular interterritorial collagen fibres is only found in adult cartilage (Clark et al., 1997; Cluzel et al., 2013; van Turnhout et al., 2010). These interterritorial fibres contain crosslinking oblique collagen fibres (Kääb et al., 1998). Another study of bovine knee articular cartilage identified the presence of parallel-oriented fibres in the deep zone of mature tissue (Rieppo et al., 2008). Therefore, the appearance of parallel intersecting fibres within the deep zone provides an indication of tissue maturity. So, it can be reasoned that BMP9 induces maturational changes in the collagen organisation of mature chondrocyte pellets that more closely recapitulate the structural architecture of native adult cartilage. Interestingly the deep zone tissue of mature chondrocyte pellets closely resembles that of immature control pellets, suggesting that BMP9 may induce patterning of tissue organisation and limit the depth of changes in cartilage produced by mature chondrocytes.

Mature chondrocytes cultured with BMP9 media had increased concentrations of proteoglycan and water content relative to controls. However, both immature and mature chondrocytes cultured with BMP9 media contained relatively similar levels of collagen (Figure 33). Indicating that increased proteoglycan content and water uptake in mature pellets are responsible for the differences in the collagen networks. Thus, the changes in collagen organisation of BMP9 cultured immature and mature pellets are dependent on increasing proteoglycan and water content not the synthesis of new collagen. Therefore, collagen reorganisation, as with explants, is due to expansion of the pellet tissue. However, in this circumstance tissue expansion is caused by proteoglycan accumulation, in contrast to explants in which swelling of the tissue is modulated by proteoglycan loss. Supporting the literature in which an *in vitro* study of BMP9's anabolic effects on juvenile and adult bovine articular cartilage found that BMP9 functions as a potent anabolic factor for juvenile cartilage inducing an 8-fold increase in proteoglycan expression and a 6.4-fold increase in collagen expression, whilst adult cartilage had little to no response to BMP9 (Morgan et al., 2020).

BMP9 is known to signal via ALK1 and to a lesser extent ALK2 receptors via activation of SMAD and MAPK signalling pathways (Luo et al., 2010). Dorsomorphin, a broad-spectrum inhibitor of ALK receptor signalling, arrested collagen reorganisation of immature and mature chondrocytes cultured with BMP9 media (Figure 34). Inhibition of collagen reorganisation of mature chondrocytes was achieved at a 10-fold lower concentration than immature chondrocytes. This corroborates the potency of BMP9 on immature chondrocytes relative to matures. Therefore, the latter data suggests that the differential response of chondrocytes to BMP9 directly correlates to ALK receptor signalling. It has been shown in previous studies

that ALK1 receptor concentrations are unaffected by ageing however ALK2 receptor concentrations decrease 3-fold with maturity (van Caam et al., 2016). Thus, the reduction in BMP9 stimulation of mature chondrocytes may be due in part to a developmentally encoded reduction in ALK2. Therefore, we believe ALK1 and -2 signalling are required for BMP9 induced maturation of articular cartilage corroborating previous studies.

5.7 Conclusion

In this study we have shown that BMP9 induces structural and morphological changes recapitulating key hallmarks of mature cartilage via histological, biochemical, and genetic methods. We have shown qualitatively and quantitatively that BMP9 induces a transition of the collagen network from one that is isotropic to one that is anisotropic, forming collagen fibres perpendicular to the surface within the mid and deep zones of the tissue. We have identified that these zonal changes in collagen structure are closely associated with the concomitant change in the organisation and morphology of chondrocytes. Combined with the changes in tissue morphology we observed a loss of proteoglycan staining within the reorganised regions combined with an increase in proteoglycan turnover and water uptake, modulated by shifts in *MMP3* and *TIMP1/2* expression. However, no changes were observed in collagen content, expression or turnover. Doxycycline-induced inhibition of MMP activity stopped the changes in collagen reorganisation. We therefore hypothesise that explants cultured *in situ* with BMP9 undergo changes in the existing collagen network through tissue degradation of proteoglycans resulting in swelling caused by increases in interstitial and interfibrillar water content. This change in the collagen fibril network organisation precipitates reorganisation of the existing chondrocyte population into columns. There is evidence of both proliferation and hypertrophy of chondrocytes contributing to the expansion of the tissue. The swelling of cartilage results in vertical expansion of the tissue drawing with it collagen fibrils which extend to form perpendicularly aligned networks. Using pellet cultures we proved that the latter process was regulated by BMP receptor signalling through ALK1 and 2 by inhibiting changes in collagen organisation using dorsomorphin. This information casts light on BMP9's ability to remodel cartilage tissue *in vitro and in situ* highlighting its potential applications for the development of tissue constructs with enhanced structural properties.

5.8 Limitations and future outlook

Following on from the research I have conducted there are still some key gaps in the knowledge base that I was unable to investigate. The next steps for the project would be to complete *in situ* hybridisation to pinpoint the precise location of *TIMP1* and -2 expression, as well as *MMP3*, in BMP9 cultured explants. MMP activity analysis will provide critical insight into which ones are functional, either through antibody labelling or zymography-based approaches. It will also be important to complete mechanical testing of the cultured explants to determine if the structural and organisational changes observed correlate with changing mechanical properties and how these compare to native articular cartilage tissue. Cartilage is a well-documented mechanosensitive tissue, known to be influenced by mechanical stimulation and this may play a significant role in the remodelling process of maturation. Thus, it will be important in future works to reproduce experiments under cyclic mechanical loading to identify its impact on BMP9 induced cartilage maturation. Finally, the next steps in generating structurally mature cartilage will be sequential co-culture of explants with BMP9, FGF2 and TGFβ1 to identify if the entire sequence of maturation can be recapitulated. With the accumulation of all the data collected the potential for development of mechanically and

structurally advanced cartilage constructs will be possible using BMP9 (and other growth factors) to direct organisational maturation of the ECM for the purpose of graft implantation. Current grafts lack the same level of collagenous and cellular organisation as we have been able to promote in our cultured explants. The application of this knowledge to scaffold-based grafts may be the solution to producing structurally mature grafts prior to implantation providing improved tissue regeneration and long-term survival.

Chapter 6: References

Abu-Hijleh, G., Reid, O., & Scothorne, R. J. (1997). Cell death in the developing chick knee joint: I. Spatial and temporal patterns. *Clinical Anatomy*, *10*(3), 183–200. https://doi.org/10.1002/(SICI)1098-2353(1997)10:3<183::AID-CA4>3.0.CO;2-V

al Kabbani, A. (2019). Synovial joint. *Radiopaedia.Org*. https://doi.org/10.53347/RID-69143

Bechtold, T. E. et al. (2019) 'The roles of Indian hedgehog signaling in TMJ formation', International Journal of Molecular Sciences, 20(24). doi: 10.3390/ijms20246300.

Bedi, A., Feeley, B. T., & Williams, R. J. (2010). Management of articular cartilage defects of the knee. *Journal of Bone and Joint Surgery*, *92*(4), 994–1009. https://doi.org/10.2106/JBJS.I.00895

Bellamy, N., Campbell, J., Welch, V., Gee, T. L., Bourne, R., & Wells, G. A. (2006). Viscosupplementation for the treatment of osteoarthritis of the knee. *Cochrane Database of Systematic Reviews*, *2006*(2). https://doi.org/10.1002/14651858.CD005321.pub2

Benninghoff, A. (1925). Form und Bau der Gelenkknorpel in ihren Beziehungen zur Funktion - Zweiter Teil: Der Aufbau des Gelenkknorpels in seinen Beziehungen zur Funktion. *Zeitschrift Für Zellforschung Und Mikroskopische Anatomie*, *2*(5), 783–862. https://doi.org/10.1007/BF00583443

Bergeron, E., Senta, H., Mailloux, A., Park, H., Lord, E., & Faucheux, N. (2009). Murine preosteoblast differentiation induced by a peptide derived from bone morphogenetic proteins-9. *Tissue Engineering. Part A*, *15*(11), 3341–3349. https://doi.org/10.1089/TEN.TEA.2009.0189

Blaney Davidson, E. N., Remst, D. F. G., Vitters, E. L., van Beuningen, H. M., Blom, A. B., Goumans, M.-J., van den Berg, W. B., & van der Kraan, P. M. (2009). Increase in ALK1/ALK5 Ratio as a Cause for Elevated MMP-13 Expression in Osteoarthritis in Humans and Mice. *The Journal of Immunology*, *182*(12), 7937–7945. https://doi.org/10.4049/jimmunol.0803991

Blaschke, U. K., Eikenberry, E. F., Hulmes, D. J. S., Galla, H. J., & Bruckner, P. (2000). Collagen XI nucleates self-assembly and limits lateral growth of cartilage fibrils. *Journal of Biological Chemistry*, *275*(14), 10370–10378. https://doi.org/10.1074/jbc.275.14.10370

Blunk, T., Sieminski, A. L., Appel, B., Croft, C., Courter, D. L., Chieh, J. J., Goepferich, A., Khurana, J. S., & Gooch, K. J. (2003). Bone morphogenetic protein 9: A potent modulator of cartilage development in vitro. *Growth Factors*, *21*(2), 71–77. https://doi.org/10.1080/0897719031000148822

Brama, P. A. J., Tekoppele, J. M., Bank, R. A., Barneveld, A., & van Weeren, P. R. (2000). Functional adaptation of equine articular cartilage: The formation of regional biochemical characteristics up to age one year. *Equine Veterinary Journal*, *32*(3), 217–221. https://doi.org/10.2746/042516400776563626

Brittberg M., Lindahl A., Nilsson A., Ohlsson C., Isaksson O., P. L. (1994). Treatment of deep cartilage defects in the knee with autologous chondrocyte transplantation. *New England Journal of Medicine*, *331*(14), 889–895.

Brunet, L., Mcmahon, J., Mcmahon, A., & Harland, R. M. (1998). Noggin, Cartilage Morphogenesis, and Joint Formation in the Mammalian Skeleton. *Science*, *1 1*, 15–17.

Bush, P. G., & Hall, A. C. (2003). The volume and morphology of chondrocytes within non-degenerate and degenerate human articular cartilage. *Osteoarthritis and Cartilage*, *11*(4), 242–251. https://doi.org/10.1016/S1063-4584(02)00369-2

Butler, R. J., Marchesi, S., Royer, T., & Davis, I. S. (2007). Distinct Roles of Bone Morphogenetic Proteins in Osteogenic Differentiation of Mesenchymal Stem Cells Hue. *Journal of Orthopaedic Research September*, *25*(June), 1121–1127. https://doi.org/10.1002/jor

Carter, D. R., Beaupré, G. S., Wong, M., Smith, R. L., Andriacchi, T. P., & Schurman, D. J. (2004). The mechanobiology of articular cartilage development and degeneration. *Clinical Orthopaedics and Related Research*, *427*(SUPPL.), 69–77. https://doi.org/10.1097/01.blo.0000144970.05107.7e

Chang, J. and Poole, C. A. (1996) 'Sequestration of type VI collage in the pericellular microenvironment of adult chondrocytes cultured in agarose', Osteoarthritis and Cartilage, 4(4), pp. 275–285. doi: 10.1016/S1063-4584(05)80105-0.

Chen, A., Gupte, C., Akhtar, K., Smith, P., & Cobb, J. (2012). The Global Economic Cost of Osteoarthritis: How the UK Compares. *Arthritis*, *2012*, 1–6. https://doi.org/10.1155/2012/698709

Cheng, H., Jiang, W., Phillips, F. M., Haydon, R. C., Peng, Y., Zhou, L., Luu, H. H., An, N., Breyer, B., Vanichakarn, P., Szatkowski, J. P., Park, J. Y., & He, T. C. (2003). Osteogenic activity of the fourteen types of human bone morphogenetic proteins (BMPs). *The Journal of Bone and Joint Surgery. American Volume*, *85*(8), 1544–1552. https://doi.org/10.2106/00004623-200308000-00017

Chijimatsu, R. and Saito, T. (2019) 'Mechanisms of synovial joint and articular cartilage development', Cellular and Molecular Life Sciences. Springer International Publishing, 76(20), pp. 3939–3952. doi: 10.1007/s00018-019-03191-5.

Cissell, D. D., Link, J. M., Hu, J. C., & Athanasiou, K. A. (2017). A Modified Hydroxyproline Assay Based on Hydrochloric Acid in Ehrlich's Solution Accurately Measures Tissue Collagen Content. *Tissue Engineering - Part C: Methods*, *23*(4), 243–250. https://doi.org/10.1089/ten.tec.2017.0018

Clark, J. M., Norman, A., & Notzli, H. (1997). Postnatal development of the collagen matrix in rabbit tibial plateau articular cartilage. *Journal of Anatomy*, *191*(2), 215–227. https://doi.org/10.1046/j.1469-7580.1997.19120215.x

Cluzel, C., Blond, L., Fontaine, P., Olive, J., & Laverty, S. (2013). Foetal and postnatal equine articular cartilage development: Magnetic resonance imaging and polarised light microscopy. *European Cells and Materials*, *26*, 33–48. https://doi.org/10.22203/eCM.v026a03

Cohen, N. P., Foster, R.), Mow, V. C., & Foster, R. J. (1998). *Composition and Dynamics of Articular Cartilage: Structure, Function, and Maintaining healthy State*. www.jospt.org

Crawford, D. C., Heveran, C. M., Cannon, W. D., Foo, L. F., & Potter, H. G. (2009). An autologous cartilage tissue implant neocart for treatment of grade III chondral injury to the distal femur: Prospective clinical safety trial at 2 years. *American Journal of Sports Medicine*, *37*(7), 1334–1343. https://doi.org/10.1177/0363546509333011

Cross, M., Smith, E., Hoy, D., Nolte, S., Ackerman, I., Fransen, M., Bridgett, L., Williams, S., Guillemin, F., Hill, C. L., Laslett, L. L., Jones, G., Cicuttini, F., Osborne, R., Vos, T., Buchbinder, R., Woolf, A., & March, L. (2014). The global burden of hip and knee

osteoarthritis: Estimates from the Global Burden of Disease 2010 study. *Annals of the Rheumatic Diseases*, *73*(7), 1323–1330. https://doi.org/10.1136/annrheumdis-2013-204763

Culliford, D., Maskell, J., Judge, A., Cooper, C., Prieto-Alhambra, D., & Arden, N. K. (2015). Future projections of total hip and knee arthroplasty in the UK: Results from the UK Clinical Practice Research Datalink. *Osteoarthritis and Cartilage*, *23*(4), 594–600. https://doi.org/10.1016/j.joca.2014.12.022

da Silva, C. M. L., Spinelli, E., & Rodrigues, S. V. (2015). Fast and sensitive collagen quantification by alkaline hydrolysis/hydroxyproline assay. *Food Chemistry*, *173*, 619–623. https://doi.org/10.1016/J.FOODCHEM.2014.10.073

David, L., Mallet, C., Keramidas, M., Lamandé, N., Gasc, J. M., Dupuis-Girod, S., Plauchu, H., Feige, J. J., & Bailly, S. (2008). Bone morphogenetic protein-9 is a circulating vascular quiescence factor. *Circulation Research*, *102*(8), 914–922. https://doi.org/10.1161/CIRCRESAHA.107.165530

Decker, R. S., Koyama, E., & Pacifici, M. (2015). Articular Cartilage: Structural and Developmental Intricacies and Questions. *Current Osteoporosis Reports*, *13*(6), 407–414. https://doi.org/10.1007/s11914-015-0290-z

Decker, R. S., Um, H. bin, Dyment, N. A., Cottingham, N., Usami, Y., Enomoto-Iwamoto, M., Kronenberg, M. S., Maye, P., Rowe, D. W., Koyama, E., & Pacifici, M. (2017). Cell origin, volume and arrangement are drivers of articular cartilage formation, morphogenesis and response to injury in mouse limbs. *Developmental Biology*, *426*(1), 56–68. https://doi.org/10.1016/j.ydbio.2017.04.006

Dowthwaite, G. P., Edwards, J. C. W., & Pitsillides, A. A. (1998). An essential role for the interaction between hyaluronan and hyaluronan binding proteins during joint development. *Journal of Histochemistry and Cytochemistry*, *46*(5), 641–651. https://doi.org/10.1177/002215549804600509

Dumanian, Z. P., Tollemar, V., Ye, J., Lu, M., Zhu, Y., Liao, J., Ameer, G. A., He, T. C., & Reid, R. R. (2017). Repair of critical sized cranial defects with BMP9-transduced calvarial cells delivered in a thermoresponsive scaffold. *PLoS ONE*, *12*(3), 1–13. https://doi.org/10.1371/journal.pone.0172327

Fomby, P., Cherlin, A. J., Hadjizadeh, A., Doillon, C. J., Sueblinvong, V., Weiss, D. J., Bates, J. H. T., Gilbert, T., Liles, W. C., Lutzko, C., Rajagopal, J., Prockop, D. J., Chambers, D., Giangreco, A., Keating, A., Kotton, D., Lelkes, P. I., Wagner, D. E., & Prockop, D. J. (2010). Repair of articular cartilage defects in the patello-femoral joint with autologous bone marrow mesenchymal cell transplantation: three case reports involving nine defects in five knees. *Annals of the American Thoracic Society*, *12*(3), 181–204. https://doi.org/10.1002/term

Franke, O., Durst, K., Maier, V., Göken, M., Birkholz, T., Schneider, H., Hennig, F., & Gelse, K. (2007). Mechanical properties of hyaline and repair cartilage studied by nanoindentation. *Acta Biomaterialia*, *3*(6), 873–881. https://doi.org/10.1016/j.actbio.2007.04.005

Galli, M., de Santis, V., & Tafuro, L. (2003). Reliability of the Ahlbaäck classification of knee osteoarthritis. *Osteoarthritis and Cartilage*, *11*(8), 580–584. https://doi.org/10.1016/S1063-4584(03)00095-5

Gao, Y., Liu, S., Huang, J., Guo, W., Chen, J., Zhang, L., Zhao, B., Peng, J., Wang, A., Wang, Y., Xu, W., Lu, S., Yuan, M., & Guo, Q. (2014). *The ECM-Cell Interaction of Cartilage Extracellular Matrix on Chondrocytes*. https://doi.org/10.1155/2014/648459

Gepstein, A., Shapiro, S., Arbel, G., Lahat, N., & Livne, E. (2002). Expression of matrix metalloproteinases in articular cartilage of temporomandibular and knee joints of mice during growth, maturation, and aging. *Arthritis and Rheumatism*, *46*(12), 3240–3250. https://doi.org/10.1002/art.10690

Gille, J., Behrens, P., Volpi, P., de Girolamo, L., Reiss, E., Zoch, W., & Anders, S. (2013). Outcome of Autologous Matrix Induced Chondrogenesis (AMIC) in cartilage knee surgery: Data of the AMIC Registry. *Archives of Orthopaedic and Trauma Surgery*, *133*(1), 87–93. https://doi.org/10.1007/s00402-012-1621-5

Gomoll, A. H. (2012). Microfracture and augments. *The Journal of Knee Surgery*, *25*(1), 9–15. https://doi.org/10.1055/s-0031-1299654

Grigolo, B., Lisignoli, G., Piacentini, A., Fiorini, M., Gobbi, P., Mazzotti, G., Duca, M., Pavesio, A., & Facchini, A. (2002). Evidence for redifferentiation of human chondrocytes grown on a hyaluronan-based biomaterial (HYAFF®11): Molecular, immunohistochemical and ultrastructural analysis. *Biomaterials*, *23*(4), 1187–1195. https://doi.org/10.1016/S0142-9612(01)00236-8

Guilak, F., Alexopoulos, L. G., Upton, M. L., Youn, I., Choi, J. B., Cao, L., Setton, L. A., & Haider, M. A. (2006). The pericellular matrix as a transducer of biomechanical and biochemical signals in articular cartilage. *Annals of the New York Academy of Sciences*, *1068*(1), 498–512. https://doi.org/10.1196/annals.1346.011

Hamze, A. B., Wei, S., Bahudhanapati, H., Kota, S., Acharya, K. R., & Brew, K. (2007). Constraining specificity in the N-domain of tissue inhibitor of metalloproteinases-1; gelatinase-selective inhibitors. *Protein Science*, *16*(9), 1905–1913. https://doi.org/10.1110/ps.072978507

Hartmann, C., & Tabin, C. J. (2001). Wnt-14 plays a pivotal role in inducing synovial joint formation in the developing appendicular skeleton. *Cell*, *104*(3), 341–351. https://doi.org/10.1016/S0092-8674(01)00222-7

Haywood, L., & Walsh, D. A. (2001). Vasculature of the normal and arthritic synovial joint. *Histology and Histopathology*, *16*(1), 277–284. https://doi.org/10.14670/HH-16.277

Hefti, E., Müller, W., Jakob, R. P., & Stäubli, H. U. (1993). Evaluation of knee ligament injuries with the IKDC form. *Knee Surgery, Sports Traumatology, Arthroscopy*, *1*(3–4), 226–234. https://doi.org/10.1007/BF01560215

Holmes, D. F., Graham, H. K., Trotter, J. A., & Kadler, K. E. (2001). STEM/TEM studies of collagen fibril assembly. *Micron*, *32*(3), 273–285. https://doi.org/10.1016/S0968-4328(00)00040-8

Horton, W. E., Bennion, P., & Yang, L. (2006). Cellular, molecular, and matrix changes in cartilage during aging and osteoarthritis. *Journal of Musculoskeletal Neuronal Interactions*, *6*(4), 379–381.

Houard, X., Goldring, M. B., & Berenbaum, F. (2013). Homeostatic mechanisms in articular cartilage and role of inflammation in osteoarthritis. *Current Rheumatology Reports*, *15*(11). https://doi.org/10.1007/s11926-013-0375-6

Hughes, L. C., Archer, C. W., & Ap Gwynn, I. (2005). The ultrastructure of mouse articular cartilage: Collagen orientation and implications for tissue functionality. A polarised light and scanning electron microscope study and review. *European Cells and Materials*, *9*(0), 68–84. https://doi.org/10.22203/eCM.v009a09

Hui, A. Y., McCarty, W. J., Masuda, K., Firestein, G. S., & Sah, R. L. (2012). A systems biology approach to synovial joint lubrication in health, injury, and disease. *Wiley Interdisciplinary Reviews: Systems Biology and Medicine*, *4*(1), 15–37. https://doi.org/10.1002/wsbm.157

Hunziker, E. B. (2009). The elusive path to cartilage regeneration. *Advanced Materials*, *21*(32–33), 3419–3424. https://doi.org/10.1002/adma.200801957

Hunziker, E. B., Kapfinger, E., & Geiss, J. (2007). The structural architecture of adult mammalian articular cartilage evolves by a synchronized process of tissue resorption and neoformation during postnatal development. *Osteoarthritis and Cartilage*, *15*(4), 403–413. https://doi.org/10.1016/j.joca.2006.09.010

Hunziker, E. B., Quinn, T. M., & Häuselmann, H. J. (2002). Quantitative structural organization of normal adult human articular cartilage. *Osteoarthritis and Cartilage*, *10*(7), 564–572. https://doi.org/10.1053/joca.2002.0814

Hyde, G., Boot-Handford, R. P., & Wallis, G. A. (2008). Col2a1 lineage tracing reveals that the meniscus of the knee joint has a complex cellular origin. *Journal of Anatomy*, *213*(5), 531–538. https://doi.org/10.1111/j.1469-7580.2008.00966.x

Imai, K., Hiramatsu, A., Fukushima, D., Pierschbacher, M. D., & Okada, Y. (1997). Degradation of decorin by matrix metalloproteinases: Identification of the cleavage sites, kinetic analyses and transforming growth factor-β1 release. *Biochemical Journal*, *322*(3), 809–814. https://doi.org/10.1042/bj3220809

Ito, M. M., & Kida, M. Y. (2000). Morphological and biochemical re-evaluation of the process of cavitation in the rat knee joint: Cellular and cell strata alterations in the interzone. *Journal of Anatomy*, *197*(4), 659–679. https://doi.org/10.1017/S0021878299006974

Jadin, K. D., Wong, B. L., Bae, W. C., Li, K. W., Williamson, A. K., Schumacher, B. L., Price, J. H., & Sah, R. L. (2005). Depth-varying density and organization of chondrocytes in immature and mature bovine articular cartilage assessed by 3D imaging and analysis. *Journal of Histochemistry and Cytochemistry*, *53*(9), 1109–1119. https://doi.org/10.1369/jhc.4A6511.2005

Joronen, K., Salminen, H., Glumoff, V., Savontaus, M., & Vuorio, E. (2000). Temporospatial expression of tissue inhibitors of matrix metalloproteinases-1, -2 and -3 during development, growth and aging of the mouse skeleton. *Histochemistry and Cell Biology*, *114*(2), 157–165. https://doi.org/10.1007/s004180000177

Kääb, M. J., Gwynn, I. A., & Nötzli, H. P. (1998). Collagen fibre arrangement in the tibial plateau articular cartilage of man and other mammalian species. *Journal of Anatomy*, *193*(1), 23–34. https://doi.org/10.1017/S0021878298003744

Kang, Q., Sun, M. H., Cheng, H., Peng, Y., Montag, A. G., Deyrup, A. T., Jiang, W., Luu, H. H., Luo, J., Szatkowski, J. P., Vanichakarn, P., Park, J. Y., Li, Y., Haydon, R. C., & He, T. C. (2004). Characterization of the distinct orthotopic bone-forming activity of 14 BMPs using recombinant adenovirus-mediated gene delivery. *Gene Therapy*, *11*(17), 1312–1320. https://doi.org/10.1038/sj.gt.3302298

Kellgren, J. H., & Lawrence, J. S. (1956). RADIOLOGICAL ASSESSMENT OF OSTEO-ARTHROSIS Ann Rheum Dis 1957. *Ann. Rheum. Dis*, *3*, 494–503. http://ard.bmj.com/

Kessler, E., Takahara, K., Biniaminov, L., Brusel, M., & Greenspan, D. S. (1996). Bone morphogenetic protein-1: The Type I procollagen C-proteinase. *Science*, *271*(5247), 360–362. https://doi.org/10.1126/science.271.5247.360

Kevorkian, L., Young, D. A., Darrah, C., Donell, S. T., Shepstone, L., Porter, S., Brockbank, S. M. V., Edwards, D. R., Parker, A. E., & Clark, I. M. (2004). Expression Profiling of Metalloproteinases and Their Inhibitors in Cartilage. *Arthritis and Rheumatism*, *50*(1), 131–141. https://doi.org/10.1002/art.11433

Khan, I. M., Evans, S. L., Young, R. D., Blain, E. J., Quantock, A. J., Avery, N., & Archer, C. W. (2011). Fibroblast growth factor 2 and transforming growth factor β1 induce precocious maturation of articular cartilage. *Arthritis and Rheumatism*, *63*(11), 3417–3427. https://doi.org/10.1002/art.30543

Klein, T. J., Chaudhry, M., Bae, W. C., & Sah, R. L. (2007). Depth-dependent biomechanical and biochemical properties of fetal, newborn, and tissue-engineered articular cartilage. *Journal of Biomechanics*, *40*(1), 182–190. https://doi.org/10.1016/j.jbiomech.2005.11.002

le Pen, C., Reygrobellet, C., & Gérentes, I. (2005). Financial cost of osteoarthritis in France: The "COART" France study. *Joint Bone Spine*, *72*(6), 567–570. https://doi.org/10.1016/j.jbspin.2005.01.011

Lewis, R. J., Macfarland, A. K., Anandavijayan, S., & Aspden, R. M. (1998). Material properties and biosynthetic activity of articular cartilage from the bovine carpo-metacarpal joint. In *Osteoarthritis Research Society* (Vol. 6).

Li, R. D., Deng, Z. L., Hu, N., Liang, X., Liu, B., Luo, J., Chen, L., Yin, L., Luo, X., Shui, W., He, T. C., & Huang, W. (2021). Biphasic effects of TGFβ1 on BMP9-induced osteogenic differentiation of mesenchymal stem cells. *BMB Reports*, *54*(5), 284–284. https://doi.org/10.5483/BMBRep.2021.54.5.053

Li, X., Chen, L., Ke, Z. Y., Yin, L. J., & Deng, Z. L. (2012). BMP9-induced osteogenetic differentiation and bone formation of muscle-derived stem cells. *Journal of Biomedicine and Biotechnology*, *2012*. https://doi.org/10.1155/2012/610952

Lin, P. M., Chen, C. T. C., & Torzilli, P. A. (2004). Increased stromelysin-1 (MMP-3), proteoglycan degradation (3B3- and 7D4) and collagen damage in cyclically load-injured articular cartilage. *Osteoarthritis and Cartilage*, *12*(6), 485–496. https://doi.org/10.1016/j.joca.2004.02.012

Luo, J., Tang, M., Huang, J., He, B. C., Gao, J. L., Chen, L., Zuo, G. W., Zhang, W., Luo, Q., Shi, Q., Zhang, B. Q., Bi, Y., Luo, X., Jiang, W., Su, Y., Shen, J., Kim, S. H., Huang, E., Gao, Y., … He, T. C. (2010). TGFβ/BMP type I receptors ALK1 and ALK2 are essential for BMP9-induced osteogenic signaling in mesenchymal stem cells. *Journal of Biological Chemistry*, *285*(38), 29588–29598. https://doi.org/10.1074/jbc.M110.130518

Luther, G., R. Wagner, E., Zhu, G., Kang, Q., Luo, Q., Lamplot, J., Bi, Y., Luo, X., Luo, J., Teven, C., Shi, Q., H. Kim, S., Gao, J.-L., Huang, E., Yang, K., Rames, R., Liu, X., Li, M., Hu, N., … He, T.-C. (2011). BMP-9 induced osteogenic differentiation of mesenchymal stem cells: molecular mechanism and therapeutic potential. *Current Gene Therapy*, *11*(3), 229–240. https://doi.org/10.2174/156652311795684777

Macri, L., Silverstein, D., & Clark, R. A. F. (2007). Growth factor binding to the pericellular matrix and its importance in tissue engineering. *Advanced Drug Delivery Reviews*, *59*(13), 1366–1381. https://doi.org/10.1016/j.addr.2007.08.015

Madej, W., van Caam, A., Blaney Davidson, E. N., Hannink, G., Buma, P., & van der Kraan, P. M. (2016). Ageing is associated with reduction of mechanically-induced activation of Smad2/3P signaling in articular cartilage. *Osteoarthritis and Cartilage*, *24*(1), 146–157. https://doi.org/10.1016/j.joca.2015.07.018

Majumdar, M. K., Wang, E., & Morris, E. A. (2001). BMP-2 and BMP-9 promote chondrogenic differentiation of human multipotential mesenchymal cells and overcome the inhibitory effect of IL-1. *Journal of Cellular Physiology*, *189*(3), 275–284. https://doi.org/10.1002/jcp.10025

Mankin, H. J. (1962). Localization of Tritiated Thymidine in Articular Cartilage of Rabbits. *Journal of Bone and Joint Surgery*, *44*(4), 682–688. https://doi.org/10.2106/00004623-196244040-00008

Maroudas, A. (1968). Physicochemical Properties of Cartilage in the Light of Ion Exchange Theory. *Biophysical Journal*, *8*(5), 575–595. https://doi.org/10.1016/S0006-3495(68)86509-9

Mehana, E. S. E., Khafaga, A. F., & El-Blehi, S. S. (2019). The role of matrix metalloproteinases in osteoarthritis pathogenesis: An updated review. *Life Sciences*, *234*(August), 116786. https://doi.org/10.1016/j.lfs.2019.116786

Mérida-Velasco, J. R. et al. (1999) 'Development of the human temporomandibular joint', Anatomical Record, 255(1), pp. 20–33. doi: 10.1002/(SICI)1097-0185(19990501)255:1<20::AID-AR4>3.0.CO;2-N.

Meyerowitz, E. s. C. and E. M. (1991). Homeobox gene expression correlated with the birfurcation process of limb cartilage development. *Nature*, *354*, 56–58.

Mitrovic, D. (1978). Development of the diarthrodial joints in the rat embryo. *American Journal of Anatomy*, *151*(4), 475–485. https://doi.org/10.1002/aja.1001510403

Mollon, B., Kandel, R., Chahal, J., & Theodoropoulos, J. (2013). The clinical status of cartilage tissue regeneration in humans. *Osteoarthritis and Cartilage*, *21*(12), 1824–1833. https://doi.org/10.1016/j.joca.2013.08.024

Morgan, B. J., Bauza-Mayol, G., Gardner, O. F. W., Zhang, Y., Levato, R., Archer, C. W., Weeren, R. van, Malda, J., Conlan, R. S., Francis, L. W., & Khan, I. M. (2020). Bone Morphogenetic Protein-9 Is a Potent Chondrogenic and Morphogenic Factor for Articular Cartilage Chondroprogenitors. *Stem Cells and Development*, *29*(14), 882–894. https://doi.org/10.1089/scd.2019.0209

Morgan, O. J., Hillstrom, H. J., Ellis, S. J., Golightly, Y. M., Russell, R., Hannan, M. T., Deland, J. T., & Hillstrom, R. (2019). Osteoarthritis in England: Incidence Trends From National Health Service Hospital Episode Statistics. *ACR Open Rheumatology*, *1*(8), 493–498. https://doi.org/10.1002/acr2.11071

Munhoz, F. B. A., Godoy-Santos, A. L., & Santos, M. C. L. G. (2010). MMP-3 polymorphism: Genetic marker in pathological processes (review). *Molecular Medicine Reports*, *3*(5), 735–740. https://doi.org/10.3892/mmr.2010.340

Murphy, G., Allan, J. A., Willenbrock, F., Cockett, M. I., O'Connell, J. P., & Docherty, A. J. P. (1992). The role of the C-terminal domain in collagenase and stromelysin specificity. *Journal of Biological Chemistry*, *267*(14), 9612–9618. https://doi.org/10.1016/s0021-9258(19)50134-x

Nakamura, T., Shirakata, Y., Shinohara, Y., Miron, R. J., Hasegawa-Nakamura, K., Fujioka-Kobayashi, M., & Noguchi, K. (2017). Comparison of the effects of recombinant

human bone morphogenetic protein-2 and -9 on bone formation in rat calvarial critical-size defects. *Clinical Oral Investigations*, *21*(9), 2671–2679. https://doi.org/10.1007/s00784-017-2069-3

Oinas, J., Ronkainen, A. P., Rieppo, L., Finnilä, M. A. J., Iivarinen, J. T., van Weeren, P. R., Helminen, H. J., Brama, P. A. J., Korhonen, R. K., & Saarakkala, S. (2018). Composition, structure and tensile biomechanical properties of equine articular cartilage during growth and maturation. *Scientific Reports*, *8*(1), 1–12. https://doi.org/10.1038/s41598-018-29655-5

Ortega, N., Behonick, D. J., & Werb, Z. (2004). Matrix remodeling during endochondral ossification. *Trends in Cell Biology*, *14*(2), 86–93. https://doi.org/10.1016/j.tcb.2003.12.003

Pacifici, M., Koyama, E., & Iwamoto, M. (2005). Mechanisms of synovial joint and articular cartilage formation: Recent advances, but many lingering mysteries. *Birth Defects Research Part C - Embryo Today: Reviews*, *75*(3), 237–248. https://doi.org/10.1002/bdrc.20050

Poole, C. A. (1997). Articular cartilage chondrons: Form, function and failure. *Journal of Anatomy*, *191*(1), 1–13. https://doi.org/10.1017/S0021878297002185

Poole, C. A., Ayad, S., & Schofield, J. R. (1988). Chondrons from articular cartilage: I. Immunolocalization of type VI collagen in the pericellular capsule of isolated canine tibial chondrons. *Journal of Cell Science*, *90 (Pt 4)*, 635–643. https://doi.org/10.1242/jcs.90.4.635

Poole, C. A., Flint, M. H., & Beaumont, B. W. (1984). Morphological and functional interrelationships of articular cartilage matrices. *Journal of Anatomy*, *138*(Pt 1), 113. /pmc/articles/PMC1164314/?report=abstract

Quiros, N., Abinzano, F., Plomp, S., Giessen, E., Levato, R., Tryfonidou, M., & Moller, N. te. (2020). Combination of bone morphogenetic protein 9 and transforming growth factor BETA-1 improves cartilaginous matrix formation by equine chondrocytes in three-dimensional culture. *Osteoarthritis and Cartilage*, *28*(2020), S496. https://doi.org/10.1016/j.joca.2020.02.776

Rich, A., & Crick, F. H. C. (1955). The structure of collagen. *Nature*, *176*(4489), 915–916. https://doi.org/10.1038/176915A0

Rieppo, J., Hallikainen, J., Jurvelin, J. S., Kiviranta, I., Helminen, H. J., & Hyttinen, M. M. (2008). Practical considerations in the use of polarized light microscopy in the analysis of the collagen network in articular cartilage. *Microscopy Research and Technique*, *71*(4), 279–287. https://doi.org/10.1002/jemt.20551

Rieppo, J., Hyttinen, M. M., Halmesmaki, E., Ruotsalainen, H., Vasara, A., Kiviranta, I., Jurvelin, J. S., & Helminen, H. J. (2009). Changes in spatial collagen content and collagen network architecture in porcine articular cartilage during growth and maturation. *Osteoarthritis and Cartilage*, *17*(4), 448–455. https://doi.org/10.1016/j.joca.2008.09.004

Rutjes, A. W. S., Nüesch, E., Reichenbach, S., & Jüni, P. (2009). Doxycycline for osteoarthritis of the knee or hip. *Cochrane Database of Systematic Reviews*, *4*. https://doi.org/10.1002/14651858.CD007321.pub2

Saito, T., Bokhove, M., Croci, R., Zamora-Caballero, S., Han, L., Letarte, M., de Sanctis, D., & Jovine, L. (2017). Structural Basis of the Human Endoglin-BMP9 Interaction: Insights into BMP Signaling and HHT1. *Cell Reports*, *19*(9), 1917–1928. https://doi.org/10.1016/j.celrep.2017.05.011

Sakaguchi, Y., Sekiya, I., Yagishita, K., & Muneta, T. (2005). Comparison of human stem cells derived from various mesenchymal tissues: Superiority of synovium as a cell source. *Arthritis and Rheumatism*, *52*(8), 2521–2529. https://doi.org/10.1002/art.21212

Salmon, R. M., Guo, J., Wood, J. H., Tong, Z., Beech, J. S., Lawera, A., Yu, M., Grainger, D. J., Reckless, J., Morrell, N. W., & Li, W. (2020). Molecular basis of ALK1-mediated signalling by BMP9/BMP10 and their prodomain-bound forms. *Nature Communications*, *11*(1), 1–16. https://doi.org/10.1038/s41467-020-15425-3

Scheller, G., Sobau, C., & Bülow, J. U. (2001). Arthroscopic partial lateral meniscectomy in an otherwise normal knee: Clinical, functional, and radiographic results of a long-term follow-up study. *Arthroscopy*, *17*(9), 946–952. https://doi.org/10.1053/jars.2001.28952

Schumacher, B. L., Su, J. L., Lindley, K. M., Kuettner, K. E., & Cole, A. A. (2002). Horizontally oriented clusters of multiple chondrons in the superficial zone of ankle, but not knee articular cartilage. *Anatomical Record*, *266*(4), 241–248. https://doi.org/10.1002/ar.10063

Servin-Vences, M. R., Richardson, J., Lewin, G. R., & Poole, K. (2016). Mechanoelectrical transduction in chondrocytes. *International Journal of Laboratory Hematology*, *38*(1), 42–49. https://doi.org/10.1111/ijlh.12426

Sophia Fox, A. J., Bedi, A., & Rodeo, S. A. (2009). The basic science of articular cartilage: Structure, composition, and function. *Sports Health*, *1*(6), 461–468. https://doi.org/10.1177/1941738109350438

Stockwell, R. A. (1978). Chondrocytes. *J Clin Pathol Suppl (R Coll Pathol)*, *x 8000*, 7–13.

Stolz, M., Gottardi, R., Raiteri, R., Miot, S., Martin, I., Imer, R., Staufer, U., Raducanu, A., Düggelin, M., Baschong, W., Daniels, A. U., Friederich, N. F., Aszodi, A., & Aebi, U. (2009). Early detection of aging cartilage and osteoarthritis in mice and patient samples using atomic force microscopy. *Nature Nanotechnology*, *4*(3), 186–192. https://doi.org/10.1038/nnano.2008.410

Storm, E. E., & Kingsley, D. M. (1996). Joint patterning defects caused by single and double mutations in members of the bone morphogenetic protein (BMP) family. *Development*, *122*(12), 3969–3979. https://doi.org/10.1242/dev.122.12.3969

Storm, E. E., & Kingsley, D. M. (1999). GDF5 coordinates bone and joint formation during digit development. *Developmental Biology*, *209*(1), 11–27. https://doi.org/10.1006/dbio.1999.9241

Takahashi, K., & Yamanaka, S. (2006). Induction of Pluripotent Stem Cells from Mouse Embryonic and Adult Fibroblast Cultures by Defined Factors. *Cell*, *126*(4), 663–676. https://doi.org/10.1016/j.cell.2006.07.024

Thomas, K. S., Muir, K. R., Doherty, M., Jones, A. C., O'Reilly, S. C., & Bassey, E. J. (2002). Home based exercise programme for knee pain and knee osteoarthritis: Randomised controlled trial. *British Medical Journal*, *325*(7367), 752–755. https://doi.org/10.1136/bmj.325.7367.752

Tillet, E., & Bailly, S. (2014). Emerging roles of BMP9 and BMP10 in hereditary hemorrhagic telangiectasia. *Frontiers in Genetics*, *5*(DEC), 1–7. https://doi.org/10.3389/fgene.2014.00456

Tübingen, G. A. S. H. L. G. and I. of T. M. U. of T. (2011). A Randomized Trial of Arthroscopic Surgery for Osteoarthritis of the Knee Alexandra. *New England Journal of Medicine*, *365*, 687–696.

Urist, M. R., & McLean, F. C. (1950). Bone repair in rats with multiple fractures. *The American Journal of Surgery*, *80*(6), 685–695. https://doi.org/10.1016/0002-9610(50)90593-9

van Caam, A. et al. (2016) 'Expression of TGFβ-family signalling components in ageing cartilage: Age-related loss of TGFβ and BMP receptors', Osteoarthritis and Cartilage. Elsevier Ltd, 24(7), pp. 1235–1245. doi: 10.1016/j.joca.2016.02.008.

van Caam, A., Blaney Davidson, E., Garcia de Vinuesa, A., van Geffen, E., van den Berg, W., Goumans, M. J., ten Dijke, P., & van der Kraan, P. (2015). The high affinity ALK1-ligand BMP9 induces a hypertrophy-like state in chondrocytes that is antagonized by TGFβ1. *Osteoarthritis and Cartilage*, *23*(6), 985–995. https://doi.org/10.1016/j.joca.2015.02.007

van Caam, A., Davidson, E. B., & van der Kraan, P. (2017). TGFβ Signaling Via ALK1 Requires ALK5 Kinase Activity In Chondrocytes. *Osteoarthritis and Cartilage*, *25*(2017), S167–S168. https://doi.org/10.1016/j.joca.2017.02.286

van Caam, A., Madej, W., Thijssen, E., Garcia de Vinuesa, A., van den Berg, W., Goumans, M. J., ten Dijke, P., Blaney Davidson, E., & van der Kraan, P. M. (2016). Expression of TGFβ-family signalling components in ageing cartilage: Age-related loss of TGFβ and BMP receptors. *Osteoarthritis and Cartilage*, *24*(7), 1235–1245. https://doi.org/10.1016/j.joca.2016.02.008

van der Kraan, P., Matta, C., & Mobasheri, A. (2016). Age-Related Alterations in Signaling Pathways in Articular Chondrocytes: Implications for the Pathogenesis and Progression of Osteoarthritis - A Mini-Review. *Gerontology*, *63*(1), 29–35. https://doi.org/10.1159/000448711

van Turnhout, M. C., Schipper, H., van Lagen, B., Zuilhof, H., Kranenbarg, S., & van Leeuwen, J. L. (2010). Postnatal development of depth-dependent collagen density in ovine articular cartilage. *BMC Developmental Biology*, *10*, 1–16. https://doi.org/10.1186/1471-213X-10-108

Vanlauwe, J., Saris, D. B. F., Victor, J., Almqvist, K. F., Bellemans, J., & Luyten, F. P. (2011). Five-year outcome of characterized chondrocyte implantation versus microfracture for symptomatic cartilage defects of the knee: early treatment matters. *American Journal of Sports Medicine*, *39*(12), 2566–2574. https://doi.org/10.1177/0363546511422220

Wallingford, J. B., Fraser, S. E., & Harland, R. M. (2002). Convergent extension: The molecular control of polarized cell movement during embryonic development. *Developmental Cell*, *2*(6), 695–706. https://doi.org/10.1016/S1534-5807(02)00197-1

Watt, S. L., Lunstrum, G. P., McDonough, A. M., Keene, D. R., Burgeson, R. E., & Morris, N. P. (1992). Characterization of collagen types XII and XIV from fetal bovine cartilage. *Journal of Biological Chemistry*, *267*(28), 20093–20099. https://doi.org/10.1016/s0021-9258(19)88670-2

Whitelock, J. M., Murdoch, A. D., Iozzo, R. v., & Underwood, P. A. (1996). The degradation of human endothelial cell-derived perlecan and release of bound basic fibroblast growth factor by stromelysin, collagenase, plasmin, and heparanases. *Journal of Biological Chemistry*, *271*(17), 10079–10086. https://doi.org/10.1074/jbc.271.17.10079

Wiberg, C., Klatt, A. R., Wagener, R., Paulsson, M., Bateman, J. F., Heinegård, D., & Mörgelin, M. (2003). Complexes of matrilin-1 and biglycan or decorin connect collagen VI microfibrils to both collagen II and aggrecan. *Journal of Biological Chemistry*, *278*(39), 37698–37704. https://doi.org/10.1074/jbc.M304638200

Williamson, A. K., Chen, A. C., Masuda, K., Thonar, E. J. M. A., & Sah, R. L. (2003). Tensile mechanical properties of bovine articular cartilage: Variations with growth and relationships

to collagen network components. *Journal of Orthopaedic Research*, *21*(5), 872–880. https://doi.org/10.1016/S0736-0266(03)00030-5

Williamson, A. K., Chen, A. C., & Sah, R. L. (2001). Compressive properties and function-composition relationships of developing bovine articular cartilage. *Journal of Orthopaedic Research*, *19*(6), 1113–1121. https://doi.org/10.1016/S0736-0266(01)00052-3

Wong, M., Wuethrich, P., Eggli, P., & Hunziker, E. (1996). Zone-specific cell biosynthetic activity in mature bovine articular cartilage: A new method using confocal microscopic stereology and quantitative autoradiography. *Journal of Orthopaedic Research*, *14*(3), 424–432. https://doi.org/10.1002/jor.1100140313

Wu, J. J., Woods, P. E., & Eyre, D. R. (1992). Identification of cross-linking sites in bovine cartilage type IX collagen reveals an antiparallel type II-type IX molecular relationship and type IX to type IX bonding. *Journal of Biological Chemistry*, *267*(32), 23007–23014. https://doi.org/10.1016/s0021-9258(18)50048-x

Xu, D. J., Zhao, Y. Z., Wang, J., He, J. W., Weng, Y. G., & Luo, J. Y. (2012). Smads, p38 and ERK1/2 are involved in BMP9-induced osteogenic differentiation of C3H10T1/2 mesenchymal stem cells. *BMB Reports*, *45*(4), 247–252. https://doi.org/10.5483/BMBRep.2012.45.4.247

Yan, B., Pan, Y., & Yan, J. (2018). Radiographic grading of the severity of knee grade to a grade based on joint space narrowing, and osteoarthritis: relation of the kellgren and lawrence correlation with arthroscopic evidence of articular cartilage degeneration. *Journal of the Indian Society of Remote Sensing*, *46*(4), 617–624. https://doi.org/10.1007/s12524-017-0734-2

Young, R. D., Lawrence, P. A., Duance, V. C., Aigner, T., & Monaghan, P. (2000). Immunolocalization of collagen Types II and III in single fibrils of human articular cartilage. *Journal of Histochemistry and Cytochemistry*, *48*(3), 423–432. https://doi.org/10.1177/002215540004800312

Yu, L., Dawson, L. A., Yan, M., Zimmel, K., Lin, Y. L., Dolan, C. P., Han, M., & Muneoka, K. (2019). BMP9 stimulates joint regeneration at digit amputation wounds in mice. *Nature Communications*, *10*(1), 1–9. https://doi.org/10.1038/s41467-018-08278-4

Zhang, Y., Morgan, B. J., Smith, R., Fellows, C. R., Thornton, C., Snow, M., Francis, L. W., & Khan, I. M. (2017a). Platelet-rich plasma induces post-natal maturation of immature articular cartilage and correlates with LOXL1 activation. *Scientific Reports*, *7*(1), 1–12. https://doi.org/10.1038/s41598-017-02297-9

Zhang, Y., Morgan, B. J., Smith, R., Fellows, C. R., Thornton, C., Snow, M., Francis, L. W., & Khan, I. M. (2017b). Platelet-rich plasma induces post-natal maturation of immature articular cartilage and correlates with LOXL1 activation. *Scientific Reports*, *7*(1), 1–12. https://doi.org/10.1038/s41598-017-02297-9